MECHANISMS INFLUENCING THE POLAR DISTRIBUTION OF CELL WALL COMPONENTS IN SEED COAT EPIDERMAL CELLS OF ARABIDOPSIS

by

Yi-Chen Lee

B.Sc., National Taiwan University, 2007
M.Phil., The University of Cambridge, 2009

A THESIS SUBMITTED IN PARTIAL FULFILLMENT OF
THE REQUIREMENTS FOR THE DEGREE OF

DOCTOR OF PHILOSOPHY
in
THE FACULTY OF GRADUATE AND POSTDOCTORAL STUDIES
(Botany)

THE UNIVERSITY OF BRITISH COLUMBIA
(Vancouver)

April 2018

Abstract

Compositions of plant cell walls are important for morphogenesis and cellular function. Cell wall components are often distributed asymmetrically in the cell wall, but the mechanism for the polar distribution remains unknown. In my research, I used Arabidopsis seed coat epidermal cells as a model system because they deposit large amounts of pectin-rich mucilage in a polar manner to the outer periclinal side of the cell forming a large apoplastic pocket. MUM2 is a β-galactosidase modifying pectin in the mucilage. Using an engineered version of MUM2 fused to a Citrine fluorescent protein (Citrine), distribution pattern of MUM2 in the epidermal cell was determined. MUM2-Citrine is found to preferentially accumulate in the mucilage pocket concomitantly with pectin deposition. The amino acid sequence of MUM2 is not required for the secretion to the pocket. Rather, the polar distribution of MUM2-Citrine is caused by a rearrangement of the secretory pathway that appears to target all secretion to the outer periclinal side of the cell.

At the end of mucilage synthesis, the fluorescence of MUM2-Citrine rapidly disappears from the mucilage pocket. The results of western blot analyses shows that the amount of MUM2-Citrine decreases, suggesting that the disappearance of MUM2-Citrine signal is due to protein degradation. Loss-of-function mutations in the genes encoding ASPG1 and RD21A, two proteases that have been detected in mucilage from mature seeds, resulted in a delay of MUM2-Citrine degradation. Also, RD21A, tagged with red fluorescent protein (RFP), accumulated in the vacuole during MUM2 secretion and was translocated to the mucilage pocket at the end of secretion. Taken together, these data suggest that ASPG1 and RD21A are responsible for MUM2 degradation. Mucilage

properties were changed in the protease mutants, suggesting that the regulation of distribution of cell wall-modifying enzymes by proteases plays an important role in determining cell wall properties.

It has been found that PER36, a peroxidase required for mucilage extrusion, was deposited in a pattern distinct from other mucilage proteins in seed coats. I showed the amino acid sequences of PER36 was required for the unique distribution pattern, suggesting that an unknown distribution mechanism may be involved.

Lay Summary

Plant cells are encapsulated by cell walls composed of carbohydrates and proteins, which are synthesizd inside the cell and transported outside the cell. Cell wall properties affect plant growth and are determined by the types and amount of protein and carbohydrate made and transported. The distribution of cell wall components is not always even resulting in cell wall asymmetry. However, mechanisms establishing asymmetric distribution remain elusive. I show that a cell wall protein, MUM2, is distributed asymmetrically in a polarized cell type through two mechansims. First, MUM2 is preferentially delivered to a certain area of the cell wall. The machinery of protein delivery is reorganized, so that most materials are exported to a specific region of the cell. Second, MUM2 is removed in certain area of cell walls at specific time by protein-degrading proteins. The distinct distribution of another cell wall protein, PER36 suggests the involvement of a distinct mechanism.

Preface

This dissertation contains three research chapters. The experiments in chpater 3 were designed by Dr. George Haughn, Dr. Erin Gilchrist, and Yi-Chen Lee. Yi-Chen Lee performed all the experiments, except for making *genomic MUM2-Citrine* transgenic plants, which was done by Dr Erin Gilchrist. The experiments in chapter 4 were designed by Dr. George Haughn and Yi-Chen Lee. All the experiments were carried out by Yi-Chen Lee, except for crossing *genomic MUM2-Citrine* into the protease mutants, which was done by Dr. Allen Yi-Lun Tsai. The design of the research project in chapter 5 was contributed by Dr. George Haughn and Yi-Chen Lee. Yi-Chen Lee did all the experiments, except for the following experiments: Tiffany Lee, an undergraduate working under my supervision screened for *PER36(322Q)-Citrine* transgenic plants and tested if PER36(N224Q) is glycosylated via deglycosylation with enzymes, with help from Yi-Chen Lee. Data in all reseach chapters were analyzed by Dr. George Haughn and Yi-Chen Lee.

Table of Contents

List of Tables

List of Figures

List of Abbreviations

ARA12 or SBT1.7	SUBTILISIN-LIKE SERINE PROTEASE 1.7
ASPG1	ASPARTIC PROTEASE IN GUARD CELL 1
BXL1	Bifunctional β-D-Xylosidase/α-L-arabinofuranosidase 1
CESA	cellulose synthase
Col	Columbia ecotype
Cyto	cytosol
DPA	Day Post Anthesis
ECH	ECHIDNA
GAP	GTPase-activating protein
GEF	guanine nucleotide exchange factor
HG	homogalacturonan
kD	kilodalton
mRFP	monomeric red fluorescent protein
MVB	multivesicular bodies
PER36	PEROXIDASE 36
PME	pectin methyesterases
PMEI	pectin methyesterases inhibitor
ROP	Rho of plants
PRX	peroxidase
RD21A	RESPONSIVE TO DEHYDRATION 21A
RG-I	rhamnogalacturonan-I
RG-II	rhamnogalacturonan-II
VAMP	vesicle-associated membrane protein
sec	secretory
SCPL35	SERINE CARBOXYPEPTIDASE-LIKE 35
SNARE	soluble N-ethylmaleimide-sensitive factor activating protein receptor
SP	signal peptide
T-DNA	transfer DNA
TGN	*trans*-Golgi network
YFP	yellow fluorescent protein

Acknowledgements

I would like to thank many people without whose help I would not have been able to finish my research project and this dissertation. First, I would like to thank my supervisor, Dr. George Haughn, for his instruction, support and endless patience. I am grateful for being included in his lab and being given such a wonderful project. I appreciate having had the chance to make my own mistakes without too much criticism. Finally, I would like to give special thanks for the huge amount of time and energy that Dr. Haughn spent in editing my dissertation.

I would like to thank my supervisory committee: Dr. Jae-Hyeok Lee, Dr. Linda Matsuuchi, Dr. Lacey Samuels, and Dr. Yuelin Zhang for guidance and advice. Thank you very much for valuable insight and helpful suggestions. I would like to give another thank you to Dr. Lacey Samuels for critically reviewing my manuscript. Dr. Ljerka Kunst, as an unofficial committee member, provided welcome constructive criticism of my research and presentations.

Thank you to members of the Haughn and Kunst labs for making such a great work environment. Dr. Erin Gilchrist provided assistance, support and kindness, especially during the beginning of my degree. Dr. Gill Dean and Dr. Allen Tsai provided many suggestions and technical assistance for my experiments. I had many valuable discussions with fellow graduate students Kresimir Sola and Robert McGee that taught me a lot. In addition, I would like to thank them for generously sharing experimental material with me. Thanks to Joyce Liu for her encouragement when I was writing my dissertation and to Tiffany Lee for helping me with the PER36 project as a summer student.

I would like to thank people in UBC Bioimaging Facility for technical support and all the friendly people in the Botany department for support in many different ways . I am really happy to be a member of this department.

Thanks to Studying Aboard Scholarship from Minister of Education of Taiwan for funding the first two years of my PhD degree.

I would like to thank my parents, my brother, and other family members for their love, understanding and encouragement and my friends for encouragement and friendship. Finally, I would like to thank many people whose names I didn't list here, including many enthusiastic instructors, passionate researchers, and talented peers I met. I received a lot of inspiration from my interactions with them.

Chapter 1   : Introduction

The composition and structure of plant cell walls can vary significantly both between cell types as well as throughout the life of a single cell type. Such differences are necessary to accomplish diverse functions and morphologies in different developmental and environmental conditions. The heterogeneity of cell wall is determined by how cell wall components are synthesized, when and where they are deposited to the apoplast, and how cell walls are modified by cell wall-modifying enzymes after deposition. In this dissertation, I investigate polar distribution mechanisms in an attempt to understand how cell walls achieve heterogeneity. My main focus is on the polar secretion of two cell wall-modifying enzymes MUCILAGE MODIFIED 2 (MUM2) and PEROXIDASE 36 (PER36) in Arabidopsis seed coat epidermal cells, a polarized cell type.

Below, I briefly introduce cell wall structure and biosynthesis followed by a description of our current knowledge of the molecular mechanism underlying endomembrane trafficking, especially post-Golgi trafficking to the plasma membrane/apoplast, and mechanisms of cell polarity and polar distribution in general. I then focus on secretion and polar distribution of plant cell wall components. Finally, I introduce my model system, Arabidopsis seed coat epidermal cells, with an emphasis on mucilage-related studies that include MUM2 and PER36, the two proteins that are the focal point of my research.

1.1   Dynamic plant cell wall structure

Plant cells are encapsulated by primary cell walls that are composed mainly of polysaccharides, including cellulose, hemicellulose, and pectin. The classical view of plant cell

wall structure has the fibrous cellulose tethered by hemicellulose to form a mesh-like load-bearing structure or network. The cellulose and hemicellulose network is embedded in a gel-like matrix termed pectin (Cosgrove, 2014; Chebli and Geitmann, 2017). In addition to polysaccharides, 10% of the cell wall consists of proteins, including cell wall enzymes, signaling proteins, and structural proteins.

The traditional concept of plant cell wall structure has been challenged recently due to evidence suggesting a more important role for pectin. First, studies show that there are more cellulose-pectin connections than those of cellulose-hemicellulose (Wang et al., 2015). Second, it has been shown that pectin may function as the loading-bearing structure when hemicellulose or cellulose is absent (Chebli and Geitmann, 2017). Third, pectin has been shown to be connected with hemicellulose, phenolic compounds, and proteins (Caffall and Mohnen, 2009) and pectin and hemicelluloses can be covalently linked to arabinoglycan proteins (AGPs) (Tan et al., 2013). The actual cell wall structure is likely to be more complicated than what has been proposed in the past.

The identity and relative amounts of the major cell wall carbohydrates and proteins can vary significantly between different species, tissues, cell types or even between different domains of a single cell (Burton et al., 2010; Worden et al., 2012). In addition, cell walls are highly dynamic; their composition and structure can change during development and in response to environmental cues. Cells produce different kinds of cell wall components and secrete cell-wall-modifying enzymes to change the properties of the walls depending on the needs of the cell (Cosgrove, 2005; Somssich et al., 2016; Chebli and Geitmann, 2017).

According to cell wall proteome data from Arabidopsis, one quarter of cell wall proteins, including glycoside hydrolases and expansins, act on carbohydrates. These cell wall-modifying proteins form and/or break both covalent and non-covalent bonds between cell wall components

and thus change cell wall properties (Albenne et al., 2013). Fifteen percent of cell wall proteins are oxido-reductases, including peroxidases (Albenne et al., 2013). Those enzymes may also be involved in modification of linkages between cell wall polymers (Passardi et al., 2004). The abundance of cell wall-modifying enzymes highlights the dynamic nature of cell walls.

1.2   Biosynthesis of cell wall components

The major classes of carbohydrate synthesized by the cell are cellulose, hemicellulose and pectin. Much of cell wall heterogeneity is determined by the specific cell wall components made and their relative proportions for a given cell type.

Celluloses are unbranched β-1,4-linked-D-glucan chains, which are synthesized by the cellulose synthase (CESA) protein complex in the plasma membrane (McFarlane et al., 2014). Microtubules underneath the plasma membranes guide the movement of CESA complexes and thus determine the orientation of cellulose microfibrils, which can limit the direction of cell expansion (Cosgrove, 2005).

Hemicelluloses are diverse non-cellulosic polysaccharides, such as xyloglucan, xylan, and mannan. The backbones of hemicellulose are synthesized by cellulose synthase-like enzymes (CSL) and other glycosyltransferases in the Golgi, while the side chains are synthesized by glycosyltransferases (reviewed by Scheller and Ulvskov, 2010). For example, the glucoside backbone of xyloglucan is synthesized by CSLC4 while xylosyltransferases XXT1/XXT2/XXT5 add side chains to the backbone (Cocuron et al., 2007). After synthesis, hemicelluloses are secreted to the apoplast via vesicles (Caffall and Mohnen, 2009; Driouich et al., 2012).

Pectins are non-cellulosic polysaccharides that contain galacturonic acids (GalA). There are three main kinds of pectins, homogalacturonan (HG), rhamnogalacturonan-I (RG-I), and rhamnogalacturonan-II (RG-II). HG is an unbranched polymer of α-1,4-linked-D-galacturonic

acid, which account for ~65% pectin in the primary plant cell wall (Atmodjo et al., 2013). HG is methylesterified at the *O*-6 position when it is secreted but can be partially de-esterified by pectin methyesterases (PME) in the apoplast. Blocks of unesterified HG interact via Ca^{2+} salt bridges to form dimeric HG molecules (Caffall and Mohnen, 2009; Atmodjo et al., 2013). Such interactions make pectin much more cohesive. Thus, plants are able to alter the stiffness of the cell wall by changing the degree of HG methylation, which, in turn, is controlled by the spatiotemporal distribution of PME and its inhibitor PMEI (Wolf and Greiner, 2012). RG-II, which has an HG backbone with four structurally conserved side chains, accounts for up to ~10% of pectin in primary cell walls in dicotyledonous species (Atmodjo et al., 2013). RG-II can form dimeric molecules via boron ester bonds that contribute to cell wall strength. The RG-I backbone is made of alternating galacturonic acid and rhamnose (Rha), with a repeat unit of $[4]$-α-D-GalA-(1,2)-α-L-Rha-(1,$]_n$. RG-I constitutes 20-35% of primary cell wall pectin. RG-I is branched at the *C*-4 position of rhamnose by arabinan, galactan, or arabinoglalctan side chains. The degree of branching varies from tissue to tissue (Caffall and Mohnen, 2009; Atmodjo et al., 2013).

Pectin is synthesized in the Golgi, with different residues of the polysaccharide side chains added in different cisternae, and delivered by vesicle to the apoplast (Worden et al., 2012). Because of the complicated array of glycosidic linkages, it has been proposed that pectin synthesis requires 65 glycosyltransferases. So far only a few enzymes have been characterized, including galacturonosyltransferases GAUT1 and GAUT7 for HG backbone synthesis, QUASIMODO 2 (QUA2), QUASIMODO 3 (QUA3), COTTON GOLGI-RELATED2 (CGR2) and COTTON GOLGI-RELATED 3 (CGR3) for HG methylation, ARABINAN DEFICIENT 1 (ARAD1) and ARABINAN DEFICIENT 2 (ARAD2) for adding arabinose to RG-I side chains, GALS1 for adding galactose to RG-I side chains, and Rhamnogalacturonan-II

Xylosyltransferase RGXT1, RGXT2, RGXT3, and RGXT4 for adding xylose to RG-II side chains (Driouich et al., 2012; Atmodjo et al., 2013; Anderson, 2016).

An increasing amount of data has suggested that these cell wall biosynthetic enzymes work in complexes (Oikawa et al., 2013). The interaction may help enzymes related to a particular pathway to be localized together for efficient synthesis. For example, the membrane anchor of GAUT1 is cleaved off. GAUT1 is retained in the Golgi by interacting with GAUT7, which doesn't have any enzymatic activity itself (Atmodjo et al., 2011). Interactions between polypeptides may also be important for enzyme activity. For example, CSLC4 only shows enzyme activity when co-expressed with XXT1 in yeasts (Oikawa et al., 2013).

Plant cells secrete both polysaccharide matrix and cell wall proteins to the apoplast, but studies of secretion in plants have mainly focused on proteins as cargo. The proteins carrying signal peptides at their N-terminal ends are synthesized by the ribosome on the ER membrane and travel through the endomembrane system. These proteins are transferred from the ER to the Golgi apparatus by vesicles. Then they are sorted in the *trans*-Golgi network (TGN) and transported to other organelles or the plasma membrane depending on the type of sorting signal the proteins carry (Alberts et al., 2002). Proteins without a specific sorting signal are secreted to the apoplast.

The mechanisms for polysaccharide secretion are largely unknown. Hemicellulose and pectin are non-cellulosic polysaccharide components of the cell wall, which are synthesized in the Golgi and secreted via vesicles to the apoplast in growing cells or the cell plate in dividing cells (Driouich et al., 2012). Most of the evidence supporting this hypothesis comes from the study of immuno-electron microscopy; when using anti-xyloglucan antibody (for hemicellulose) or anti-polygalacturonic acid or anti-RGI (for pectin), Golgi stacks and vesicles were labeled (Moore et al., 1991; Zhang and Staehelin, 1992; Young et al., 2008; Kang et al., 2011). Also, the secretion

of hemicellulose and pectin was disrupted by BFA, an inhibitor of ER-Golgi trafficking (Driouich et al., 1993; Satiat-Jeunemaitre and Hawes, 1993), inferring that they are secreted via a Golgi-mediated secretion pathway.

No matter which pathway(s) non-cellulosic polysaccharides use, the pathway(s) must be under tight environmental and developmental regulation. Pectin deposition in the root was investigated by feeding Arabidopsis with alkynyl fucose. The fucose was incorporated into RG-I side chains, while the alkenes were covalently linked to fluorophores by click chemistry. The deposition patterns observed for RG-I differ in different parts of the roots. The dividing and elongating cells exhibited a diffuse pattern in the cell wall. Fucose in cells of the early differentiation zone was found in the cell wall in large globular bodies while fucose in cells of the late differentiation zone was found in fibrillar structures (Anderson et al., 2012).

1.3 Mechanisms of vesicular trafficking in the endomembrane system

To maintain proper functioning of the cell, proteins, polysaccharides, and cargo must be directed to the proper location. As mentioned above, proteins and polysaccharides are sorted in the TGN and transported by vesicle to different organelles or the plasma membrane/extracellular space. Proteins can also be retained in the ER or Golgi before they reach the TGN or recycled back from the plasma membrane after secretion. Because of the complexity of the endomembrane system, a precisely regulated trafficking mechanism is required.

Our knowledge about mechanisms of vesicular trafficking comes mainly from the studies in animal and yeast species and focuses on proteins as a cargo (Alberts et al., 2002). Successful protein trafficking involves packing a specific cargo into a vesicle and targeting the vesicle to the correct membrane. Soluble proteins carry a sorting signal, which can be recognized by the proper receptor, which, in turn, is bound by an adaptor complex that stimulates specific coat protein

assembly. Coat proteins curve the membrane and thus allows vesicle budding. Different coat proteins are found in the vesicles in different intracellular trafficking routes. COPI and COPII are found in Golgi-to-ER and ER-to-Golgi vesicles, respectively. COPI is also involved in intra-Golgi transport (Paul and Frigerio, 2007). Clathrin coats are found on endocytosed vesicles budding from the plasma membrane. Clathrin is also on the vesicles targeted to the plasma membrane in animals but not in plants; the vesicles in plants are coatless. Clathrin coats assemble at the trans-Golgi network in plants, though. It has been suggested that they are involved in protein transportation to the vacuole (Robinson and Pimpl, 2014). The sorting signals are often short domains of a polypeptide, but also can be glycans or lipids attached to proteins in animals (Stoops and Caplan, 2014). Traditionally, coat protein was thought to dissociate after vesicle budding. However, some data suggest that coat protein remains on the vesicles during trafficking and contributes to targeting specificity by interacting with the tethering complex on the acceptor membrane (Cai et al., 2007; Angers and Merz, 2011). The vesicles are moved by motor proteins along the cytoskeleton cableway, which can be either actin or microtubules, to the destined membrane, although the involvement of microtubules in vesicle trafficking has not yet been observed in plants. When vesicles reach the destination, the tethering components on the vesicle interact with the tethering components on the target membrane to form a tethering complex that helps vesicles dock. Finally, the *v*-SNARE or R-SNARE (Soluble N-ethylmaleimide-sensitive factor activating protein receptor) protein on the vesicle interacts with *t*-SNAREs consisting of Qa-, Qb- and Qc-SNARE or Qa- and Qb,*c*-SNARE on the target membrane to promote vesicle fusion and cargo release (Lipka et al., 2007).

Vesicular trafficking is regulated by a family of small GTPases, the RAB GTPases. RABs have been shown to be involved in vesicle uncoating, mobility, and fusion (reviewed by Stenmark, 2009). They regulate these processes by interacting directly or indirectly with

trafficking components, including motor proteins, tethering factors and SNAREs (Stenmark, 2009). RAB GTPases are switched on and off by conversion between a GTP- and GDP-bound form. The inactive RAB GDP protein is present in the cytosol and associates with GDP-displacement inhibitor (GDI). The recruitment of RAB to the membrane, where it can function, requires replacing the GDP with GTP using guanine nucleotide exchange factor (GEF). GDI disassociates from active RAB GTP and thus the C20 prenyl group of RAB is unmasked for membrane attachment. In contrast, GTPase-activating protein (GAP) promotes RAB GTPase to hydrolyze GTP and switch back to a GDP-bound form. The inactive RAB is taken away from the membrane by GDI (Saito and Ueda, 2009). The coordination of GEF and GAP determines the spatiotemporal activation of RAB and thus allows proper vesicular trafficking (Rehman and Sansebastiano, 2014).

The correct targeting of vesicles requires the correct combination of trafficking components. Different kinds of RABs, tethering complexes, and SNAREs are found in different organelle membranes (Cai et al., 2007; Saito and Ueda, 2009). The subunit of tethering complex on the vesicle only forms a complex with subunits on the acceptor membrane. Recruitment of the tethering complex requires the correct RABs in the active state for a particular membrane. Similarly, different *v*-SNAREs interact with specific *t*-SNAREs on the acceptor membrane. For example, in Arabidopsis, Vesicle-associated membrane protein VAMP721/722, specific vesicle localized *v*-SNAREs, form a complex with Syntaxin of plant 121 (SYP121) and soluble N-ethylmaleimide-sensitive factor adaptor protein 33 (SNAP33), *t*-SNAREs on the plasma membrane (Kwon et al., 2008). VAMP727 on vesicles from Multivesicular bodies (MVB) forms a complex with SYP22, VTI11 (Vesicle transport *v*-SNARE 11) and SYP51 on the vacuole membrane (Ebine et al., 2008). However, the combination of SNARE complex may change according to the specific developmental stage or environmental situation. For example,

VAMP721/722 form two different complexes by interacting either with KNOLLE (also known as SYP111) and SNAP33 or with KNOLLE, NPSN11 (Novel plant SNARE 11), and SYP71 during cytokinesis (Kasmi et al., 2013). VAMP727 forms complex with SYP121 on the plasma membrane under salt stress (Ebine et al., 2008, 2011). The specificity and flexibility of SNARE complexes may allow precise regulation of vesicular trafficking in response to different conditions.

The mechanism of vesicular tracking is conserved among different diverse eukaryotic organisms. However, the number of genes encoding trafficking components varies greatly. Typically, multicellular organisms have more such genes than single celled eukaryotes. For example, there are 11 RABs in yeast, while there are 60 RABs in a human and 57 in Arabidopsis. Similarly, for the SNARE family there are 24 in yeast in comparison with 38 in a human and 63 in Arabidopsis. This expansion of trafficking genes may reflect the complexity of vesicular trafficking in multicellular organisms, because multiple pathways may exist for each organelle and each pathway may be subject to different regulation (Saito and Ueda, 2009).

Although the vesicular trafficking is conserved, each eukaryotic lineage may acquire a lineage-specific sub-group of trafficking components. For example, there is a large family of RABA/RAB11 proteins in Arabidopsis, encoded by 26 genes in comparison to 3 and 2 genes in humans and yeast, respectively (Ueda et al., 2012). A large family of VAMP7 R-SNARE proteins (12 genes) and exocyst tether complex subunit EXO70 proteins (23 genes) are present in Arabidopsis (Fujimoto and Ueda, 2012). In addition, some members of the trafficking components acquire unique structural characteristics. For example, although VAMP727 is highly similar to other VAMP72 members, it has an insertion of many acidic amino acids in the login domain (Fujimoto and Ueda, 2012). VAMP727 is involved in trafficking from the MVB to the vacuole and the plasma membrane. The trafficking pathway from MVB to the plasma membrane

is regulated by a plant-unique RAB5 GTPase, ARA6, while the one to the vacuole is regulated by conventional RAB5, ARA7. Plants may have acquired the novel trafficking pathway from MVB to the plasma membrane through the evolution of unique trafficking components (Fujimoto and Ueda, 2012). Such expansion of certain groups and acquisition of unique members are observed throughout the land plant lineages, suggesting that these events may be required for plant lineage-specific diversification of trafficking events (Fujimoto and Ueda, 2012).

Functional analysis revealed that some trafficking components share the same function as their homologous counterparts in yeast and animals, while others evolved new functions to match the requirement in plants. For example, RAB11 in yeast and animals is involved in a post-Golgi pathway. The RAB11 counterparts in plants, the RABA proteins, are localized in the TGN, indicating they also function in post-Golgi pathways. On the other hand, some members acquire new roles in order to accomplish unique post-Golgi trafficking in plants. For example, RABA2 and RABA3 are required for TGN-derived vesicle trafficking to the cell plate to deliver plasma membrane and cell wall materials, a plant lineage-specific cytokinesis process (Seguí-Simarro et al., 2004; Chow et al., 2008).

1.4 Mechanism of post-Golgi trafficking to the plasma membrane/apoplast

The plant TGN mediates several post-Golgi pathways, including trafficking to vacuoles, plasma membrane/apoplast, or cell plate during cytokinesis. The plant TGN also functions as an early endosome, which receives the endocytosed proteins from the plasma membrane and then either recycles them back to the plasma membrane or delivers them to the vacuole for degradation (Park and Jürgens, 2012). The post-Golgi pathway to the plasma membrane/apoplast

will be emphasized here because secretion of cell wall components is the focus of my research project.

The default pathway or bulk flow is the dominant model for protein secretion in plants; proteins without a sorting signal are directly secreted to the apoplast. This model started from the observation that cytosolic proteins were secreted to the apoplast when they were fused with a signal peptide. Also, vacuolar proteins were found to be secreted to the apoplast when a vacuolar sorting signal was not present in the polypeptide (Vitale and Denecke, 1999). In addition, coat-like structures that are required for cargo sorting and vesicle budding in yeast and animals are rarely observed on plant secretory vesicles (Staehelin and Moore, 1995; Toyooka et al., 2009). Hence, it remains unclear how a vesicle is budded and how cargo is sorted in plants.

RABA4b is a RAB GTPase located in the TGN and preferentially labels the secretory vesicle-forming region in Arabidopsis (Kang et al., 2011). RABA4b is found to be involved in tip growth of root hairs (Preuss et al., 2004). RABA4b may be involved in vesicle budding by interacting with its effector, phosphatidylinositol 4-kinase β1 (PI4Kβ1). PI4Kβ1 is also localized in the secretory vesicle-budding subdomain of the TGN (Kang et al., 2011). When *PI4Kβ1* and its orthologue *PI4Kβ2* are both mutated, root hair growth is defective, vesicle budding is reduced, and the vesicles are larger and more variable in size (Preuss et al., 2006; Kang et al., 2011). PI4K is a kinase that can phosphorylate the fourth OH- group in the inositol ring of phosphatidylinositol (PI) to generate phosphatidylinositol 4-phosphate (PI4P). PI4P can be further phosphorylated, by phosphatidylinositol 4-phosphate 5-kinase (PI4P5K), at the fifth position to generate phosphatidylinositol 4,5-biphosphate PI $(4,5)P_2$. It has been found that PI4P5K3 is required for tip growth of root hairs (Stenzel et al., 2008). It is unclear if PI4P is directly involved in vesicle formation or indirectly by reducing production of PI$(4,5)P_2$. Some models have been proposed to explain how phosphoinositide is involved in vesicle budding.

Phosphoinositide has been shown to recruit different effectors, including many trafficking components (Delage et al., 2013). For example, sorting nexin (SNX) is a phosphoinositide-interaction protein that is suggested to induce membrane deformation during endocytosis in animals (van Weering et al., 2010). It is possible that PI4P or $PI(4,5)P_2$ may recruit similar proteins to stimulate membrane curvature. The other possibility is to change the lipid structure. $PI(4,5)P_2$ can recruit and activate phospholipase D (PLD). PLD converts cylindrically-shaped phosphatidylcholine (PC) into conically-shaped phosphatidic acid (PA) and thus curves the membrane. PA can be further converted to conically shaped diacylglycerol (DAG) (Delage et al., 2013; Gendre et al., 2015). DAG is also produced from cylindrically-shaped PI4P by phosphoinositide phospholipase C (PI-PLC). It is hypothesized that the structural difference between DAG- and PI4P-enriched areas leads to vesicle fission (Bard and Malhotra, 2006). In plants, PLD is activated by both PI4P and $PI(4,5)P_2$ and is able to stimulate secretory vesicle budding (Chen et al., 1997; Delage et al., 2013).

The default pathway model for secretion implies that proteins diffuse passively into vesicles because of the absence of a sorting signal, while the active selection model suggests that secretory proteins have export signals and the presence of cargo will induce vesicle formation (Vitale and Denecke, 1999). At least some of the secretion in animals is known to be mediated by sorting signals, such as exocytosis to apical or basolateral domains of epithelial cells. So far, no similar signals have been found in plants (Rodriguez-Boulan and Müsch, 2005). However, some proteins, such as auxin efflux carrier PINFORM2 (PIN2), have been shown to be secreted to the plasma membrane through pathways different from secretory GFP (secGFP), a marker used for the default pathway (Batoko et al., 2000). For example, the secretion of PIN2 was not affected when a SNARE protein SYP121 was disrupted (De Caroli et al., 2011; Hachez et al., 2014). In contrast, secretion of secGFP, plasma membrane intrinsic protein 1;4 (PIP1;4), PIP2;1,

PIP2;7 and brassinosteroid insensitive-1 (BRI1) is mediated by SYP121 (Hachez et al., 2014). Since there are different secretion routes in plants, it is hard to explain how cargos are able to be sorted into correct vesicles merely by passive diffusion. The secretion in plants is more than default; there must be mechanisms to recognize different secretory cargos.

Because sorting signals and coat proteins in secretory vesicles have not been identified in plants, plants may have other mechanism to sort cargo. In animals, cargos are segregated into different domains of the TGN according to their sorting signal, glycosylation, and interaction with proteins and lipids (Gu et al., 2001). The plant TGN also contains different domains, which can be labeled by different trafficking components (reviewed by Gendre et al., 2015). The domain labeled by RABA1b, RABA2a and VAMP721 is distinguishable from the domain labeled by V-ATPase subunit 1 (VHA-a1) and SYP61, suggesting the plant TGN has at least two domains. These two domains may carry out different functions. RABA1b and RABA2a but not VHA-a1 and SYP61 are localized at the cell plate during cell division. In contrast, VHA-a1 and SYP61 are involved in endocytosis and trafficking to the plasma membrane and the vacuole. What's more, a domain may contain many subdomains. For example, the VHA-a1-labeled domain largely overlaps with domains labeled by SYP41, SYP61 and ECHINDA (ECH) (Dettmer et al., 2006; Gendre et al., 2011). When plants are treated with endosidin 1 (ES1), a drug affecting the subdomain defined by VHA-a1 and SYP61 but not SYP41, the endocytosis of PIN2, auxin transporter protein 1 (AUX1), and BRI1 but not PIN1 and PIN7 is affected (Robert et al., 2008). On the other hand, the secretion of AUX1 is defective in the *ech* mutant, but its secretion is not affected when VHA-a1 is inhibited by Concanamycin A (Boutté et al., 2013). Some cargos show physical interaction with the trafficking components. For example, PIP2;7 interacts with SYP61 and its secretion to the plasma membrane is defective when *SYP61* is mutated (Hachez et al., 2014). It is possible that the interaction between cargo and the TGN-

localized trafficking components allows cargo to segregate into different domains and be sorted into different pathways, but the evidence remains elusive.

Cell wall polysaccharides, hemicellulose and pectin, are considered to be secreted via a default pathway because, to date no sorting signals for polysaccharide secretion have been identified (Driouich et al., 2012). Several trafficking components have been identified to be involved in polysaccharide secretion. It has been found that RABA4b labeled budding vesicles with cell wall polysaccharides inside, suggesting RAB4Ab is involved in forming polysaccharides-containing vesicles (Kang et al., 2011). On the other hand, the conserved YPT/RAB interacting proteins YIP4a and YIP4b, whose homologue in animals is involved in regulating RAB activity, are localized in the TGN and affect cell wall polysaccharide secretion. Pectin and hemicellulose are mis-sorted to the vacuole in the *yip4a/4b* double mutant (Gendre et al., 2013). In addition, YIP4a/YIP4b can form a complex with ECH, a TGN-localized protein required for proper function and structure of the TGN (Gendre et al., 2011, 2013). Cell wall polysaccharides are also mis-targeted to the vacuole in *ech* mutants (Gendre et al., 2013; McFarlane et al., 2013). These data suggest that YIP4a/YIP4b/ECH complex is involved in directing polysaccharides to the correct location, but it remains unknown if it is required for cargo sorting or vesicle targeting.

A key question concerns whether polysaccharides are secreted by the same mechanism as proteins. Some data suggest that polysaccharides and cell wall proteins may be secreted through the same pathway. Co-immunolabeling experiments showed that vesicles could carry mixed types of polysaccharides (Sherrier and VandenBosch, 1994) or both polysaccharides and glycoproteins (Driouich et al., 1994). In addition, both pectin and secGFP are secreted in vesicles marked with secretory carrier membrane protein 2 (SCAMP2) (Toyooka et al., 2009). Also, the secretion of both secGFP and pectin is disrupted when *ECH* is mutated (Gendre et al., 2011,

2013; McFarlane et al., 2013). In contrast, some data appears to contradict the idea that carbohydrate and protein are found in the same vesicles. ECH appears to be involved in more than one secretory pathway because pectin secretion and secretion of some proteins, such as ABC transporter G family member 11 (ABCG11) and PIP2, are differentially affected (McFarlane et al., 2013). Also, when the function of SYP121 is disrupted in tobacco, the secretion of secGFP, but not non-cellulosic polysaccharide, is interrupted, suggesting that they are secreted through different pathways (Leucci et al., 2007). Taken together, cell wall polysaccharides seem to share some secretory components with proteins, but the available data can't rule out the possibility that the two cargos have distinct secretory pathways.

In plants, there exists a number of mechanisms for cargo delivery to the apoplast. Some proteins, such as tobacco pectin methylesterase NtPPME 1, are directly secreted from the Golgi without passing through the TGN (Wang et al., 2016). In addition, some proteins can even be delivered to the apoplast by unconventional Golgi-bypass pathways (Ding et al., 2012; Drakakaki and Dandekar, 2013). In plants, MVBs have been observed to fuse with the plasma membrane and release the intraluminal vesicles when pathogens attack, although the cargos inside remain to be characterized (Ding et al., 2012). In addition, a novel double membrane organelle EXPO (exocyst positive organelle) identified by EXO70E2, may mediate unconventional secretion in plants (Wang et al., 2010). EXPOs fuse with the plasma membrane and release the single membrane vesicles to the apoplast, and they are not affected by BFA treatment, which interrupts the conventional ER-Golgi secretory pathway. So far, the only cargo identified in EXPO is S-adenosylmethionine synthetase (SAMS2), which is involved in lignin methylation in the cell wall (Wang et al., 2010). It is still unclear how these unconventional pathways contribute to overall secretion and the secretion of cell wall components.

1.5   Cell polarity and polar distribution in plants

To accomplish different functions and cooperate with the neighboring cells, plant cells are able to deliver cargo to specific domains of a cell. This requires plant cells to establish cell polarity. In yeast and animals, Rho GTPases are involved in cell polarity establishment (reviewed by Nelson, 2003). Rho GTPases are recruited to specific domains in response to external or internal cues and then amplify the signals for cell polarity establishment through positive feedback. Afterward, they promote polar trafficking to the specific domain by recruitment of downstream effectors such as proteins involved in cytoskeleton reorganization. In plants, the best-known case of cell polarity establishment is that of tip growth in pollen tubes and root hairs (Kost, 2008). During the elongation of pollen tubes and roots hairs, large amounts of material for building plasma membrane and cell wall are required to be delivered to the tip region. Indeed, electron microscope data show that large numbers of vesicles can be observed in the apical region of these tip-growing cells, indicating secretion is targeted to the tip region (Derksen et al., 1995; Galway et al., 1997). These vesicles are known to carry cell wall material (Lancelle and Hepler, 1992; Bove et al., 2008). How such plant cells can establish polarity and secrete cargo to specific domains of the cell is of interest.

Rho of plants (ROPs), are master regulators of cell polarity in both pollen tubes and root hairs. ROPs also switch between a GTP-bound active form and a GDP-bound inactive form like the RAB GTPases. Active ROPs, localized in the apex of the cell tip, are thought to regulate tip growth by coordinating vesicular trafficking and actin reorganization. RIC (ROP-interactive CRIB motif-containing protein) is one class of ROP effector that is involved in cytoskeleton dynamics. ROP1 is involved in tip growth of pollen tubes, and RIC4 and RIC3 are two downstream effectors of ROP1 that are involved in actin dynamics in opposing ways; RIC4 promotes F-actin assembly, while RIC3 stimulates F-actin disassembly (Gu et al., 2005) (Figure 1.1A). RIC4-dependent actin assembly doesn't require actin-related protein 2/3 (ARP2/3)

complex, suggesting that other nucleation mechanisms may be involved (Fu et al., 2005). In contrast, RIC3 promotes Ca^{2+} accumulation in the cytosol. The high level of cytosolic Ca^{2+} stimulates actin disassembly. Actin assembly is required for vesicle delivery to the apex of the pollen tube, while actin disassembly is important for vesicle docking/fusion (Lee et al., 2008). The RIC3-mediated actin disassembly is found to lag behind RIC4-mediated actin assembly. This temporal control may allow the two opposing pathways to function coordinately. However, it is still unknown how RIC3- and RIC4-mediated pathways are able to be controlled by Ca^{2+} alone.

ROP2 is involved in tip growth of root hairs (Jones et al., 2002). Actin assembly and turnover, triggered by an increase in Ca^{2+} concentration, are also important for proper growth of root hairs (Ringli et al., 2002; Pei et al., 2012). The arrangement of actin is altered in the root hairs of constitutively active and dominant negative ROP2 transgenic plants. ROP2 can interact with RHD2 NADPH oxidase that produces ROS. The ROS burst then activates influx of Ca^{2+} (Jones et al., 2007). The Ca^{2+} in turn activates RHD2 forming a positive feedback loop (Takeda et al., 2008). This ROS/Ca^{2+} loop can also be observed in pollen tubes (Potocký et al., 2007). However, the direct effectors of ROP2 in actin dynamics in the root hairs have not been identified yet (Figure 1.1B).

In addition to tip growth, ROPs are also involved in other kinds of polarized growth. For example, ROP2 and ROP6 are involved in the morphogenesis of the jigsaw-puzzle pattern in pavement cell of leaf epidermis. The lobe and indentation of the pavement cell require coordination of neighboring cells. ROP2 is involved in lobe formation, while ROP6 is involved in indentation formation (Fu et al., 2005). ROP2 can interact with RIC4 and promote actin assembly. Besides RIC4, ROP2 can interact with interactor of constitutive active ROP1 (ICR1)/ROP-interacting partner (RIP1). ICR/RIPs are plant-unique effectors of ROPs. ICR1/RIP1 acts

as a scaffold protein to link ROP2 to SEC3, a subunit of the exocyst tethering complex, and thus allow vesicle docking in the lobe region. ROP6 activates RIC1 to promote cortical microtubule organization that restricts cell expansion in the region of indenting (Fu et al., 2005). The ROP2-RIC4 pathway acts antagonistically with the ROP6-RIC1 pathway, allowing the zigzag pattern of pavement cells (Figure1.1C).

Like RAB GTPases, the local activation of ROPs is achieved by the cooperation of GAPs, GEFs, and GDIs and thus allows the spatial regulation of ROPs in different domains of the cells. ROPs can be activated by GEFs. Plants contain only a single conventional type of GEF, SPIKE1 (SPK1). The morphogenesis of pavement cell is defective in the *spk1* mutant; the pattern is similar to what has been observed when ROP2 is downregulated, suggesting SPK1 can activate ROP2 (Qiu et al., 2002). On the other hand, tip growth of pollen tubes and root hairs is not affected, implying that other types of GEF may exist. Indeed, plants have a plant-specific GEF family, RopGEF. Members of this family contain a conserved PRONE (plant-specific Rop nucleotide exchanger) domain (Nagawa et al., 2010). The N- and C-termini of RopGEF bind to the PRONE domain inhibiting the ability of RopGEF to activate ROP (Gu et al., 2006). RopGEF1 and RopGEF12 may be involved in activation of ROP1 in pollen tubes (Figure1.1A), because overexpression of RopGEF1 and RopGEF12 causes depolarization of pollen tubes, which has also been observed when ROP1 is overexpressed. Also, the uninhibited RopGEF1 and RopGEF12 are localized at the apex of the pollen tubes where active ROP1 accumulates (Gu et al., 2006; Zhang and McCormick, 2007).

Active ROPs can be deactivated by GAPs. Plants contain two types of GAPs, RopGAP and REN. RopGAPs have a conserved GAP-like domain and a CRIB motif that can promote the binding to active ROP and the hydrolyzation of ROP GTP. RENs have a GAP domain, a PH domain at the N-terminus, and two coiled-coil domains at the C-terminus (Nagawa et al., 2010).

In tobacco pollen tubes, overexpression of NtRhoGAP1 causes narrow tubes (Klahre et al., 2006). NtRhoGAP1 is localized at the flanking region of the pollen tubes. This suggests that RhoGAPs restricts ROPs activity (Klahre et al., 2006). However, REN1 is thought to negatively regulate ROP1 in Arabidopsis pollen tubes globally, because it is localized at the apex where ROP1 is activated. The location of REN1 to the apex is found to oscillate between the activation and deactivation of ROP1 (Hwang et al., 2008). In addition, ROPs are also regulated by GDI. ROP2 is localized at the apex of root hairs in wildtype plants, while in the *scn1/gdi1* mutant, ROP2 is mis-localized and numerous root hairs are initiated (Carol et al., 2005). Taken together, in tip-growing cells, GEFs co-localize at the cell apex with active ROPs, while GAPs are present in the flanking region of the apex. GEFs activate ROPs at the place where they should function, while GAPs and GDIs are required for local restriction of ROPs (Kost, 2008).

The fact that GEF, GAP or any other upstream regulators are distributed in a polar manner begs the question what influences their distribution? Polarity requires stimulation by asymmetric external or internal cues. Some receptors, that receive such cues and then generate downstream signaling to establish cell polarity, have been identified. In tomato pollen tubes, two pollen-specific receptor-like kinases, LePRK1 and LePRK2 have been identified (Muschietti et al., 1998). Both of them are localized at the surface of pollen tubes. These two receptor-like kinases interact with each other, suggesting they may work together (Wengier et al., 2003). It has been found that LePRK2 interacts with a pollen-specific RopGEF and downregulation of LePRK2 causes a defect in pollen tube growth (Kaothien et al., 2005; Zhang et al., 2008). Similarly, it has been found that a receptor-like kinase PRK2a phosphorylates the C-terminal regions of RopGEF1 and RopGEF12. The phosphorylation releases the kinases from self-inhibition, so that they can activate ROP1 in Arabidopsis pollen tubes (Chang et al., 2013). PRK2a can also directly interact with ROP1 and activate it. In addition, the constitutively active form of

RopGEF1 rescues the pollen germination defect caused by a dominant negative PRK2 (Chang et al., 2013). Taken together, these data suggest that PRK2a may function as the upstream receptor to receive external cues and turn the downstream ROP1 signaling either by direct interaction or through RopGEF1 and RopGEF12 or both (Figure1.1A). The next question is what are the cues that stimulate PRK activity for establishing cell polarity. LeSTIG1 is a small cysteine-rich protein from the pistils of tomato. This protein can bind to the external domains of LePRK1 and LePRK2. Also, the growth of pollen tubes is promoted when exogenous LeSTIG1 is applied. This suggests that LeSTIG1 may be the cue that stimulates pollen tube growth (Huang et al., 2014).

Auxin, an important hormone for plant morphogenesis, may act as a polarity signal. For example, the pavement cells of a leaf have fewer lobes when auxin biosynthesis is defective. Also, the application of exogenous auxin can rapidly activate ROP2 and ROP6 (Xu et al., 2010). The auxin activation requires the receptor-like kinases transmembrane kinase 1-4 (TMK1-4). TMK1 physically interacts with the putative auxin receptor auxin binding protein 1 (ABP1). Pavement-cell-lobing defects can be observed in the quadruple mutant *tmk1/2/3/4* and exogenous application of auxin doesn't rescue the mutant phenotype. Active ROP2 and ROP6 also decreases in the quadruple mutant when treated with auxin. Consistently, the amount of RIC4 localized in the plasma membrane and RIC1 interacting with microtubules decreases in the mutant (Xu et al., 2014). These data suggest that auxin is an external cue for the polarized growth of pavement cells through ABP1-TMK-ROP2/ROP6 signaling pathways (Figure1.1C).

ROP can increase the concentration of auxin by positive feedback. Auxin concentration gradients are often required for auxin to function properly. The polar distribution of auxins is achieved by the polar localization of auxin efflux carrier proteins, PINFORMs (PINs). Polar distribution of PINs is achieved by polar endocytosis and constitutive recycling. The endocytosis

is inhibited by auxins, so the presence of auxins can promote the accumulation of PINs and thus their own transportation. Auxins can activate ROPs (Tao et al., 2002), while the ROPs can inhibit the endocytosis of PINs and promote the recycling of endocytic PINs. For example, ROP2 inhibits PIN1 endocytosis in the lobe regions of the pavement cells through RIC4-dependent actin accumulation (Figure1.1C) (Nagawa et al., 2012). Auxins may function as positive regulators of ROPs in these tip-growing cells. The auxin gradient induces ROP accumulation at the base of trichoblasts to mark the position of root hair initiation (Fischer et al., 2006). However, a detailed mechanism remains to be determined.
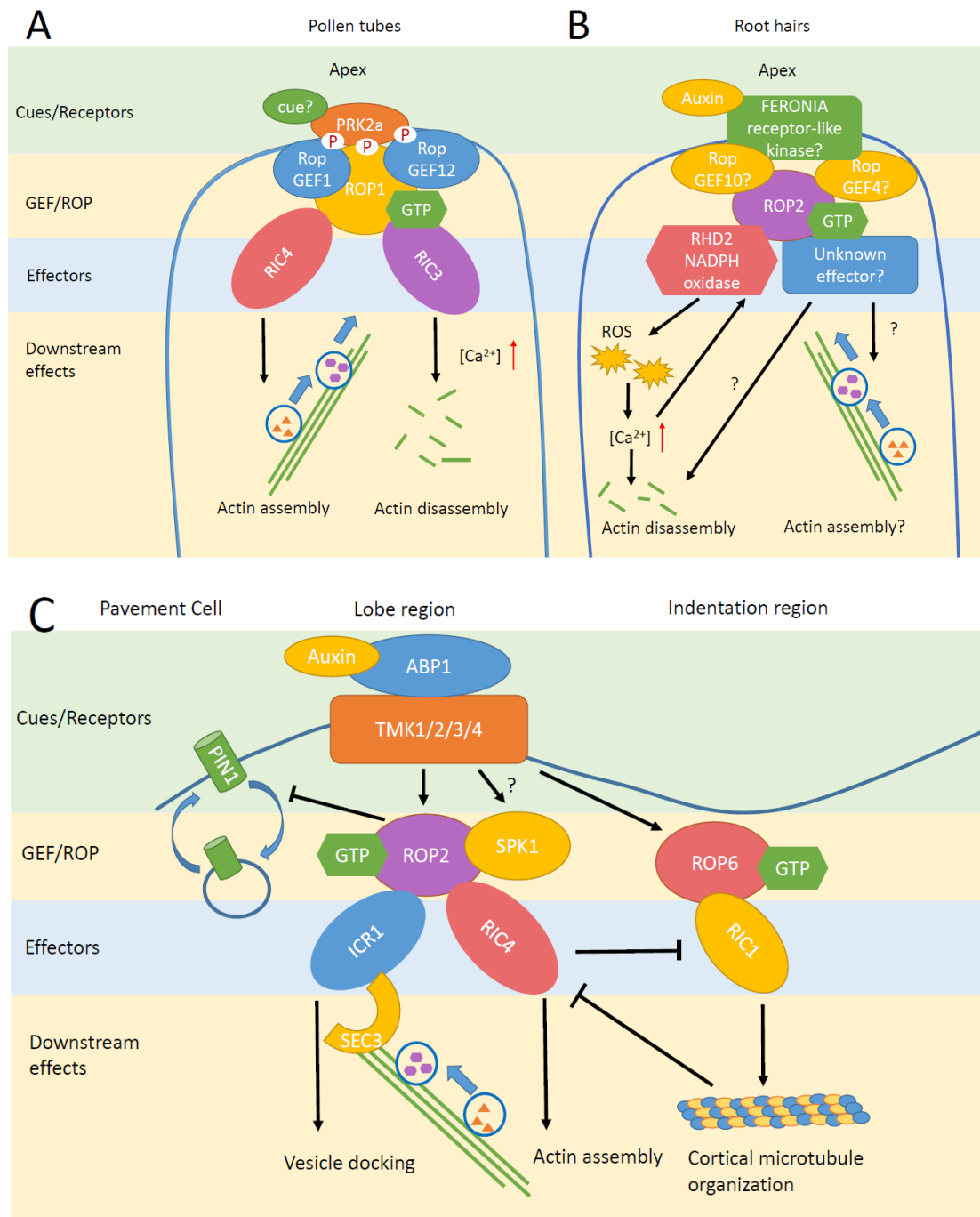
Figure 1.1: A diagram illustrating proposed mechanisms of cell polarity establishment in pollen tubes (A), root hairs (B), and pavement cells (C)

ABP1: auxin binding protein 1; GEF: guanine nucleotide exchange factor; ICR1: interactor of constitutive active ROP 1; PIN1: PINFORM 1; PRK2a: pollen receptor-like kinase 2a; ROP: Rho of Plants; RIC: ROP-interactive CRIB motif-containing protein; TMK: transmembrane kinase.

The polarized cells described above only account for a small number of the cell types in plants. The majority of plant cells appear symmetrical, but even such morphologically nonpolar cells still need to deliver cargo to different domains of the cells following cessation of elongation. In polarized cells, the direction of cargo movement can be different from that of cell growth. It has been found that many plasma membrane proteins are localized in different domains of cells. The members of the PIN family show a variety of distribution patterns depending on tissue type. For example, PIN1, PIN2, and PIN7 can be localized either in the apical domain or the basal domain. PIN3 is distributed in the lateral domain or evenly distributed around the cell. Some plasma membrane proteins not belonging to the PIN family also show a polar distribution pattern (Dettmer and Friml, 2011). For example, NOD26-like intrinsic protein 5;1 (NIP5;1), a boron transport protein, is localized in the outer lateral domain of the root epidermal cell (Takano et al., 2010; Wang et al., 2017). In contrast, boron transporter 1 (BOR1) is localized in the inner lateral domain of many tissues in the root (Takano et al., 2002).

To date, the best studied polarized membrane proteins are PIN1 and PIN2. PIN proteins were found to be secreted in a nonpolar manner and then become polar through endocytotic recycling (Kleine-Vehn et al., 2008; Kleine-Vehn et al., 2011), although a recent study has suggested that they may be secreted in a polar manner (Łangowski et al., 2016). Similarly, the polarity of lateral-distributed proteins such as BOR4 and ABCG36 is established by polar secretion or endocytotic recycling (Łangowski et al., 2010; Mao et al., 2016). Thus, it appears that it is hard to distinguish between mechanisms that depend on targeted secretion from ones that depend on recycling.

Different trafficking mechanisms are involved in establishing the polarity of basal- and apical-localized PINs. GNOM and its homolog GNOM-LIKE 1 (GNL1) are endosome-localized GEF of ARF (another class of small GTPase) involved in the basal localization of PIN1 (Geldner et

al., 2003; Naramoto et al., 2010), but not the apical localization of PIN2 and AUX1 (Fischer et al., 2006; Klahre et al., 2006; Doyle et al., 2015). On the other hand, a drug, Endosidin 16 (ES16), affects apical-localized PIN2 in root epidermal cells but not basal-localized PIN1 in the same cells or PIN3 and PIN7 in root stele cells (Li et al., 2017). This drug also affects the distribution of lateral-distributed BOR1 and NIP5;1 and nonpolar PIP2a. Thus, ES16 only inhibits the trafficking components involved in non-basal targeting. It has been suggested that RABA2a may be the target of ES16, but the mechanism of how RABA2a is involved in trafficking of apical, lateral, and nonpolar proteins remain to be resolved (Li et al., 2017).

Proteins are able to be distributed in a polar manner in diffusively growing cells, indicating that the distribution of proteins can be uncoupled with the direction of the expansion of growing cells. ROP proteins may also be important for the polar distribution of protein in less polarized cells. PIN proteins maintain polarity by endocytosis (Kitakura et al., 2011). It has been found that ROP6 inhibits the endocytosis of PIN2 in root epidermal cells because PIN2 is internalized into cells when ROP6 or its GEF SPK1 is mutated, although the polarity is unaffected (Lin et al., 2012). A remaining question is whether ROPs are involved in cell polarity establishment and maintenance only in tip-growing cells or also in other less polarized cells.

Cell polarity is reflected not only in the polarized cell shape or polarized protein distribution, but also in the heterogeneity of cell wall properties in different domains of the polarized cell. The best characterized example is the pollen tube cell wall (Geitmann and Steer, 2006; Hepler et al., 2013). The apex region of the pollen tube cell wall is composed mainly of pectin, which is synthesized in a methylesterified form (O'Neill et al., 1990). A gradient of highly esterified pectin at the apex to less esterified pectin in the periphery has been observed (Bosch et al., 2005; Bosch and Hepler, 2005; Geitmann and Parre, 2004; Parre and Geitmann, 2005). As mentioned previously, de-methylesterified HG can dimerize via Ca^{2+} bridges and thus stiffen the cell wall.

The gradient of demethylesterification in the pollen tube suggests that the pollen tube tip is relatively pliable whereas the flanks are mechanically stiff (Geitmann and Parre, 2004; Fayant et al., 2010). PME, an enzyme that removes methyl groups from the HG, and its inhibitor PMEI control the degree of methylation of pectin. In Arabidopsis, a pollen-specific PME, AtPPME1, is distributed throughout the pollen tube, while the inhibitor, AtPMEI1, only appears in the apex therefore preventing the dimerization of pectin via Ca^{2+} bridges at the tip region (Rockel et al., 2008). It has been shown previously that secretion is targeted to the tip region in pollen tube. PMEs and methylesterified pectin are likely secreted in the same vesicles (Li et al., 2002). PMEs are often secreted as pro-proteins that are inactive because the pro-region in the N-terminus acts as an endogenous inhibitor. The pro-regions are cleaved from the full-length PMEs by proteases in the cell wall following secretion (Bosch et al., 2005; Bosch and Hepler, 2005). Therefore, pectin can remain esterified even when secreted with PMEs. It is unknown if PMEIs are also secreted with esterified pectin and PMEs. However, some evidence suggests that PMEIs are retrieved through endocytosis and maybe, in this way, prevented from functioning outside of the pollen tube apex (Röckel et al., 2008). The coordination of secretion, endocytosis, and spatiotemporal regulation of cell wall modifying-enzyme allows cells to have cell wall heterogeneity in different domains of the cells, thus affecting the polarity of cell growth.

Cell walls formed after cessation of cell growth are typically referred to as secondary cell walls. Depending on the cell type, secondary cell walls are not always deposited uniformly. For example, the patterns of secondary cell wall deposition in the xylem of vascular tissues are very diverse; the cell wall can be deposited in an annular, helical, or scalariform pattern. In the most extreme case, xylem cells have secondary cell wall deposited throughout the cell surface except for small regions scattered uniformly over the surface, referred to as pits. ROP11 is found to be located in the pit regions (Oda and Fukuda, 2012). The constitutive activation of ROP11 in

developing metaxylem results in the formation of abnormal secondary cell wall lacking pits, suggesting that the spatial activation of ROP11 is required for proper secondary cell wall patterning (Oda and Fukuda, 2012). Like other ROPs, the distribution of ROP11 is controlled by GEF and GAP. RopGEF11 and RopGAP3 are co-localized in the pit regions (Oda and Fukuda, 2012). In addition, the co-introduction of both RopGEF11 and RopGAP3 into other cell types causes dispersed patterning of ROP11, similar to what has been observed in xylem cells. This data infers that the RopGEF11 and RopGAP11 mediate the local activation of ROP11, but the mechanism remains unknown (Oda and Fukuda, 2012). After ROP11 is activated, it can recruit a RIP/ICR protein, MIDD1, to the pit regions (Oda and Fukuda, 2012). MIDD1 is a plant-specific microtubule-associated protein that can in turn interact with a microtubule-depolymerizer, kinesin-13A (Oda et al., 2010; Oda and Fukuda, 2013). The loss or overexpression of kinesin-13A causes smaller or larger pits respectively. The organization of microtubules is important for the trajectory of cellulose synthase complexes (Paredez et al., 2006; Chan et al., 2010). The ROP11-MIDD1-kinesin-13A signaling pathway may affect the deposition of secondary cell wall, which is mainly composed of cellulose, by affecting cellulose synthesis (Oda, 2015). The pathway may also affect the deposition of non-cellulosic material (Oda, 2015). It has been shown that microtubules are involved in pectin secretion (Zhu et al., 2015). A subunit of the exocyst, EXO70A1, was found to be involved in the deposition of tracheary element secondary cell wall (Li et al., 2013). The cell wall thickness in the *exo70a1* mutant is variable and the pattern of pits irregular. EXO70A and another exocyst subunit SEC3 are located in the target membrane in yeast, and they can interact with other subunits located on the vesicle to promote vesicle docking (He and Guo, 2009). It has been found that EXO7OA1 is recruited to the microtubules (Oda, 2015). ROP11 signaling pathway may control the pattern of secondary cell wall by regulating exocytosis of non-cellulosic material and/or cellulose synthase complexes.

So far, it has been illustrated that cell wall deposition can be regulated in a polar manner. However, the cell wall itself also acts as a mechanism of polar distribution. After cell walls are removed to generate protoplasts, the previously polarized membrane proteins, regardless of the domains of the cells in which they were positioned, become distributed evenly throughout the cell membrane (Feraru et al., 2011; Łangowski et al., 2016). It is known that different membrane proteins have different diffusion rates in the plasma membrane, and the removal of the cell wall can promote their diffusion to varying extents. For this reason, it has been hypothesized that cell walls may help polarized proteins keep their polarity by constraining their ability to move in the membrane (Feraru et al., 2011; Martinière et al., 2012). Certain cell wall components may affect the polarity of certain proteins in a more specific manner. For example, PIN1 is localized to the basal domain of root epidermal cells but shifts to the apical domain when cellulose synthesis is disrupted genetically or chemically (Feraru et al., 2011). Also, interference with cellulose synthesis by genetic or pharmacological manipulation results in an increased mobility of apical-localized PIN2 in the plasma membrane, suggesting cellulose maintains polarity of PIN by reducing lateral diffusion (Feraru et al., 2011). In addition, certain cell types may have a specialized cell wall structure that helps maintain cell polarity. The Casparian Strip may function as a diffusion barrier separating the outer tangential and inner tangential plasma membranes of endodermal cells (Alassimone et al., 2010; Lee et al., 2013; Nakayama et al., 2017), although how it is involved in polar distribution of proteins remains elusive.

There are several plant-specific mechanisms for the establishment of cell polarity (Dettmer and Friml, 2011). First, cortical microtubules, instead of transporting secretory vesicles, influence a variety of polar events in the cell. They guide cellulose synthase complexes and, in this way, affect the orientation of cellulose microfibrils which in turn influences cell shape by limiting the direction of cell expansion. In diffusely growing cells, cortical microtubules may

serve a similar role to delimit the growing area. Cortical microtubules label the position where

the cell plate will form in dividing cells (Žárský et al., 2009). Also, in Arabidopsis seed-coat

cells, microtubules delineate the domain where the mucilage pectin will be secreted and cellulose

is deposited (Young et al., 2008; Griffiths et al., 2015). Second, as mentioned previously, the cell

wall may affect cell polarity. Lateral diffusion of PIN and other proteins is restricted by the cell

wall (Feraru et al., 2011; Martinière et al., 2012). Third, the constitutive recycling of protein may

also be important for maintenance of cell polarity (Žárský et al., 2009; Dettmer and Friml, 2011).

1.6   Seed coat epidermal cell – a model system for cell wall biosynthesis and secretion

Arabidopsis seed coat epidermal cells accumulate a large amount of cell wall materials in a

polar manner, so it is a good model system to ask questions concerning the mechanism of polar

distribution of cell wall components. Seeds of angiosperms contain three structures, embryo,

endosperm, and seed coat. The seed coat of Arabidopsis differentiates from the ovule

integuments after double fertilization of the embryo and endosperm.

Arabidopsis seed coats are composed of five layers, which differentiate from the integument

cells, two layers of cells derived from the outer integument and three layers of cells derived from

the inner integument (Windsor et al., 2000). After fertilization, these five layers undergo cell

division and cell growth for four days. The innermost layer of the inner integument differentiates

into the seed coat endothelium (pigmented layer). Large amounts of proanthocyanidins (PA)

accumulates in the central vacuole of the endothelium. Once released from the vacuole,

molecules of PA condense to form tannin oligomers that gives the seed coat a brown color. The

other two layers of inner integuments undergo programmed cell death without further

differentiation (Windsor et al., 2000; Haughn and Chaudhury, 2005).

The two outer integument cell layers differentiate into epidermal and palisade cells. The

accumulation of amyloplasts is observed in both layers. The layer of palisade cells deposits a secondary cell wall in the inner side of the cell and then undergoes programmed cell death. Meanwhile, the epidermal cells accumulate large amounts of pectinaceous mucilage between the primary cell wall and the membrane on the outer tangential side, forming a ring-shaped mucilage pocket surrounding a volcano-shaped cytoplasmic column (Western et al., 2000; Young et al., 2008). At this stage, the amyloplasts are distributed in the cytoplasmic column (Figure 1.2). After mucilage secretion is finished, the amyloplasts degenerate and a secondary cell wall is deposited along the outer membrane, gradually displacing the cytoplasmic column toward the bottom of the cell. Ultimately the cytoplasm is replaced by a volcano-shaped secondary cell wall called the columella (Figure 1.2) (Western et al., 2000; Young et al., 2008). After seed maturation, when seeds are hydrated, the mucilage expands and extrudes from the cell to form a mucilage halo around the seed. The abundance and easy accessibility of cell wall materials from a single cell type makes the Arabidopsis seed-coat epidermal cells a good model to study cell wall biosynthesis and secretion (Haughn and Chaudhury, 2005; Arsovski et al., 2010).
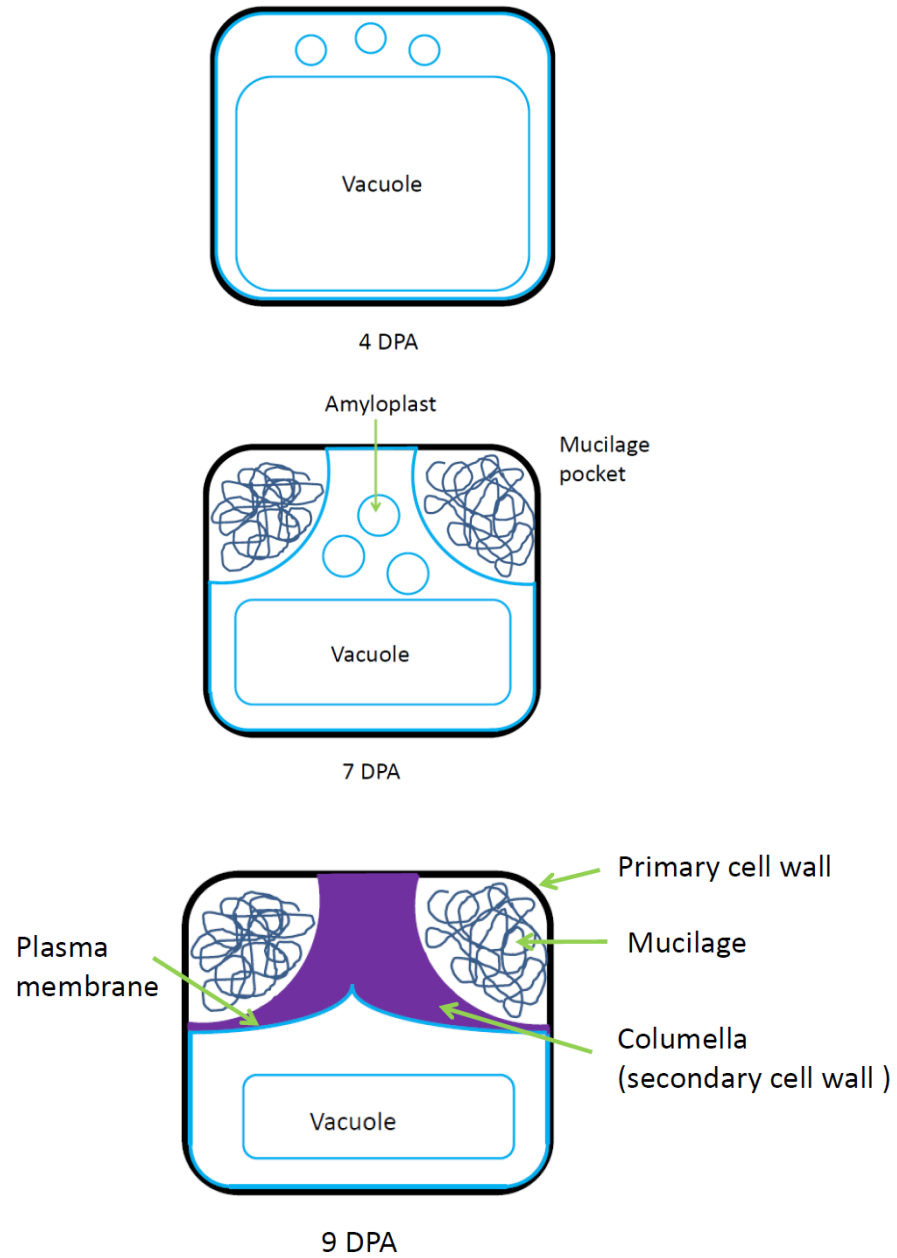
Figure 1.2: The diagram of seed coat epidermal cells at 4 DPA, 7 DPA, and 9 DPA (Day Post Anthesis)

The mucilage halo has two distinct layers, a non-adherent diffusive outer layer that is easily removed by gentle shaking and a dense adherent inner layer which is tightly associated with the seed (Western et al., 2000). The non-adherent layer accounts for 65% of total mucilage, while the adherent layer represents the remaining 35%. The molecular sizes of the polysaccharides are also quite different, with ~600 kD in non-adherent layer and ~ 5000 kD in adherent layer (Macquet et al., 2007a). The composition of mucilage includes all the major carbohydrate classes found in other cell walls, pectin, hemicellulose and cellulose. The non-adherent layer is composed mainly of unbranched RG-I (> 80% - 90% of the sugars) with only small amounts of HG, branched RG-I and arabinoxylan (Willats et al., 2001; Macquet et al., 2007a). The increased density in the adherent layer is explained by an increase of chemical complexity (Haughn and Western, 2012). The inner layer is also mainly composed of unbranched RG-I, but it also contains HG, branched RG-I, galactoglucomannans, xylans and celluloses (Dean et al., 2007; Macquet et al., 2007b; Arsovski et al., 2009; Yu et al., 2014; Voiniciuc et al., 2015a, 2015b, Hu et al., 2016a, 2016b).

Through a combination of genetic manipulation and cytology, the structure of the adherent layer, has been partly determined (Griffiths et al., 2015; Voiniciuc et al., 2015b; Griffiths and North, 2017). A cluster of cellulose microfibrils extends from the top of the columella to the outer edge of the adherent layer forming a linear structure called a ray (Mendu et al., 2011; Sullivan et al., 2011; Griffiths et al., 2014, 2015). The xylan and galactoglucomannans are closely associated with this cellulose ray (Yu et al., 2014; Voiniciuc et al., 2015a, 2015b; Ralet et al., 2016; Hu et al., 2016a, 2016b). The RG-I and HG surround the ray. HG with either low or high degrees of methyl-esterification have distinct distribution patterns in the adherent layer. The JIM5 antibody that recognizes moderately methyl-esterified HG strongly labels the adherent layer. In contrast, JIM7 antibody against highly methyl-esterified HG only labels the outer edge of adherent layer (Macquet et al., 2007a; Griffiths et al., 2014).

In addition to polysaccharides, mucilage also contains small amount of proteins. Proteomic analysis of mature mucilage shows there are many carbohydrate-active enzymes and oxido-reductases that may be involved in modification of the cell wall components. The adherent and non-adherent layer share many cell wall proteins, except that proteins involved in lipid metabolism are only identified in the adherent layer (Tsai et al., 2017).

Several enzymes involved in mucilage polysaccharide biosynthesis and modification have been identified through molecular genetic analyses. Synthesis of the RG-I backbone requires the nucleotide sugars UDP-Rha and UDP-GalA (reviewed by Atmodjo et al., 2013). MUM4/RHM2 is a rhamnose synthase required for synthesizing the UDP-Rha for RG-I synthesis (Usadel et al., 2004; Western et al., 2004; Oka and Jigami, 2006). UDP-GalA is first synthesized as UDP-glucuronic acid (GlcA) in the cytosol, and then UDP-GlcA is converted to UDP-GalA after transport into the Golgi. UUAT1 is the Golgi-localized uronic acid transporter that is required for synthesis of UDP-GalA in seed coats (Saez-Aguayo et al., 2017). The RG-I backbone is composed of alternating Rha and GalU. Galactosyltransferase-like 5 (GALT5) appears to be needed to add at least some of the UDP-Rha and GalA to the RG-I backbone (Kong et al., 2013). The arabinan needed for RGI side chains is synthesized using UDP-arabinose, which, like UDP-GalA, is converted from UDP-GlcA. This suggests that UUAT1 is also required for synthesis of arabinan (Saez-Aguayo et al., 2017). The arabinogalactan side chains of RG-I appear to play an important role in determining mucilage properties. MUCILAGE-MODIFIED 2 (MUM2) discussed in more detail below, is a β-galactosidase that is believed to remove galatan side chains from mucilage RG-I. In *mum2* mutant seed-coat epidermal cells (Dean et al., 2007; Macquet et al., 2007b), the mucilage fails to extrude when seeds are hydrated. Similarly, normal mucilage extrusion is dependent on BXL1, a bifunctional β-D-xylosidase/α-L-arabinofuranosidase that appears to remove arabinose from RG-I side chains (Arsovski et al., 2009). The increase of side

chains may enhance the attachment of RG-I to other cell wall components in the mucilage. It has been found that the partitioning of polysaccharide to the mucilage adherent layer is increased in the *mum2* mutant (Macquet et al., 2007b).

Mucilage also contains some HG. The putative glycosyltransferase GAUT11 has been suggested to be involved in the biosynthesis of HG in the non-adherent layer (Caffall et al., 2009), but stronger evidence is needed to support this hypothesis. As mentioned previously, the degree of methyl-esterification is controlled by PMEs and PMEIs. PME58 and PMEI6 are involved in controlling methyl-esterification of the HG in mucilage which influences both the ability of mucilage to extrude and the overall structure of the adherent and non-adherant layers(Saez-Aguayo et al., 2013; Turbant et al., 2016). It is unknown if PME58 is the target of PMEI6. Proteins in addition to PME and PMEI affect the methyl-esterification of HG in mucilage. One of these, Subtilisin-like protease 1.7 (SBT1.7 or ARA12) is required for normal extrusion and may target HG modifying enzymes (Rautengarten et al., 2008; Saez-Aguayo et al., 2013). In addition to ARA12, FLYING SAUCER 1 (FLY1), a transmembrane RING E3 ligase in a late endosome compartment, is also involved in limiting methyl-esterification of HG and therefore the ability of the mucilage to extrude. FLY1 may control the degradation of methyltransferase or retention of PMEs (Voiniciuc et al., 2013).

The cellulosic rays are synthesized by CESAs, including CESA3, CESA5, CESA10 and possibly CESA1. These CESAs move unidirectionally around the cytoplasmic column parallel to the seed surface. The mucilage cellulose is important for mucilage adherence and to a limited extent, mucilage extrusion (Mendu et al., 2011; Sullivan et al., 2011; Griffiths et al., 2014, 2015).

MUCILAGE-MODIFIED 5/MUCILAGE-RELATED 21 (MUM5/MUCI21); IRREGULAR XYLEM 7 (IRX7) and IRREGULAR XYLEM 14 (IRX14) are putative xylosyltransferases that

are required for synthesis of mucilage xylan and are needed for adherence of mucilage as well as cellulose ray structure (Voiniciuc et al., 2015a; Ralet et al., 2016; Hu et al., 2016a, 2016b). It has been shown that mucilage xylan has a high affinity for cellulose and facilitates RG-I binding to cellulose (Ralet et al., 2016). These data suggest that these enzymes are responsible for synthesis of xylans that may be side chains of RGI and anchor it to the cellulose ray (Voiniciuc et al., 2015a; Ralet et al., 2016; Hu et al., 2016a, 2016b).

In addition to xylans, adherent mucilage also contains another kind of hemicellulose, galactoglucomannan (GGM). GGM is synthesized by CELLULOSE-SYNTHASE-LIKE A2 (CSLA2) and MUCILAGE-RELATED 10 (MUCI10) and is required for maintainance of the ray structure (Yu et al., 2014; Voiniciuc et al., 2015b)). It has been proposed that GGM affects the mucilage polysaccharide spacing (Voiniciuc et al., 2015b).

AGPs, like xylans, affect cellulose structure and mucilage adherence. This pathway involves SALT-OVERLY SENSITIVE 5 (SOS5), an AGP, and FEI2, a receptor-like kinase (Shi et al., 2003; Harpaz-Saad et al., 2011; Griffiths et al., 2014; Steinwand et al., 2014). It is still not clear how SOS5 and FEI2 are involved in cellulose organization and pectin adherence. It has been proposed that SOS5 and FEI2 initiate a signaling cascade that alters cellulose biosynthesis (Steinwand et al., 2014), although this hypothesis has been challenged by evidence showing that the influence of SOS5 on mucilage structure and function is distinct from that of CESA5 (Griffiths et al., 2014).

The production of seed coat mucilage begins abruptly four to five days after fertilization. At this time changes occur in the endomembrane system with the cisternae of the Golgi becoming much wider and an extensive TGN appearing (Young et al., 2008). These changes do not occur in the RG-I deficient *mum4* mutant suggesting that they are a consequence of secretion of matrix polysaccharides. Consistent with this, mucilage RG-I has been detected in the Golgi and vesicles

of seed coat epidermal cells during the period of mucilage synthesis (Young et al., 2008). The deposition of mucilage is polar but as yet the mechanism underlying the polar secretion is unknown. Golgi stacks are randomly distributed all around the cell, instead of clustering at the site of secretion and all of the Golgi seems to have RGI (Young et al., 2008). Microtubules are found in the cytoplasm underneath the mucilage pocket, but they do not seem to be involved in vesicle trafficking (McFarlane et al., 2008). As mentioned previously secretion of cell wall components is defective in *ech* and *yip4a/yip4b* mutants (Gendre et al., 2011, 2013). The secretion of mucilage is also disrupted in these mutants (Gendre et al., 2013; McFarlane et al., 2013). YIP4a and YIP4b form a complex with ECH at the TGN (Gendre et al., 2013) and therefore must be involved in the same secretory pathway. The precise function of ECH/YIP4a/4b is still unknown, but a large proportion of mucilage is mis-sorted to the vacuole in the mutants, suggesting ECH/YIP4a/4b are involved in protein sorting or targeting. However, the accumulation of small amounts of mucilage in the pocket is still observed in the mutants, suggesting the cell polarity is not affected (Gendre et al., 2013; McFarlane et al., 2013). Two subunits of the excyost, including SEC8 and EXO70A1, have been suggested to be involved in secretion of mucilage (Kulich et al., 2010).

1.7   Cell wall proteins MUM2 and PER36

It has been shown that the location of cell wall deposition influences cell morphogenesis and function. Some cells, such as pollen tubes, secrete cell wall polysaccharides in a polar manner, while many others secrete such material uniformly along the plasma membrane. In addition to carbohydrates, cell walls also contain many cell wall proteins, including both structural proteins and enzymes that can modify carbohydrates to control cell wall properties. It would be interesting to know where and when these enzymes work on their substrates.

Arabidopsis seed coat epidermal cells deposit large amount of pectin-rich mucilage in a polar manner at a specific development stage. Recently, a proteomic analysis has identified many proteins in mature mucilage, including many characterized cell wall-modifying enzymes (Tsai et al., 2017). Thus, mucilage represents a good model system to understand the spatiotemporal relationship between cell wall components and the modifying enzymes. MUM2 and PEROXIDASE 36 (PER36) are of interest here because they are the focus of the research described in this thesis.

Mutation of MUM2 and PER36 results in two distinct mucilage defect phenotypes. The *mum2* mutant was identified by the failure of its seeds to extrude mucilage when exposed to water (Dean et al., 2007; Macquet et al., 2007b). This defect is due to an alteration in the chemical properties of the mucilage. According to monosaccharide composition and linkage analysis, the *mum2* mutant mucilage has an increase in Ara and Gal relative to Rha and GalA and an increased number of Rha branch points compared with the wild type, suggesting that the MUM2 protein removes RG-I side chains (Dean et al., 2007). Consistent with this hypothesis, *MUM2* encodes a β-galactosidase that contains in its primary sequence a signal peptide, a glycosyl hydrolase domain, and a galactose binding domain. Thus, MUM2 appears to be a β-galactosidase that works to remove galactan side chains from RGI. In addition, *mum2* mucilage contains more type II arabinogalactan, which can be linked to either RGI or AGPs. It is possible that MUM2 is involved in modification of AGP (Dean et al., 2007). *MUM2* is expressed not only in the seed coat, but also in siliques, leaves, roots, stems, and flowers (Dean et al., 2007; Macquet et al., 2007b). MUM2 has been shown to be secreted to the apoplast when introduced into tobacco epidermal cells (Dean et al., 2007). However, the details of the timing of MUM2 synthesis and its actual intracellular location in seed coat cells have not been investigated. In addition, the

relationship of MUM2 secretion in seed coats relative to that of pectin remains to be characterized.

PER36 belongs to class III peroxidase family. Class III peroxidase are only found in plants. They reduce H_2O_2 by transferring electrons from molecules such as phenolic compounds. They could also generate reactive oxygen species (ROS) by a separate hydroxylic cycle (Mathé et al., 2010). These peroxidases are able to stiffen the cell wall by oxidizing and cross-linking aromatic compounds when H_2O_2 is available. In contrast, peroxidases can generate ROS that break covalent bonds of cell wall polysaccharides and thus loosen the cell walls (Francoz et al., 2015). The mucilage of *per36* mutant only partially extrudes, suggesting that PER36 is involved in loosening cell walls (Kunieda et al., 2013). PER36 is located in the outer corner of the primary cell wall of seed coat epidermal cells but not in the mucilage pocket, suggesting that the PER36 works on the polysaccharides in the primary cell wall instead of mucilage (Kunieda et al., 2013). Thus, the poor mucilage extrusion of the *per36* mutant may be due to the inability of the expanding mucilage to break a primary cell wall that has not been loosened.

PER36 is localized to the outer corners of the primary cell wall which is presumed to be its substrate. The substrate of MUM2 lies in the mucilage pocket so it is likely MUM2 is also localized there. If correct, both the substrates and the enzymes must be secreted in a polar manner by the seed coat epidermal cells. Thus, the seed coat epidermal cells represent a good model for investigating the polar secretion of carbohydrates and the proteins that modify them.

1.8   Research objectives

Cell wall modifying enzymes are important for establishing cell wall properties, which in turn affect cell growth and function. Often these cell wall components are distributed asymmetrically but the mechanisms underlying such spatiotemporal distribution remain to be determined.

In my thesis research, I explored polar secretion in seed coat epidermal cells by finding answers to the following questions:

1. How is MUM2 distributed in seed coat epidermis at different developmental stages and how is the timing of secretion and distribution of MUM2 related to its substrate, RG-I?

2. What is the mechanism of polar distribution of MUM2 if it is distributed in a polar manner?

3. What is the mechanism of polar distribution of PER36 and how does it differ from that of MUM2?

Chapter 2 : Materials and methods

2.1 Plant materials and growth conditions

Seeds of Arabidopsis were germinated on AT medium (Haughn and Somerville, 1986) with appropriate antibiotics when necessary. Seeds were stratified in the dark at 4ºC for 2-4 d on AT plates before being transferred to continuous light (100 µEm-2s-1 of photosynthetically active radiation) at 20ºC. Ten day-old seedlings were transplanted to soil (Sunshine 4 mix, SunGro) and grown under the same conditions.

mum2-1 is an EMS mutant generated previously (Western et al., 2001). Forward primer MUM2-87f (GAAACAATGCGTATAGCTTGAG) and reverse primer MUM2-77r (ACAGGGTTCTAGTATCAGTAAACGTC) were used for genotyping; the PCR product amplified from *mum2-1* is cleaved by digestion with TatI (Fisher), while the one from wildtype is not. Seeds of all other mutants used in this thesis were obtained from Arabidopsis Biological Resource Center, Ohio USA. Mutants were verified by PCR. The genomic DNA from mutant leaves were preserved on Whatman FTA cards. The primers used for genotyping were the listed in the references (Table 2.1).

Seeds of $P_{AtVAMP721}::mRFP\text{-}VAMP721$ and $P_{AtVAMP722}::mRFP\text{-}VAMP722$ transgenic plants were kindly provided by Prof. Masa H. Sato (Ichikawa et al., 2014). Seeds of *Pro35S:PER36-GFP4g* transgenic plants were gifts from Prof. Ikuko Hara-Nishimura (Kunieda et al., 2013).

Table 2.1: Mutant alleles used in this dissertation

Mutant allele	locus	T-DNA line	Reference for genotyping	Function of encoding protein
mum2-1	*At5g63800*	N/A	This work	ß-galactosidase
echidna (*ech-1*)	*At1g09330*	SAIL_163_E09	McFarlane et al., 2013	TGN-located protein
aspg1-1	*At3g18490*	SALK_045354	Tsai et al., 2017	protease
rd21a-2	*At1g47128*	SALK_090550	Tsai et al., 2017	protease
scpl35-1	*At5g08260*	SALK_086802	Tsai et al., 2017	protease
ara12-1	*At5g67360*	GK-140B02	Tsai et al., 2017	protease
vamp721-1	*At1g04750*	SALK_037273	Zhang et al., 2011	vesicle-associated membrane protein
vamp722-1	*At2g33120*	SALK_119149	Zhang et al., 2011	vesicle-associated membrane protein
per36-1	*At3g50990*	SAIL_194_G03	Kunieda et al., 2013	peroxidase
per36-2	*At3g50990*	SALK_118195	Kunieda et al., 2013	peroxidase

2.2 Transgenic plants

2.2.1 Molecular cloning

For examining the localization of proteins, genomic sequences or coding regions were amplified with primers listed below (Table 2.2) and inserted into vectors carrying the coding region for fluorescent proteins. Those fused with Citrine were cloned into pAD vectors (DeBono, 2011) while those fused with monomeric red fluorescent protein (mRFP) were cloned into pGWB553 (Nakagawa et al., 2008). For cloning into pAD, target sequences were amplified with primers carrying restriction enzyme recognition sites. The amplicoms and vectors were cut with appropriate restriction enzymes and ligated with T4 ligases (NEB). For insertion into pGWB vectors (Nakagawa et al., 2008), target sequences were amplified with primers carrying *attB1* and *attB2* sequences, which are required for a recombination reaction. The recombination reaction was carried out according to the Gateway Technology manual (Invitrogen).

Table 2.2: Primers used for making constructs and the genetic background the constructs were transformed into

Name	sequences	constructs	background
gMUM2-F	ATCTGCAGGTGACTTGTAAGTGGACTGGTCA	For cloning genomic *MUM2*	*mum2-1*
gMUM2-R	ATCTCGAGGGAGAATTGAGATTGAGCTTGA		
MUM4p-F	ATGGTACCAATCGGTCCCATTAGTCTTTATTG	For cloning *MUM4p 1.5* promoter. The result construct was used to fuse the coding regions of different genes I tested.	It depends on the genes fused later.
MUM4p-R	ATCTCGAGCCTTGAAATCTGCAAAAAAAAAC		
MUM4p-ATG-R	ATCTGCAGCATCCTTGAAATCTGCAAAAAAAAAC	For cloning *MUM4p1.5* by pairing with MUM4p-F to generate *cytoCitrine*. A start codon was introduced at the end.	*Col-2*
cMUM2-F	ATGTCGACATGGAGATGGGTCGTCTGGT	For cloning *MUM2* cDNA.	*mum2-1*
cMUM2-R	ATCTGCAGGGAGAATTGAGATTGAGCTTGA		
cMUM2-R2	ATCTGCAGCGCCGTAGCACCGCC	For cloning *MUM2SP* by pairing with MUM2-F.	*Col-2*
PMEI-F	ATAAGCTTATGACTAATCCCATGATCATGG	For cloning *PMEI* (*At4g15750*).	*Col-2*
PMEI-R	ATCTGCAGGAGACGGTGGATCAACGTCT		
Sec-F	CTTGGCGACCACATTGCTGCAGCTCGGCCGAGGATAATGATA	For cloning *secCitrine*.	*Col-2*
Sec-R	ATGCCTCCACAAAAAGAAAACCATAGAACATTGAACAAACTCGAGATGAAGACTAATCTTTTTCTCTTTCTC		

Table 2.2: Primers used for making constructs and the genetic background the constructs were transformed into

PER36-F	ATGAATTCATGAATACAAAA ACGGTGAAGTCAA	For cloning *PER36*.	*Col-2* or *per36-2*
PER36-R	ATCTGCAGAACATCATGGTT AACCCTCCG		
PER36-R2	ATCTGCAGACAAATACATA GAGGAAACAGC	For cloning *PER36SP* by pairing with PER36-F	*per36-2*
PER36-R3	ATCTGCAGTCCTTGAAAGT TGAACATAGTGAGAA	For cloning *PER36$_{1-195}$* by pairing with PER36-F	*per36-2*
PER36-R4	ATCTGCAGAATCGGACATC CCTGCTG	For cloning *PER36$_{1-247}$* by pairing with PER36-F	*per36-2*
PER36-F2	ATCTGCAGTATCAAACACAT CAAAGCACGA	For fusing *PER36* behind *MUM2* to generate *MUM2-PER36-Citrine* by paring with PER36-R.	*mum2-1*
PRX20-F	ATGAATTCATGGAGATCAA GCAGAAGAAAGT	For cloning *PRX20*.	*per36-2*
PRX20-R	ATCTGCAGGATATTGACAA ATCTACAATTCTCCC		
PRX72-F	ATGAATTCATGGCCAAGTC ATTGAACATC	For cloning *PRX72*.	*per36-2*
PRX72-R	ATCTGCAGATAAGCATGGTT AACCCTCCG		
B1-gSCPL35-F	GGGGACAAGTTTGTACAAA AAAGCAGGCTTCGCAGTAG CCGTGAGATTATAAGAA	For cloning genomic sequence of *SCPL35*, including 1.4 kb upstream region.	*scpl35-1*
B2-gSCPL35-R	GGGGACCACTTTGTACAAG AAAGCTGGGTCGAACCGTT TTGAAGGCAAGG		

Table 2.2: Primers used for making constructs and the genetic background the constructs were transformed into

B1-gRD21A-F	GGGGACAAGTTTGTACAAA AAAGCAGGCTTCGACTGTA TATGTACTGTTCCATCCAAA	For cloning genomic sequence of *RD21A*, including 2.0 kb upstream region.	*rd21a-2*
B2-gRD21A-R	GGGGACCACTTTGTACAAG AAAGCTGGGTCGGCAATGT TCTTTCTGCCTT		

2.2.2 Site-directed mutagenesis

Primers for mutating the glycosylation sites of PER36 were designed according to Zheng et al., 2004. The plasmids were amplified by Phusion High-Fidelity DNA polymerase (Thermo Scientific) for 16 cycles. The resulting PCR products were digested with DpnI (NEB) to remove un-mutated plasmid templates before transformation into *E. coli* DH5α. Plasmid *pAD-MUM4p1.5::PER36-Citrine* was used as a template for generating *PER36(N224Q)* and *PER36(N332Q)*, while *pAD-MUM4p1.5::PER36(N224Q)-Citrine* was used to generate *PER36(N12Q)*. The primers used for site-directed mutagenesis are listed below (Table 2.3).

Table 2.3: Primers used for side-directed mutagenesis

Name	Sequence
PER36-N224Q-F	CCGACAAAGGTTATACCAACATACTG
PER36-N224Q-R	CAGTATGTTGGTATAACCTTTGTCGG
PER36-N322Q-F	GATGGGGCAAATCTCACCGTTGACGG
PER36-N322Q-R	GAGATTTGCCCCATCTTCACCATCGAC

2.2.3 Transformation

The purified constructs were transformed into the *Agrobacterium tumefaciens* GV3101 carrying pMP90 Ti plasmid by electroporation with Gene Pluser (Bio-Rad). For constructs inserted into pAD vectors, pSoup plasmids were also co-transformed (Hellens et al., 2000). The transformed Agrobacterium were then used for transforming Arabidopsis of appropriate genotypes by the floral-dip method (Clough and Bent, 1998). The genotypes of plants for transforming with each constructs are listed in Table 2.2. *per36-2* mutants were used for transformation with constructs carrying *PER(N224Q)-Citrine*, *PER36(N322Q)-Citrine* and *PER36(N12Q)-Citrine*.

2.3   Western blot analysis and de-glycosylation

2.3.1 Protein extraction

Siliques were first frozen on dry ice and then homogenized with pestles in 1.5 ml microtubes. One hundred microliter of protein extraction buffer (Lu et al., 2010) was added to the sample homogenized from four siliques. Cellular debris was removed by centrifuging at 12000g at 4 ºC for 10 min. Protein concentration of the supernatant was determined by Bradford assay (Bradford, 1976).

For leaf tissue, proteins were extracted directly in loading buffer according to Tsugama et al., 2011. Siliques of transgenic plants carrying *PER36* with mutated glycosylation sites were first

homogenized as described above and then extracted in loading buffer (Tsugama et al., 2011). The mixtures were heated at 95 °C for 10 min and loaded on SDS-PAGE gels.

2.3.2 SDS-PAGE and Western blots

Extracted proteins were mixed with 5X protein loading buffer (250 mM TrisHCl, pH 6.8, 10% SDS, 30% glycerol, 5% β-mercaptoethanol, 0.02% bromophenol blue) and denatured at 80-95 °C for 7-10 min if no other treatment was required. The protein samples were then loaded onto an 8% acrylamide gel with 1% SDS. Proteins were separated by electrophoresis at 100-110 V for 3 h.

Proteins were transferred from acrylamide gels to nitrocellulose membranes in Bjerrum Schafer-Nielsen buffer with SDS (48 mM Tris, 39 mM glycine, 20% methanol, 1.3 mM SDS, pH9.2) by Trans -Blot SD semi-dry transfer cell (Bio-Rad) at 15 V for 50 min. The membranes were blocked with 5% skim milk powder in TBS-T buffer (150 mM NaCl, 10 mM Tris, pH 8.0, 0.1% tween 20) for 30 min at RT or at 4 °C overnight. Anti-GFP (mouse) antibody (Roche) with 10,000 X dilution in TBS-T buffer was used to detect Citrine- or GFP-tagged proteins. HRP-conjugated anti-mouse IgG antibody (Santa Cruz biotechnology) with 20,000 X dilution in TBS-T buffer was used to as secondary antibody. The peroxidase activity was detected with Super Signal^{TM} West Pico PLUS Chemiluminescent substrate (Thermo Scientific).

2.3.3 De-glycosylation

To removing N-linked glycan from the proteins, proteins extracted with protein extraction buffer were treated with de-glycosylation enzymes Endo H (NEB) or PNGase F (NEB) according to the manual and incubated at 37 °C for 2 h. The treated proteins were mixed with 5X protein loading buffer, denatured and loaded to acrylamide gels for SDS-PAGE.

2.4 Microscopy

2.4.1 Confocal microscopy

Perkin-Elmer UltraView VoX Spinning Disk Confoca Microscope (PerkinElmer) was used for characterizing the distribution of fluorescent-tagged proteins. GFP tagged proteins were excited with 488 nm laser. Citrine-tagged proteins were excited with 514 nm laser. mRFP-tagged proteins and FM4-64 stained tissues were excited with 561 nm laser. Images were taken with Hamatsu C9100-02 electron multiplier CCD camera (Hamatsu) and software Velocity (PerkinElmer) under 20 X or 63 X glycerol immersion objective lenses.

2.4.2 Brightfield microscopy

Zeiss AxioSkop 2 upright light microscope (Carl Zeiss AG) was used to examine the mucilage phenotype of hydrated seeds stained with ruthenium red. The images were taken with Leica DFC450 C digital camera and software Leica Application Suite LAS v4.2 (Leica) under 5 X objective lens.

2.4.3 Seed staining

Before staining with ruthenium red, seeds were first immersed in water and left to stand in steady state for 15 min or orbitally shaken for 2 h. Water was removed, and the hydrated seeds were stained with 1 mL 0.2mg/mL Ruthenium Red (Sigma-Aldrich) for 20 min. The stained seeds were characterized by brightfield microscopy.

For staining developing seed with FM4-64 (Invitrogen), seeds were removed from siliques and immersed in 10 μM FM4-64 in 1.5 mL microtubes. Seeds were infiltrated by vacuuming for

5 min and stained for 10 min before imaging. Other tissues were stained with 10 μM FM4-64 for

5 min without vacuuming. The stained seeds and tissues were examined by confocal microscopy.

For calcofluor white staining, seeds were immersed in water, orbitally shaken for 2 h and

then stained with 0.02% calcofluor white (Sigma-Aldrich) for 1 h (Willats et al., 2001). The

stained seeds were examined by confocal microscopy using an excitation filter (BP 360-370),

dichroic mirror (DM400), and emission filter (BA 420-460).

2.4.4 Image processes

All images taken from microscope were processed with ImageJ (Abramoff et al., 2004). The

band intensity on western blots and the width of mucilage halo were also measured with ImageJ.

Chapter 3 : Polar secretion contributes to polar distribution of cell wall components in Arabidopsis seed coat epidermis

3.1 Introduction

The seed coat epidermal cells of Arabidopsis are highly polarized, with large amounts of pectin-rich mucilage deposited between the primary cell wall and plasma membrane on the outer periclinal side of the cells. MUM2, a ß-galactosidase that modifies the side chains of RG-I, has a signal sequence and is secreted to the apoplast when it is ectopically expressed in the tobacco leaves. However, its distribution in seed coat epidermal cells has not been determined. Since its substrate, mucilage RG-I is distributed in a polar manner in seed coats, I hypothesized that MUM2 is localized in the apoplast asymmetrically as well.

Asymmetry of cell wall matrix carbohydrates and proteins can be achieved by polar secretion. Pollen tubes and root hairs are the model systems where polar secretion has been best studied (; Galway et al., 1997). It has been found that vesicles accumulate in the tip region of pollen tubes (Derksen et al., 1995) and these vesicles contain cell wall materials (Lancelle and Hepler, 1992; Bove et al., 2008), indicating cell wall polysaccharides are secreted to the tip of the pollen tube. In addition, AtPMEI1 is localized only at the apex (Röckel et al., 2008), and it is possible that this localization is achieved by polar secretion. Polar secretion has also been observed in root hairs. By labeling vesicle-localized membrane proteins, VAMP721 and its homologue VAMP722 with fluorescent protein, the direction of secretion is able to be tracked and found to be localized at the tip of root hairs undergoing tip growth (Ichikawa et al., 2014).

The redirection of secretion to a specific domain of the cells has also been observed in non-polarized cells. VAMP721 predominately accumulates in the cell plates of dividing cells (Zhang et al., 2011a). The formation of cell plates includes the deposition of primary cell wall material

(Drakakaki, 2015). Consequently, cell wall materials are delivered in a polar manner during cell division. VAMP722 is found to accumulate at the sites of fungal attack (Kwon et al., 2008). A powdery mildew resistant protein RPW8.2, carried by VAMP721/722-associated vesicles is delivered asymmetrically to the plant-pathogen interface (Kim et al., 2014). Also, it has been found that polar secretion is also involved in mycorrhiza formation. During nodulation, the plant host cells deposit plasma membrane surrounding intracellular hyphae of mycorrhizal fungi. GFP-labeled exocytosis marker accumulates in the region of the plasma membrane around the tip of penetrating hyphae, suggesting the secretion is redirected (Pumplin et al., 2012; Harrison and Ivanov, 2017). These findings indicate that secretion can be redirected according to different developmental and environmental conditions.

In this chapter, I investigated how MUM2 is distributed in seed coat epidermal cell at different developmental stages and how the distribution is related to its substrate. I also examined if polar secretion is involved in the polar deposition of cell wall components and if different cell wall components share the same or at least some parts of the secretory mechanism.

3.2 Results

3.2.1 MUM2 is distributed in a polar manner in seed coat epidermal cells

To understand the spatiotemporal distribution of MUM2 relative to its substrate, genomic *MUM2* sequence including 2 kb promoter and coding region was fused with *Citrine* yellow fluorescent protein (*gMUM2-Citrine*). The construct was transformed into *mum2-1* mutant, and the mucilage extrusion defect was rescued. The localization of the resulting MUM2-Citrine in the seed coat epidermal cells from 4 DPA (Day Post Anthesis) to 10 DPA was examined with a spinning-disc confocal microscope.

No Citrine signal was detected at 4 PDA (Figure 3.1 A, E). MUM2-Citrine was first observed at 5 DPA where it was located in the primary wall with the strongest fluorescence where the radial and outer periclinal walls meet (at the future position of the mucilage pocket) and to a much lesser extent in the primary cell wall on other sides of the cell (Figure 3.1 B, F). From 6 DPA and 8 DPA, when mucilage is being deposited, the fluorescence of MUM2-Citrine was found primarily in the mucilage pocket (Figure 3.1 C, D, G, H, I, M). To ensure that the Citrine fluorescence was in the apoplast, the cells were counterstained with the membrane dye FM4-64. MUM2-Citrine was located between the membrane and the cell wall, indicating that MUM2-Citrine is indeed secreted to the apoplast (Figure 3.1 L, P). Following the completion of mucilage synthesis, the MUM2-Citrine signal abruptly disappeared from the mucilage pocket (9 DPA) but continued to accumulate in the developing columella (Figure 3.1 J, N). The YFP signal in the columella was still detected at 10 DPA but gradually decreased after this point in time (Figure 3.1 K, O). Thus, the secretion of MUM2 appears to be polar, coincident temporally and spatially with its mucilage substrate during seed coat epidermal cell differentiation (Young et al., 2008). In addition, data suggest that MUM2 is actively removed at the end of mucilage synthesis. The latter point is investigated in more detail in Chapter 4.
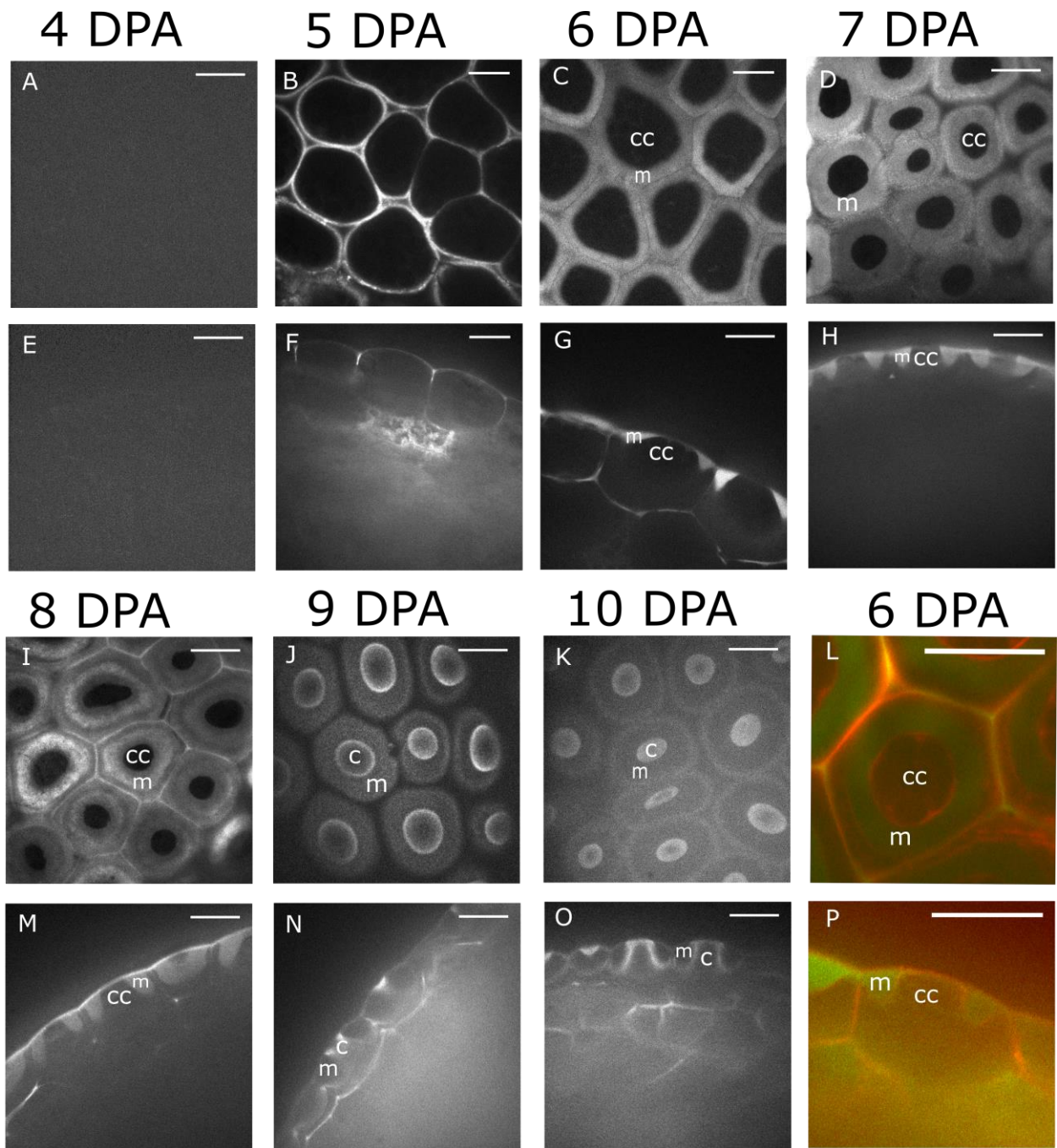
Figure 3.1: Distribution patterns of gMUM2-Citrine from 4 DPA to 10 DPA in seed coat epidermal cells

(A) to (D) and (I) to (L) show the transverse sections of seed coat epidermal cells. (E) to (H) and (M) to (P) show the longitudinal sections. (L) and (P) shows the distribution of MUM2-Citrine (in green) counterstained with FM4-64 (in red) at 6 DPA. Scale Bar = 20 μm. c: columella; cc: cytoplasmic columella; m: mucilage pocket.

3.2.2 The MUM2 distribution is not polar in tissues other than the seed coat

MUM2 is expressed by native promoter in a wide variety of cell types (Dean et al., 2007; Macquet et al., 2007b). To check if the polar distribution is unique to seed coat epidermal cells, the distribution pattern of MUM2-Citrine was examined in other tissues. MUM2-Citrine was detected in the elongation zone and mature zone of the root, but not in the division zone. In the elongation zone, MUM2-Citrine was observed in every cell layer (Figure 3.2 A), while in the mature zone, it was present in the cortex and epidermis, including root hairs (Figure 3.2 B and C), but not the stele (Figure 3.2 C). MUM2-Citrine was also present in the epidermal cells of the cotyledon (Figure 3.2 D) and young leaf (Figure 3.2 E). MUM2-Citrine was distributed in a nonpolar manner in all of these tissues. Root tissue was stained with FM4-64 to determine whether MUM2 is secreted to the apoplast. The MUM2-Citrine signal was detected between the two plasma membranes stained by FM4-64, indicating that MUM2-Citrine is located in the cell wall (Figure 3.2 F). The fact that MUM2-Citrine is distributed in a polar manner only in seed coat epidermal cells, suggests that the polar localization is a characteristic of this specialized cell type.
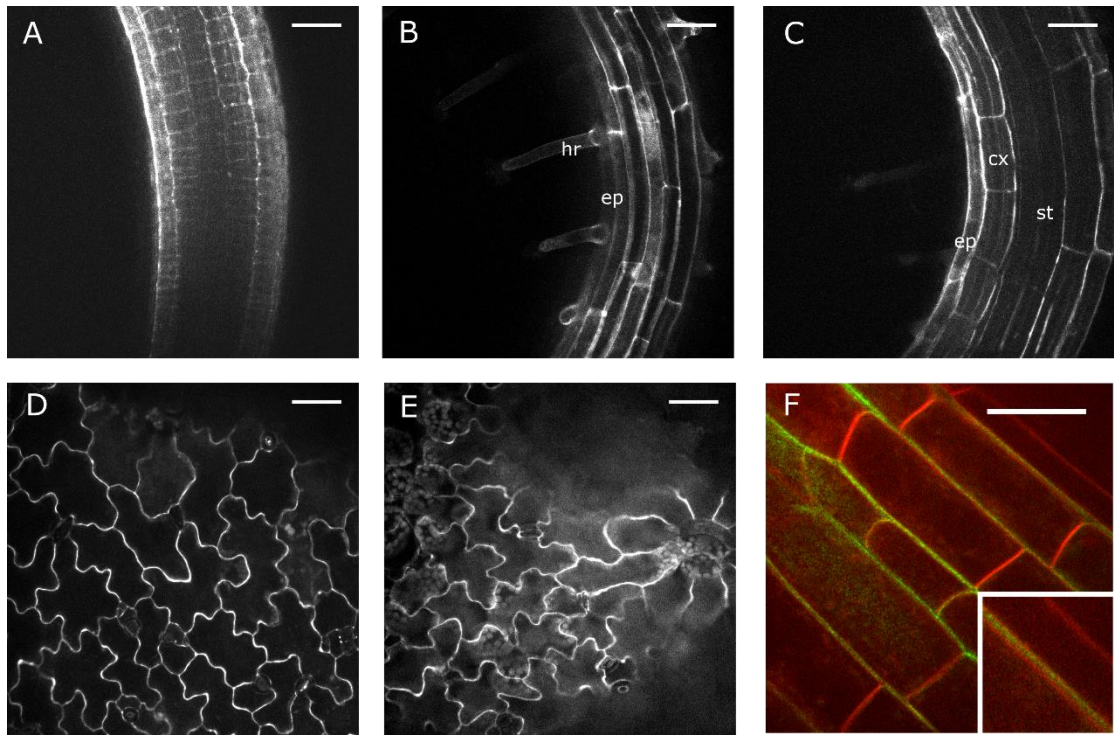
Figure 3.2: Distribution of MUM2-Citrine in root, cotyledon and leaf cells

Citrine fluorescence of MUM-Citrine in the elongation zone (A) and mature zone (B and C) of roots, and in epidermal cells of cotyledons (D) and leaves (E). (F) shows the fluorescence signal of MUM2-Citrine (in green) counterstained with FM4-64 (in red) in roots. The inset in (F) shows a cells at higher magnification where the MUM2 signal clearly lies between the membranes of two adjoining cells. Scale bar in (A) to (C) = 50 µm. Scale Bar in (F) = 20 µm. cx: cortex; ep: epidermis; hr: root hair; st: stele.

3.2.3 Polar secretion to the mucilage pocket is not dependent on the sequence of the secreted protein

Above, I showed that MUM2 is distributed to the apoplast of the seed coat epidermal cell in a polar manner. To determine whether this distribution requires MUM2 protein sequence, I employed a secretory form of Citrine in Arabidopsis where the signal sequence of either *MUM2* (a.a. 1-28; MUM2SP-Citrine) or the Arabidopsis chinitase gene (secCitrine; Batoko et al., 2000) was fused in frame with Citrine YFP. These chimeric genes were placed under the control of the Arabidopsis *MUM4* promoter (MUM4p 1.5kb, includes the 5'UTR; Dean et al., 2017) that, like the MUM2 promoter drives expression in seed coats between 4 DPA and 10 DPA with highest expression at 6-7 DPA (Dean et al., 2017). In addition, the *MUM2* cDNA fused in frame to *Citrine* (*cMUM2-Citrine*) as well as Citrine coding region alone (lacking a signal peptide; *cytoCitrine*) under the control of the *MUM4p1.5* were included as positive and negative controls respectively. In addition, an empty vector pAD was included as a negative control. Each of these four genes and empty vector pDA were individually transformed into Arabidopsis and the localization of Citrine fluorescence in developing seed coat epidermal cells examined by confocal microscopy.

As expected, the fluorescent signal of cytoCitrine (Figure 3.3 H, K) was observed only in the cytoplasm and not the apoplast, and no fluorescence signal was detected in transgenic plants carrying pAD (Figure 3.3 I, L). The localization of MUM2-Citrine derived from *MUM4p1.5::cMUM2-Citrine* was largely indistinguishable from the polar distribution of *gMUM2-Citrine* described above (Figure 3.3 A, D), indicating that the use of the *MUM4* rather than the *MUM2* promoter didn't influence protein distribution. Interestingly, both secCitrine (Figure 3.3 B, E) and MUM2SP-Citrine (Figure 3.3 C, F) also appeared primarily in the

mucilage pocket demonstrating that the polar distribution of MUM2 cannot be due to its protein sequence.

As a final test for this hypothesis, an Arabidopsis gene (At4g15750) annotated as a pectin methylesterase inhibitor and expressed in the embryo (Levesque-Tremblay, 2014) was fused in frame with *Citrine* (*PMEI-Citrine)* and introduced into Arabidopsis under the control of the *MUM4p1.5* promoter. This putative PMEI-Citrine was also localized to the mucilage pocket (Figure 3.3 G, I), implying that the mechanism leading to polar distribution can work on any protein expressed in the seed coat epidermal cells. Taken together, our data suggests that it is a feature of the cell type and not the sequence of secreted proteins that determines polar distribution in in seed coat epidermal cells.
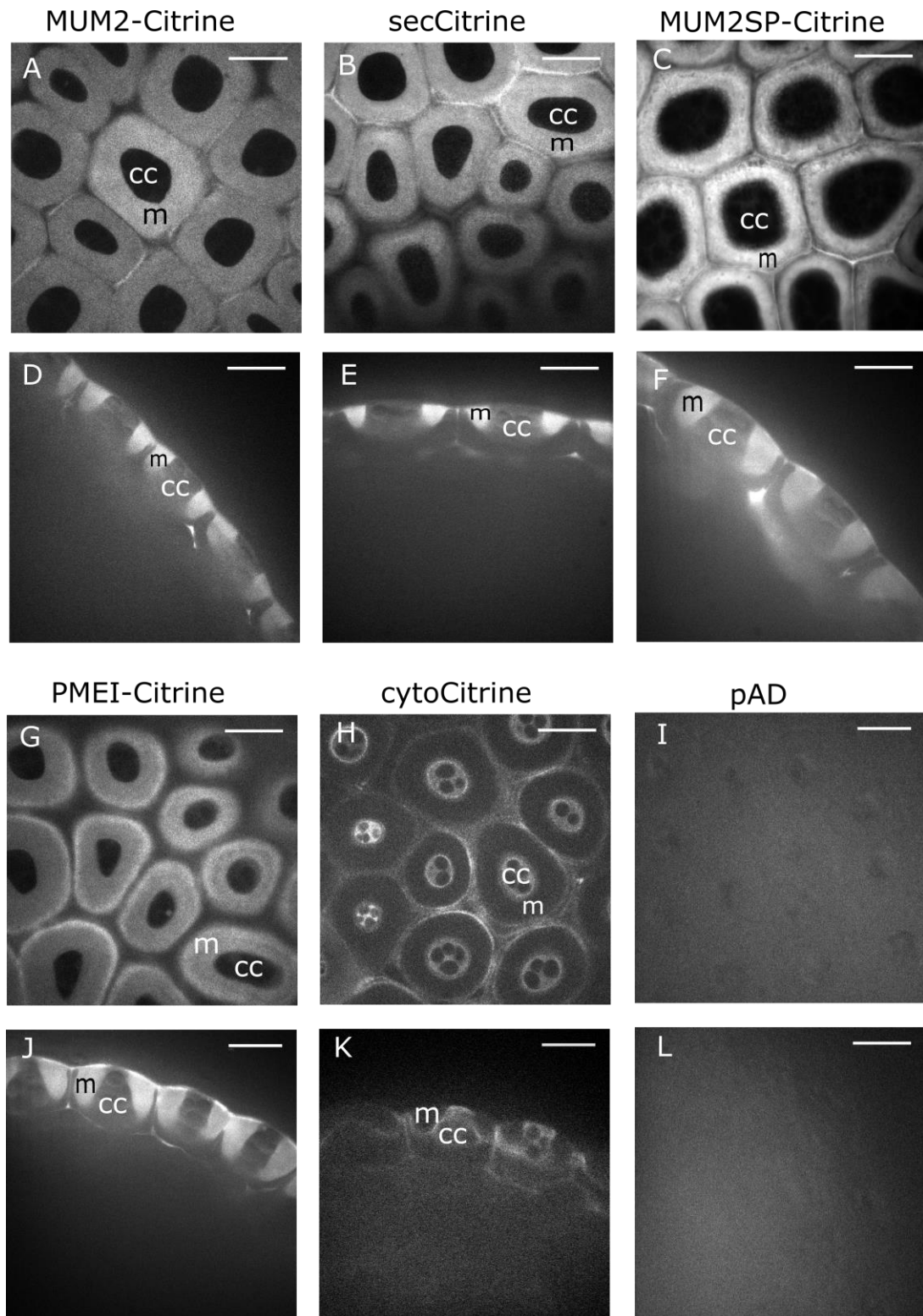
Figure 3.3: Citrine fluorescence of MUM2-Citrine, secCitrine, MUM2SP-Citrine, PMEI-Citrine, cytoCitrine and empty vector pAD in seed coat epidermis at 7 DPA

(A) to (C) and (G) to (I) show transverse sections of seed coats. (D) to (F) and (J) to (L) show longitudinal sections. Scale bar = 20 μm. cc: cytoplasmic columella; m: mucilage pocket.

3.2.4 The secretory pathway appears to be directed to the mucilage pocket in seed coat epidermal cells

Since the amino acid sequence of MUM2 doesn't determine its polar distribution in seed coat epidermal cells and MUM2 is secreted uniformly in other cell types, then the mechanism of polar distribution must be the default pathway in differentiating seed coat epidermal cells. In this case, I hypothesized that the default secretory pathway should be polar. To test this hypothesis, I determined the distribution of *v*-SNAREs, vesicle localized proteins that are involved in the fusion of vesicles to the plasma membrane. VAMP721 and VAMP722, are two redundant Arabidopsis *v*-SNARE proteins expressed in the seed coat cells (Dean et al., 2011). I obtained chimeric VAMP721 and VAMP722 genes, with their own promoters, where monomeric red fluorescence protein (mRFP) is translationally fused to the N-terminus of VAMP721 and VAMP722 (Ichikawa et al., 2014) and determined their patterns of distribution in the differentiating seed coats. mRFP-VAMP721 was distributed uniformly around the cell membrane at 4 DPA (Figure 3.4 A) but by 5 DPA was localized primarily in the membrane at the outer corner of the cell (Figure 3.4 B). During the period of mucilage secretion (6 DPA to 8 DPA), mRFP-VAMP721 was located primarily along the membrane lining the mucilage pocket (Figure 3.4 C, G, H). At 9DPA, when mucilage is no longer being secreted, the signal of mRFP-VAMP721 becomes much weaker and was no longer detected (Figure 3.4 I). VAMP722, which is redundant to VAMP721, showed a similar distribution pattern (Figure 3.4 D to F, J to L). These results suggest that the secretory pathway is targeted uniformly around the cell prior to differentiation and later redirected to the domain of the mucilage pocket. Therefore, the polar distribution of mucilage-related proteins and carbohydrate in the seed coat epidermis is probably due to rearrangement of the secretory machinery of seed coat epidermal cells during differentiation.
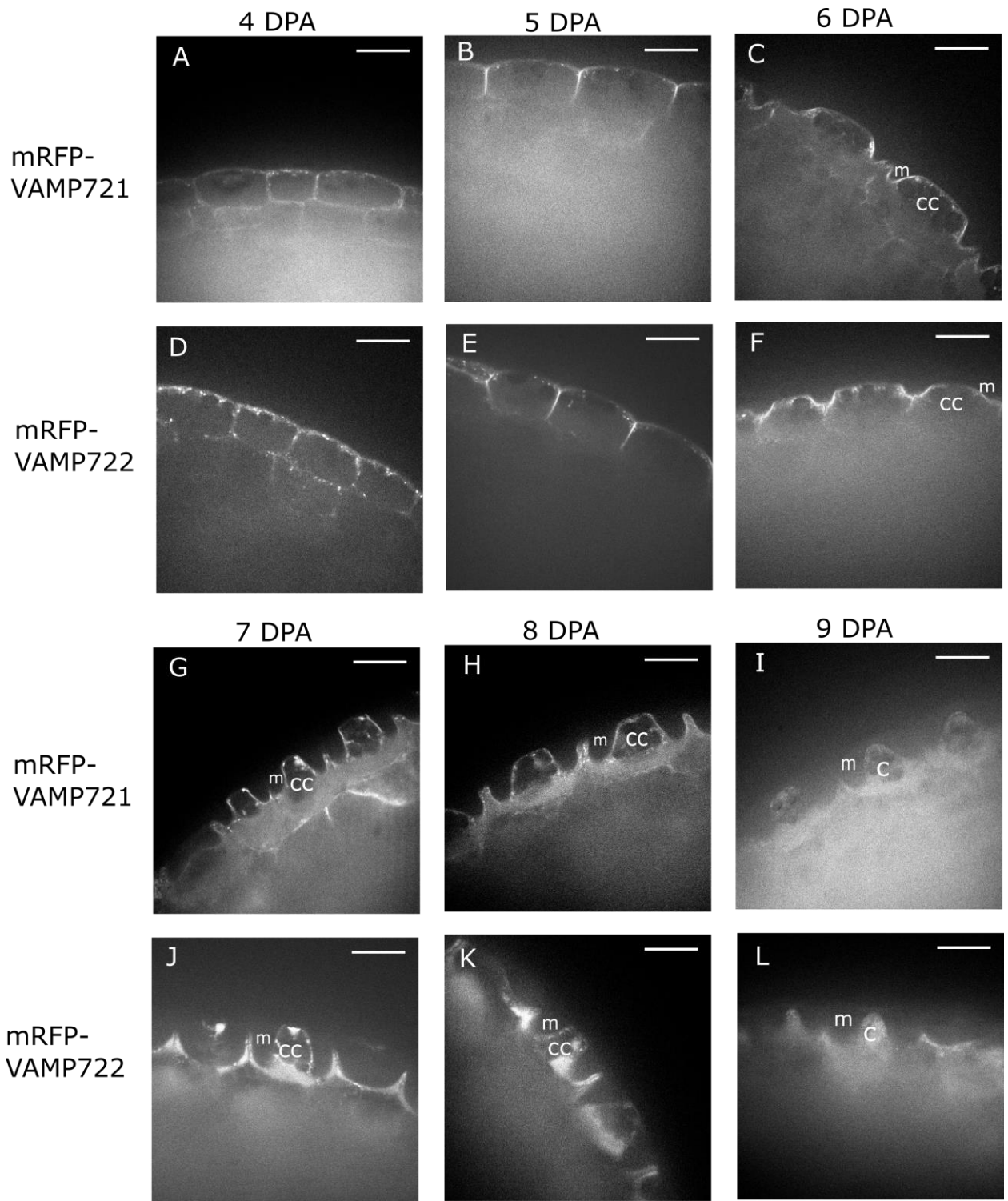
Figure 3.4: Distribution of mRFP-VAMP721 and mRFP-VAMP722 in seed coat epidermis from 4 DPA to 9 DPA

Figures show transverse sections of seed coat epidermal cells. Scale bar = 20 μm. c: columella; cc: cytoplasmic columella; m: mucilage pocket.

The distribution of VAMP721 and VAMP722 correspond to that of both mucilage and MUM2, and could be required for their secretion. For this reason, we sought to test if mucilage and/or MUM2 secretion is disrupted when both *VAMP721* and *VAMP722* are mutated. The seeds of *vamp721* and *vamp722* single mutants were shaken in water and stained with Ruthenium Red. If either mucilage or MUM2 secretion was affected in the mutants, it was expected that mucilage extrusion would be disrupted. However, no obvious differences in mucilage extrusion compared to that of wild type were observed. The function of *VAMP721* and *VAMP722* is known to be redundant and the *vamp721/722* double mutant is lethal (Zhang et al., 2011a) making it impossible to determine the effect on seed coat development directly. With the hope that lines homozygous mutant for one locus and heterozygous for the second would be viable but show a mucilage extrusion phenotype, both *vamp721(-/+)722(-/-)* and *vamp721(-/-)722(-/+)* lines were generated. Although both lines were viable neither showed defects in mucilage extrusion (Figure 3.5).
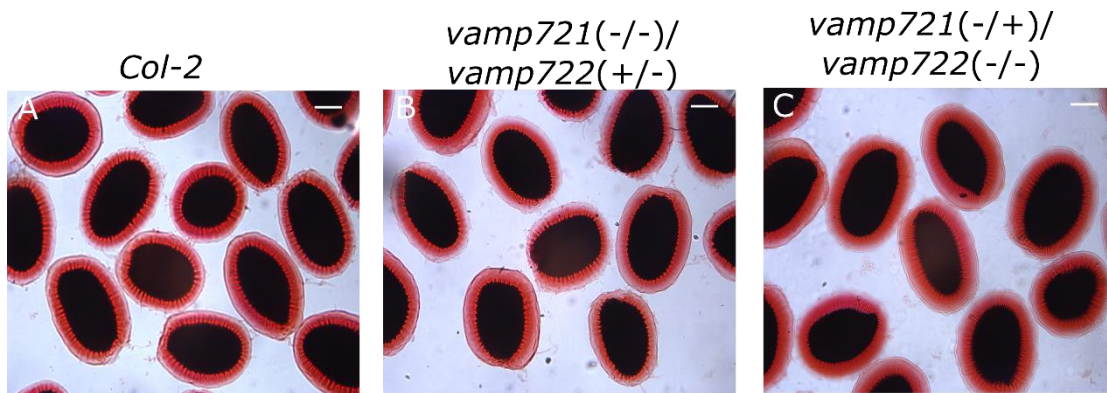
Figure 3.5: Mucilage phenotype of *Col-2*, *vamp721(-/-)722(+/-)*, and *vamp721(-/+)722(-/-)* Seeds were shaken gently in water for 15 min before staining with ruthenium red. The red halo surrounding seeds is extruded mucilage. Scale bar = 200 μm.

3.2.5 Secretion of MUM2, mucilage and VAMP721 is mediated by the same trafficking component

ECHIDNA (ECH) is a TGN-localized protein involved in vesicle targeting but not endocytosis (Gendre et al., 2011). It has been shown that the majority of mucilage is mis-sorted to the vacuole in *ech* mutants (Gendre et al., 2013; McFarlane et al., 2013). To test if the secretion of MUM2 is also dependent on ECH, MUM2-Citrine was crossed into an *ech* mutant background and the distribution of Citrine fluorescence in seed coat epidermal cells determined by confocal microscopy. Like mucilage, MUM2-Citrine signal was found primarily in the vacuole as well as in small mucilage pockets of the *ech* seed coat epidermal cells (Figure 3.6 A, C), indicating that the secretion of both mucilage and MUM2 is controlled by an ECH dependent pathway.

Since the distribution pattern of mRFP-VAMP721corresponds to the secretion pattern of MUM2-Citrine and mucilage in seed coat epidermal cells, I examined the influence of ECH on its distribution. mRFP-VAMP721 was crossed into an *ech* mutant background to test if the mRFP-VAMP721-carrying vesicles are also mis-sorted in the mutant. mRFP-VAMP721 was found lining the vacuole of seed coat epidermal cells in the *ech* mutant (Figure 3.6 B, D). These results indicate that the targeting of VAMP721-to the mucilage pocket also requires ECH. Further, the mis-localization pattern of mRFP-VAMP721 in *ech* corresponds to that of mucilage and MUM2, consistent with the hypothesis that MUM2 and mucilage are secreted through VAMP721-carrying vesicles.
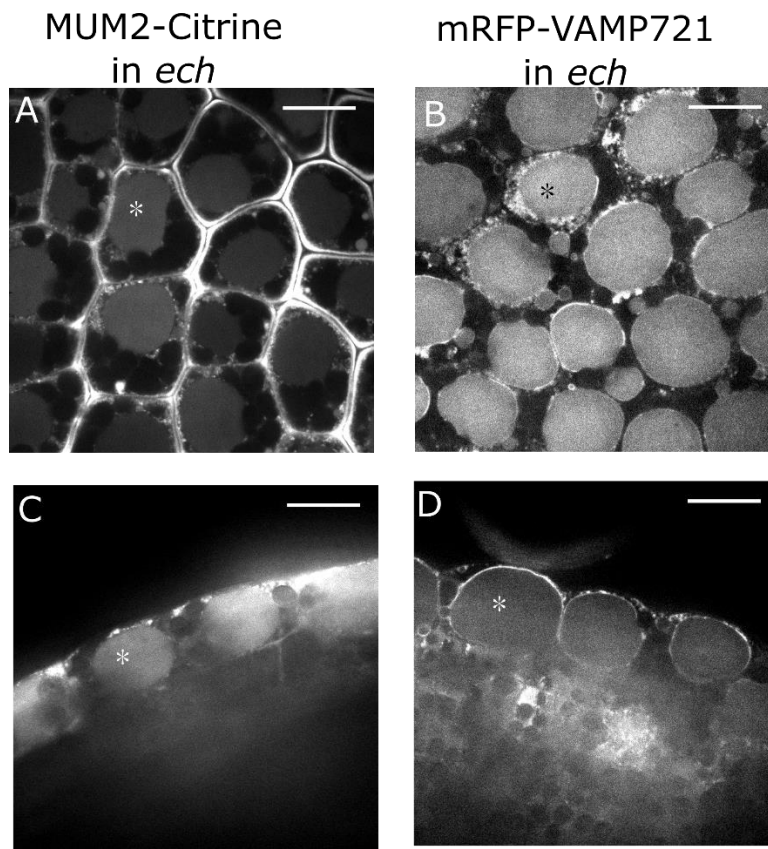
Figure 3.6: Distribution of MUM2-Citrine and mRFP-VAMP721 in the seed coat epidermal cells of the *ech* mutant

(A) and (B) are transverse sections of seed coat epidermis at 7 DPA. (C) and (D) are longitudinal sections. Star marks (*) indicate where vacuoles are. Scale bar = 20 μm.

3.3 Discussion

3.3.1 The intracellular asymmetric distribution of MUM2 is determined by the cell type but not MUM2 amino acid sequence

In this chapter, I examined the distribution of the cell wall protein, MUM2, in polarized seed coat epidermal cells. I found that like mucilage carbohydrate, MUM2 is distributed in a polar manner, accumulating in the mucilage pocket that develops from 5 to 8 DPA. I demonstrated that the polar distribution observed for MUM2 is cell type specific since its localization in other cell types is more evenly distributed in the apoplast. Further, all seed coat epidermal proteins secreted to the apoplast during mucilage synthesis that have been examined to date, including the putative PMEI encoded by At4g15750 (this study) PER36 (Kunieda et al., 2013), three proteins of unknown function, TBA1, TBA2, and TBA3 (Tsai et al., 2017) and the integral membrane proteins CESA3, CESA5, CESA10, VAMP721 and VAMP722 (Griffiths et al., 2015; this study) are distributed asymmetrically in or around the mucilage pocket. The chimeric gene secCitrine shows a similar polar pattern of distribution in seed coat epidermal cells, suggesting that the asymmetry is not determined by the amino acid sequence of the cargo. Taken together, these data demonstrate that differentiating seed coat epidermal cells have a distribution mechanism whereby secreted carbohydrates and proteins are primarily localized to a specific domain of the cell.

3.3.2 The mechanism of asymmetrical mucilage distribution requires secretion

As discussed above, during the period of seed mucilage synthesis (5 DPA to 8 DPA), secretory cargo in Arabidopsis seed coat epidermal cells is localized primarily to the region of the mucilage pocket by an unknown mechanism. Since mucilage RGI is transported to the apoplast via vesicular traffic from the Golgi (Young et al., 2008; McFarlane et al., 2013), the proteins are

likely to be delivered in a similar manner. Consistent with this hypothesis, the vesicle-localized SNARE proteins VAMP721 and VAMP722 were found to be concentrated in the membrane lining of the mucilage pocket during the period of mucilage secretion suggesting a preference for vesicle fusion at this intracellular location. In addition, the localization of VAMP721, MUM2, and mucilage was disrupted in the same way in the *ech* mutant. On the other hand, it was shown that some plasma membrane proteins display a distinct pattern in the seed coat of the *ech* mutant; ABCG11 and PIP2 accumulate in circular multilamellar membrane inclusions, which contains TGN, vacuole, and plasma membrane proteins but not mucilage (McFarlane et al., 2013). This confirms the involvement of a common secretory trafficking apparatus for mucilage, MUM2 and VAMP721.

The polar distribution of mucilage could be achieved in one of two non-mutually exclusive ways. First, polar secretion, as has been observed in some other cell types (Lancelle and Hepler, 1992; Bove et al., 2008; Röckel et al., 2008), may target all secretory cargo specifically to the mucilage pocket and not to other domains of the plasma membrane. Second, cargo could be secreted to all regions of the plasma membrane without bias but the cargo is removed by endocytosis in all regions of the plasma membrane except the mucilage pocket. The involvement of polar endocytosis in the asymmetric distribution of proteins has been observed for integral membrane proteins like PIN. In addition, there is evidence to suggest that secreted proteins such as PMEI and cell wall polysaccharides, such as pectin and hemicellulose, can be recycled back to the cells from the apoplast via endocytosis (Röckel et al., 2008). Of these two mechanisms, polar secretion seems simpler and less costly especially given the volume of mucilage to be delivered to the apoplast. However, given the available evidence, polar endocytosis cannot be ruled out.

3.3.3 Asymmetric distribution of seed coat mucilage requires establishment of cell polarity

Regardless of whether polar secretion or polar endocytosis is responsible for the distribution of seed coat mucilage, cellular asymmetry must first be established early in the differentiation process using positional information from internal or external asymmetric cues. What could act as such a cue for seed coat epidermal cells? In plants, auxin and small secreted peptides are found to be the cues for establishing polarity (Huang et al., 2014; Xu et al., 2014). For example, auxin gradient is important for positioning of ROP2 in trichoblasts to define the initiation sites of root hairs (Fischer et al., 2006). Seed coat differentiation requires auxin, which is suggested to be synthesized in the endosperms and then transported to the seed coats (Figueiredo et al., 2016). However, so far it is unknown if an auxin gradient is also a cue for cell polarity in seed coats.

In animals, the establishment of apical-basal polarity of epithelial cells requires adhesion to the basal extracellular matrix (Yeaman et al., 1999; St Johnston and Ahringer, 2010). It is possible that the cell walls of neighboring epidermal and palisade cells also provide cues for cell polarity in seed coats. Cell walls of different cells may provide different cues.

Mechanical stress could also provide a cue for cell polarity in the seed coat epidermis. In plants, epidermal cells are usually under tension and correspondingly increase the thickness of the cell wall (Kutschera, 2008). Seed coat epidermal cells stop expanding at approximately 4 DPA, but the embryo continues to grow to fill the available space (Haughn and Chaudhury, 2005). Thus after 4 DPA, at the time when mucilage synthesis begins, the fully expanded epidermal cells could be under tension from the expanding embryo. The outer corners of seed coat epidermal cells where mucilage accumulates, are inflection points of radial and outer periclinal cell walls and are likely points of high mechanical stress. Thus, mechanical stress could provide a signal with the correct temporal and spatial pattern to establish cell polarity.

The cell must also have the appropriate machinery to interpret and act on cues to establish asymmetry. Members of ROP family are widely involved in polarity establishment in many polarized cells, so it is possible that ROPs are also involved in polarity establishment in seed coat epidermal cells. Four ROPs, ROP2, ROP4, ROP9 and ROP11, have higher expression among the 11 ROPs in seed coats (Dean et al., 2011). I examined loss of function mutants for two of these ROPs, *rop2* (*rop2-1*; Jeon et al., 2008) and *rop9* (*rop9-1* and *rop9-2*; Choi et al., 2014) but did not detect any mucilage defects. The expression pattern of ROP4 and ROP11 is similar in the seed coats and overlaps with the period of mucilage synthesis so it is possible that one or both are involved in cell polarity establishment in epidermal cells. However, the *rop4-1* T-DNA mutant was in the *WS* ecotype background (Fu et al., 2005), so the comparison of mucilage phenotype with the *Columbia* wild type and the other *rop* mutants is problematic. I couldn't identify a homozygous *rop11-1* mutant (Li Zixing et al., 2012). Instead, I examined the other two T-DNA insertion lines (Salk_039681 and Salk_013327C). These two *rop11* T-DNA line has an insertion in the 5' UTR and 1st intron, respectively, but neither has a mucilage defect phenotype. The lack of mucilage phenotype may be due to gene redundancy, and thus mutants lacking multiple ROPs or a negative dominant mutation in one ROP may be required in order to see a phenotype.

3.3.4 The relationship of MUM2 to its substrates

The temporal and spatial distribution of MUM2 was found to be coincident with its substrate RGI. This suggests that MUM2 modifies mucilage either in the endomembrane system prior to secretion, in the apoplast or both.

Mucilage extrusion, which is dependent on MUM2 activity can be observed after 10 DPA (data not shown) and MUM2 appears to be degraded by 9 DPA. These data suggest that the

action of MUM2 is complete by 9 DPA but that at least one other process is required for mucilage extrusion. Several other enzymes are known to be needed for normal seed mucilage extrusion including BXL1, PER36, PMEI6 and ARA12 (SBT1.7) (Rautengarten et al., 2008; Saez-Aguayo et al., 2013; Arsovski et al., 2009; Kunieda et al., 2013), . It is possible that, unlike MUM2, one of more of these proteins have not completed their function by 9DPA.

The disappearance of fluorescent signal of MUM2-Citrine suggested that MUM2 was degraded rapidly at the end of mucilage synthesis. Investigation of this phenomenon is presented in chapter 4.

Chapter 4 : The distribution of MUM2 in the apoplast is regulated by proteases

4.1 Introduction

In the previous chapter, I showed that the fluorescent signal of MUM2-Citrine disappears from the mucilage pocket in seed coat epidermal cells abruptly at 9 DPA. It is possible that the disappearance is due to degradation by proteases. In this chapter, I investigated whether proteins in mucilage are subject to degradation at the end of mucilage synthesis.

Proteases are involved in most aspects of plant cell biology including cell differentiation, morphogenesis, programmed cell death, and resistance to pathogen attack (reviewed by Hoorn, 2008). Correspondingly, proteases are distributed in various cell compartments, such as the chloroplast, vacuole, and apoplast. However, the substrates of most proteases have not been identified (Tsiatsiani et al., 2012), so it remains largely unknown how the majority of the proteases mediate these biological processes.

Proteases account for a large portion of cell wall proteins (about 12%), suggesting that they may be involved in modification of cell wall properties. However, the biological roles remain uncharacterized for most of the secreted proteases. Some protease families are frequently identified in the cell walls including subtilisin-like serine proteases, aspartic proteases, carboxypeptidases, and papain-like cysteine proteases (Canut et al., 2016) and such proteases can alter cell wall properties. For example, *ARA12* (S*UBTILISIN-LIKE SERINE PROTEASE 1.7* or *SBT1.7*) has been identified in mucilage (Tsai et al., 2017) and when the gene encoding is mutated, mucilage extrusion is defective (Rautengarten et al., 2008). A higher enzymatic activity of PME and lower degree of methylation in the mutant mucilage suggests that ARA12 may be involved in the direct degradation of PME or the activation of PMEI, although the substrate has

not be identified yet (Rautengarten et al., 2008). In contrast, other members of subtilisin-like proteases, such as SBT6.2 and SBT3.5, are suggested to activate PMEs by removing the inhibitory pro-region (Wolf et al., 2009; Sénéchal et al., 2014).

Apart from ARA12, three other proteases have been identified in the mature mucilage: ASPARTIC PROTEASE IN GUARD CELL 1 (ASPG1), RESPONSIVE TO DEHYDRATION 21A (RD21A), and SERINE CARBOXYPEPTIDASE-LIKE 35 (SCPL35) (Tsai et al., 2017). ASPG1 is involved in drought tolerance related to ABA signaling in guard cells, but the mechanism is unknown (Yao et al., 2012). RD21A is a papain-like cysteine protease that is known to have a role in programmed cell death, plant immunity, and likely other stress responses (Shindo et al., 2012; Lampl et al., 2013; Bogamuwa and Jang, 2016; Koh et al., 2016). SCPL35 has not been studied yet, so the biological function remains unknown. Some members of the same family adopt a new function as acyltransferases for secondary metabolism, but the phylogenetic analysis shows that SCPL35 is not clustered with Clade IA (the acyltransferase clade) (Fraser et al., 2005; Mugford and Osbourn, 2010). This suggests that SCPL35 may still function as a protease. However, none of substrates for the proteases have been characterized. In this chapter, I show that the disappearance of MUM2-Citrine fluorescence is likely due to protein degradation and at least some of the proteases found in mucilage influence the rate of this degradation.

4.2 Results

4.2.1 MUM2 is degraded at 9 DPA

The secretion of seed mucilage ends by 9DPA (Young et al., 2008). At the same time, the fluorescence of MUM2-Citrine abruptly disappears from the mucilage pocket (this study, Chapter 3). This disappearance could be due to protein degradation or changes in the chemical

environment that result in quenching of the Citrine fluorescence. To distinguish between these

possibilities a western blot analysis was conducted. Proteins were extracted from siliques from 7

DPA to 10 DPA and MUM2-Citrine was detected by anti-GFP antibody. The intensity of bands

corresponding to the size of MUM2-Citrine decreases after 8 DPA (Figure 4.1) concomitant with

the loss of fluorescence. Free Citrine was also be detected from 7 DPA to 10 DPA, but like

MUM2-Citrine the amount of free Citrine decreased after 8 DPA (Figure 4.1), suggesting that

the decrease of MUM2-Citrine is likely caused by protein degradation, not simply by the

cleavage of Citrine from MUM2.
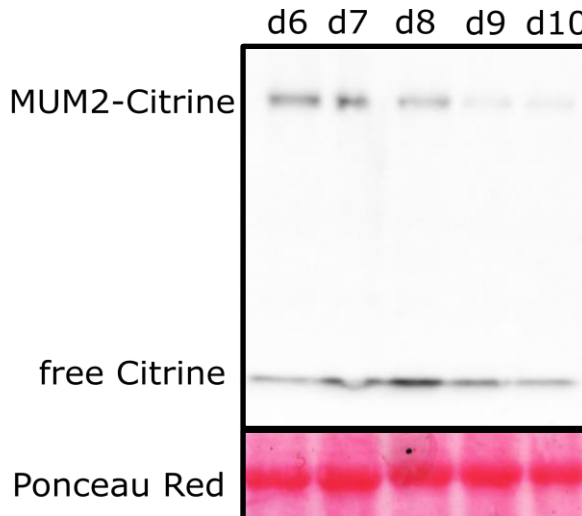
Figure 4.1: The western blot of protein extract from 7 DPA to 10 DPA old siliques with anti-GFP antibody

The large band corresponds to MUM2-Citrine (107 kD), while the small band corresponds to free Citrine (27 kD). Ponceau Red staining was used as a protein loading control.

4.2.2 Protease(s) is involved in MUM2 degradation at 9 DPA

Proteomic analysis of mature mucilage has detected four proteases, ASPG1, RD21A, SCPL35, and ARA12 (Tsai et al., 2017). One or more of these proteases might be responsible for the observed MUM2-Citrine degradation. To test this hypothesis lines with *MUM2-Citrin*e that were also homozygous for a loss-of-function mutation for one of each of the four proteases were constructed. *ara12-1* and *scpl35-1* are knock-out mutants, while *aspg1-1* and *rd21a-2* are knock-down mutant. The fluorescent signal in the mucilage pocket of 9 DPA seed coat epidermal cells of all four lines was characterized with a confocal microscope and compared to that of a *MUM2-Citrin*e line with a *mum2-1* genetic background. Similar to the wild type (Figure 4.2 A), the signal of MUM2-Citrine was not observed in the mucilage pocket at 9 DPA in lines with *scpl35-1* and *ara12*-1 genetic backgrounds (Figure 4.2 C to E). However, in the *aspg1-1* mutant background and to a lesser extent the *rd21a-2* mutant background, the YFP fluorescence appeared to be significantly higher (Figure 4.2 B). The *rad21a-2/aspg1-1* and *scpl35-1/aspg1-1* double mutants (Figure 4.2 F, G) and the *rd21a-2/scpl35-1/aspg1-1* triple mutant (Figure 4.2 H) were generated to test for synergistic effects. The intensity of fluorescent signal in all double and triple mutants appeared stronger than wild type, but the level of fluorescence was difficult to quantify because of variability of signal intensity in each seed.
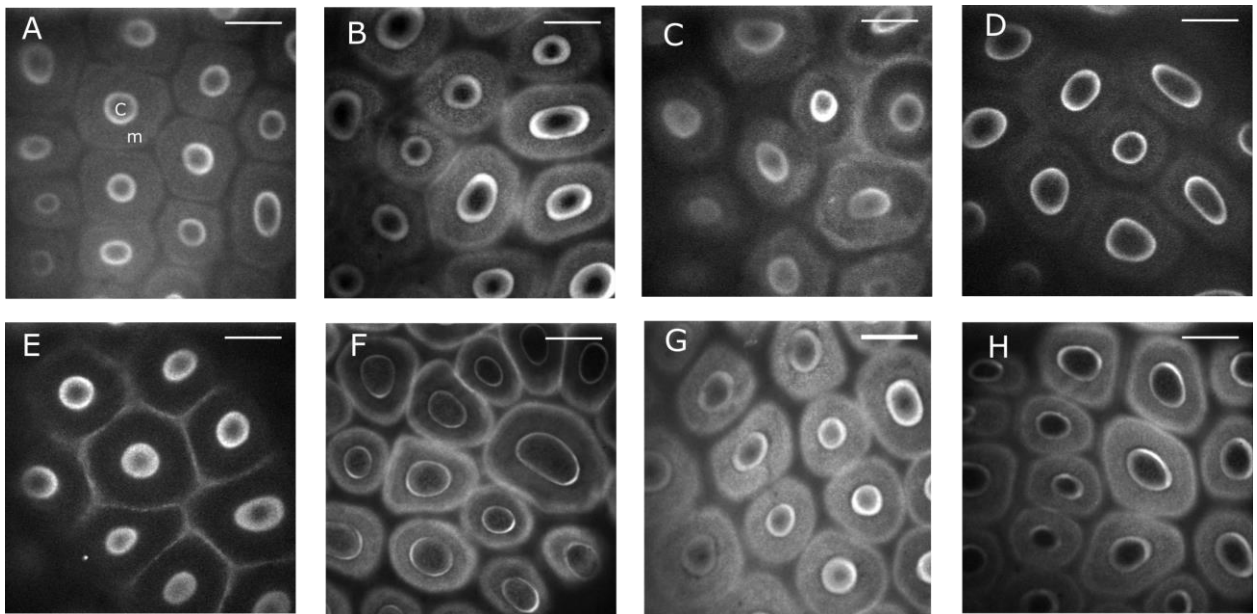
Figure 4.2: fluorescent signal of MUM2-Citrine in different protease mutants

Fluorescent signal of MUM2-Citrine was examined in transgenic plants with MUM2-Citrine in the following genetic backgrounds; *mum2-1* (A), *aspg1-1* (B), *rd21a-2* (C), *scpl35-1* (D), *ara12-1* (E), *rd21a-2/aspg1-1* (F), *scpl35-1/aspg1-1* (G), and *rd21a-2/scpl35-1/aspg1-1* (H) mutants. Scale bar = 20 μm. c: columella; m: mucilage pocket.

Western blot analysis was carried out to quantify the change in the amount of MUM2-Citrine in the siliques of the protease mutants from 7 DPA to 10 DPA. To quantify the data, the band intensity in each lane was measured by image J and normalized with loading controls. Trends of change from 7 DPA to 10 DPA in each genotype are shown in Figure 4.3 G. Consistent with confocal microscopy data, the decrease in amount of MUM2-Citrine is delayed in *aspg1-1*, *rd21a-2/aspg1-1*, *scpl35-1/aspg1-1*, and *rd21a-2/scpl35-1/aspg1-1* mutants (Figure 4.3B, D to F) at 9 DPA and 10 DPA. The degradation of MUM2-Citrine was slowest in the *rd21a-2/aspg1-1* double mutant (Figure 4.3 D) and the *rd21a-2/scpl35-1/aspg1-1* triple mutant (Figure 4.3 F), suggesting that RD21A may work redundantly with ASPG1 in degradation of MUM2, even though the amounts of MUM2-Citrine in *rd21a-2* (Figure 4.3 C) were more similar to that in the *mum2-1* mutant background (Figure 4.3 A). These data suggest that the degradation of MUM2 is

regulated by ASPG1 and possibly also RD21A, although further evidence is needed to show whether ASPG1 and RD21A are involved in degrading MUM2 directly or indirectly.
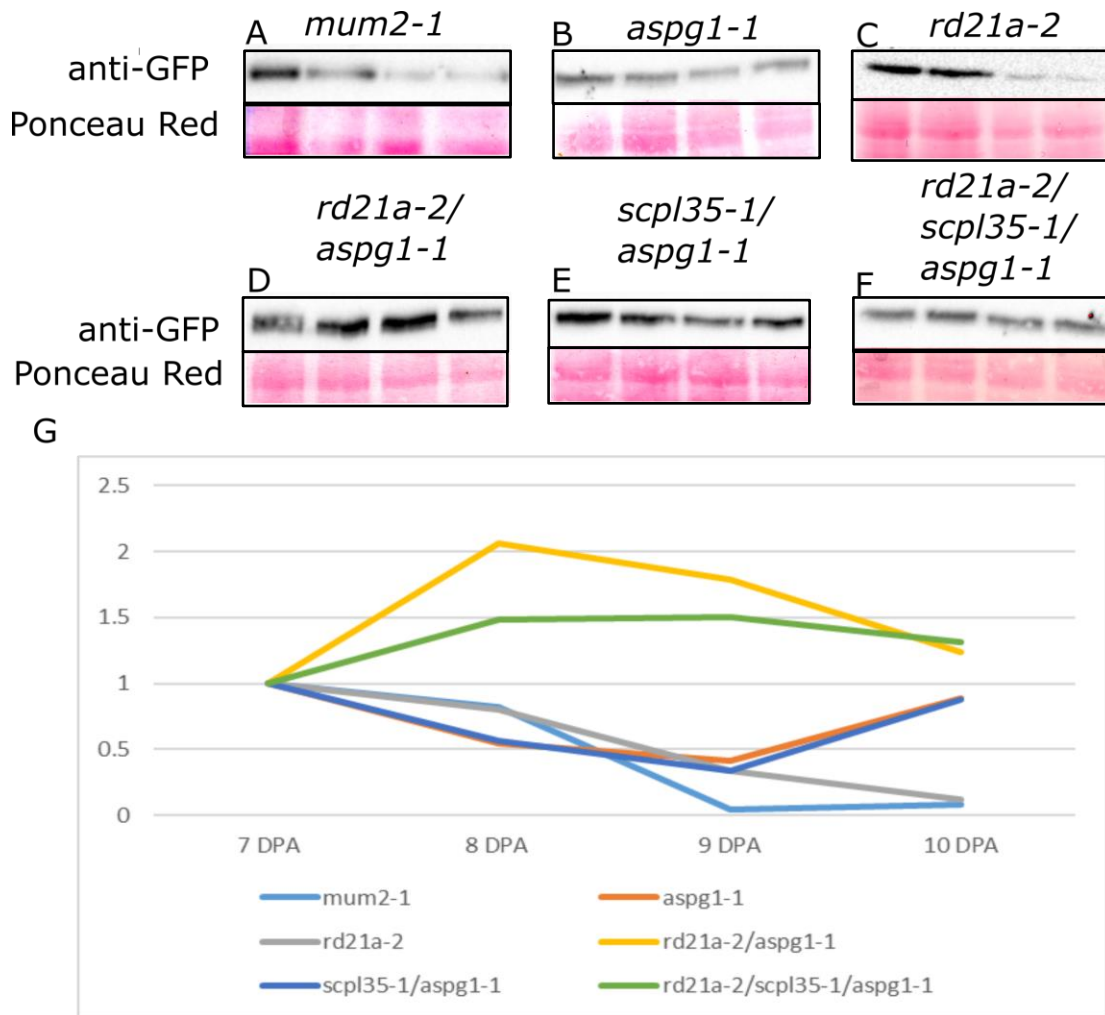
Figure 4.3: Quantification of the change in amount of MUM2-Citrine from 7 DPA to 10 DPA

Western blot analysis was carried out in protein extracted from *mum2-1* (A), *aspg1-1* (B), *rd21a-2* (C), *rd21a-2/aspg1-1* (D), *scpl35-1/aspg1-1* (E), and *rd21a-2/scpl35-1/aspg1-1* (F). MUM2-Citrine was detected with anti-GFP antibody. Ponceau Red staining was used as a loading control, showing the amount of proteins loaded in each lane. (G) shows the ratios of intensities of bands in western blots to intensities of bands in Ponceau Red staining. The ratios at different DAP were then normalized with ratio at 7 DPA in each genotypes.

4.2.3 RD21A is not translocated to the apoplast until 9 DPA

To further understand how proteases are involved in degradation of MUM2, the distribution patterns of ASPG1, RD21A and SCPL35 proteins were examined. Genomic sequences of *ASPG1*, *RD21A* and *SCPL35* including coding regions and 1.7 kb, 2 kb and 1.4 kb of upstream sequence, respectively, were fused with red fluorescent protein (RFP). *RD21A* and *SCPL35* constructs were used to transform *rd21a-2* and *scpl35-1* mutant lines carrying genomic *MUM2-Citrine* sequence, and distribution of fluorescence was determined by confocal microscopy. *ASPG1-RFP* transgenic plants have not been successfully generated yet. Due to the lack (*scpl35-1*) or subtle nature (*rd21a-2*) of the mutant phenotypes it was not possible to verify whether the RFP tagged versions of the two genes were active in the seed coat or not.

The fluorescent signal of RD21A-RFP was detected before 6 DPA and continued to 10 DPA. RD21A-RFP was observed primarily in the cytoplasm from 6 DPA and 8 DPA with strongest fluorescence toward the basal half of the cell (Figure 4.4 first two rows). The distribution pattern of RD21A-RFP is different from the pattern of cytosolic Citrine (Figure 3.3 H, K); RD21A-RFP is not distributed in the cytoplasmic column but at the bottom of the epidermal cells and the cytosolic space between the mucilage pocket and radial cell wall (Figure 4.4 second row). The size and position of the compartment where RD21A-RFP accumulates corresponds to that of the large vacuole of seed coat epidermal cells (Young et al., 2008). The overlapping image of the distribution of RD21A-RFP and MUM2-Cintrine shows that RD21A-RFP and MUM2-Cintrine were confined to two different compartments (Figure 4.4 first two rows). Thus, access of the protease to MUM2 is not possible at this stage. However, by 9 DPA RFP fluorescence signal was detected in the mucilage pocket (Figure 4.4 third row). The timing of accumulation of RD21A-RFP in the pocket coincides with the disappearance of MUM2-Citrine, suggesting that RD21A may degrade MUM2 at this time.

It is importyant to note that fluorescent signal of RD21A-RFP was not observed in the mucilage pockets of every seed coat epidermal cell (Figure 4.4 fifth row). Also, RFP fluorescent signal was detected in the vacuole (Figure 4.4 fourth row), whether RFP signal was detected in the mucilage pocket or not. The cause of the failure of translocation of RFP tagged RD21A in these lines remains unclear.

The distribution of ASPG1 is not yet characterized. Since ASPG1 functions redundantly with RD21A in the degradation of MUM2, I anticipate a distribution pattern similar to RD21A.

In contrast to RD21A-RFP, SCPL35-RFP was observed in the mucilage pocket and primary cell walls from 6 DPA to 8 DPA (Figure 4.5 first two rows) and remained in the pocket at 9 DPA (Figure 4.5 third row). SCPL35 and MUM2 were co-localized in the mucilage pocket when fluorescent signal of MUM2-Citrine was still detectable in the pocket (Figure 4.5 third row). This further confirms that SCPL35 is less likely to be involved in the degradation of MUM2
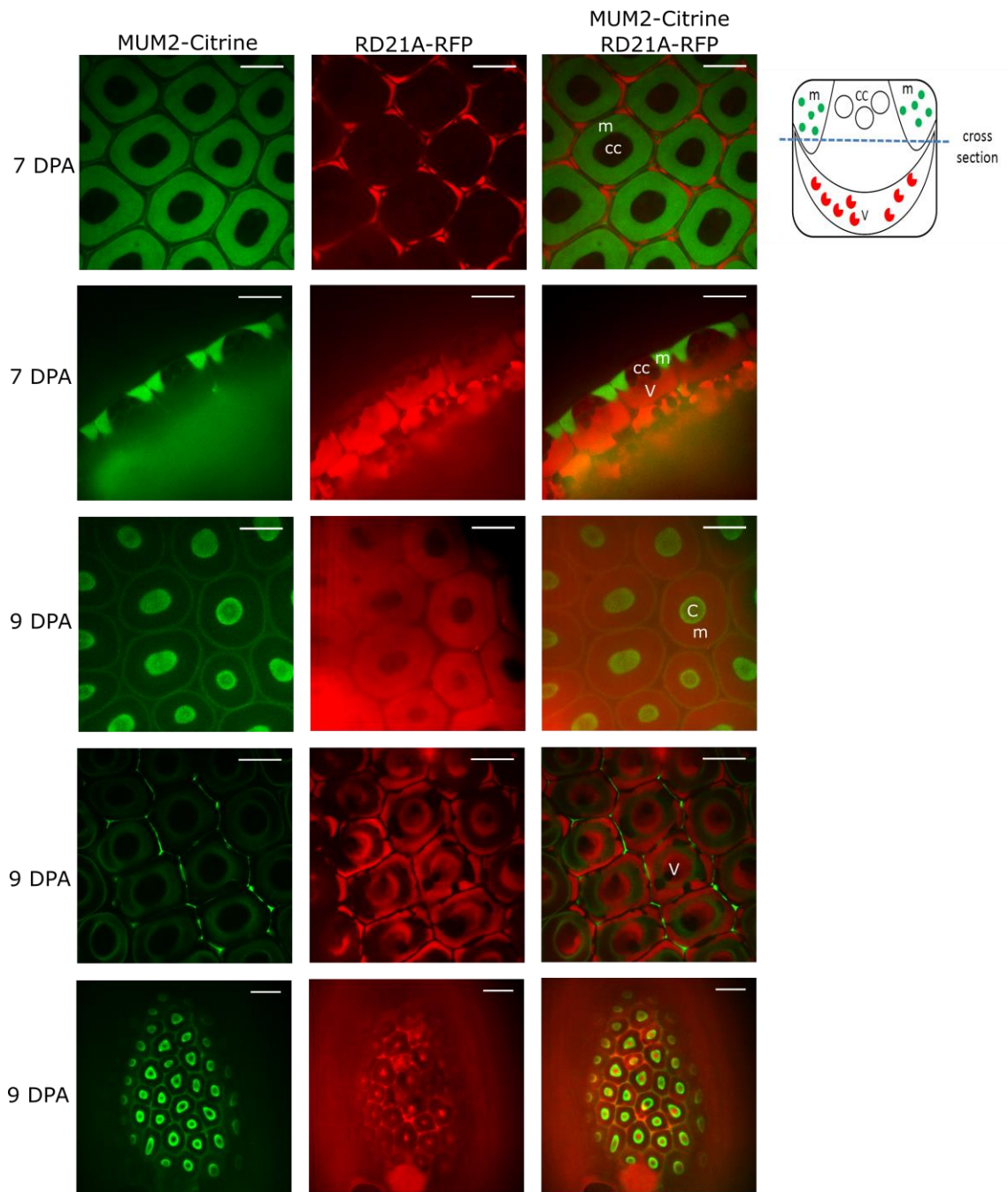
Figure 4.4: Distribution of MUM2-Citrine and RD21A-RFP in seed coat epidermal cells at 7 DPA and 9 DPA

The fluorescent signal from MUM2-Citrine is labeled in green, while the fluorescent signal from RD21A-RFP is labeled in red. Images at the first two rows show cross and longitudinal sections of seeds at 7 DPA, respectively. Images in the bottom three rows show cross sections of seeds at 9 DPA. Images in the fourth row were taken at the bottom of the cell. Scale bar for the first four rows= 20 µm. Scale bar for the fifth row = 50 µm. c: columella; cc: cytoplasmic columella; m: mucilage pocket; v: vacuole.
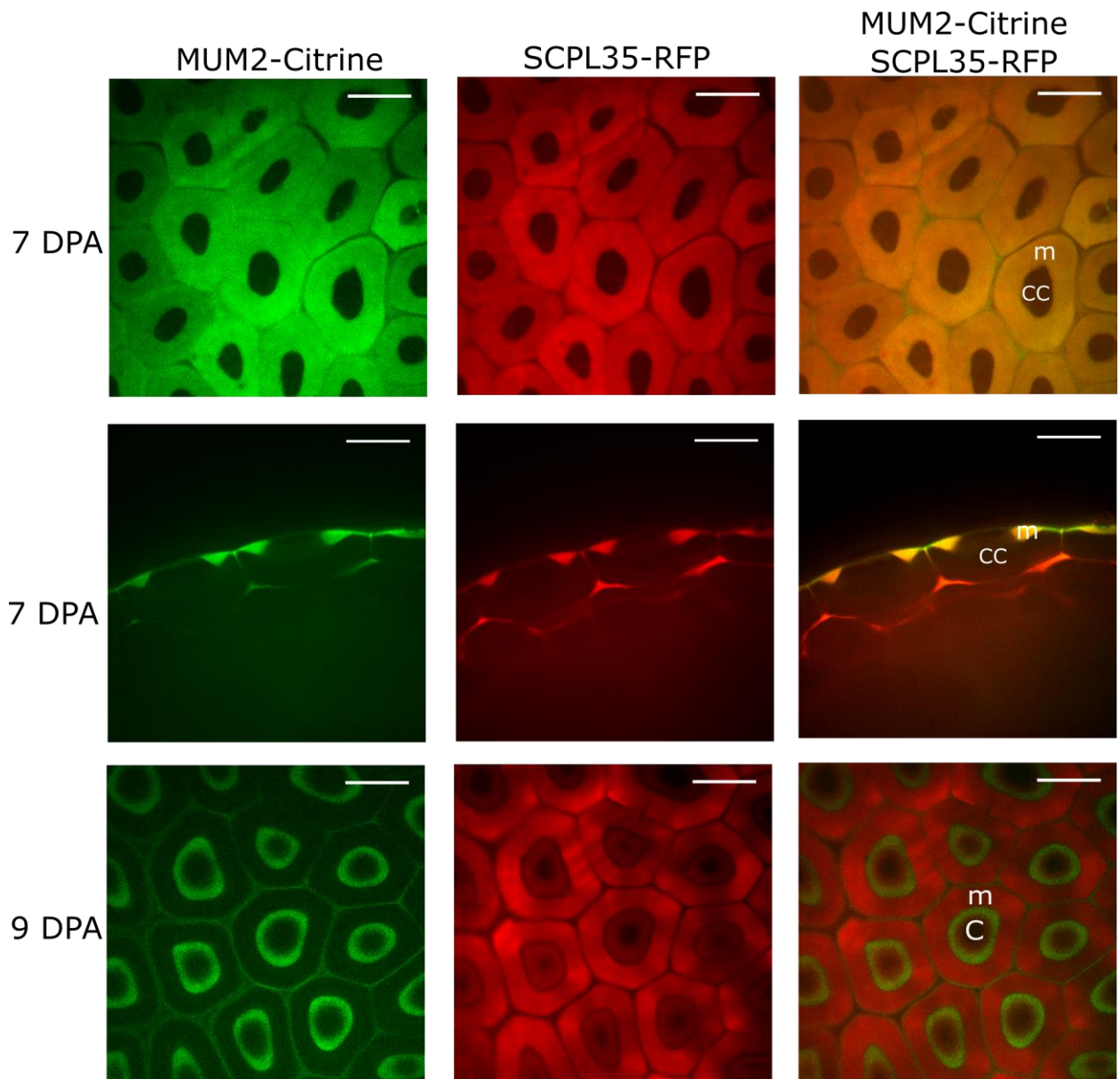
Figure 4.5: Distribution of MUM2-Citrine and SCPL35-RFP in seed coat epidermal cells at 7 DPA and 9 DPA

The fluorescent signal from MUM2-Citrine is labeled in green, while the fluorescent signal from SCPL35-RFP is labeled in red. Images in the first two rows show cross and longitudinal sections of seeds at 7 DPA, respectively. Images in the bottom row show cross sections of seeds at 9 DPA. Scale bar = 20 μm. c: columella; cc: cytoplasmic columella; m: mucilage pocket.

4.2.4   The cell wall properties are modified in the protease mutants

Since the distribution and amount of cell wall-modifying enzyme(s) is regulated by proteases, the cell wall properties may be also changed if the proteases lose function. Therefore, the seed mucilage phenotypes of the protease mutants, including all the single, double, and triple mutants, were examined by hydrating and staining the seeds with ruthenium red with or without shaking. When seeds were hydrated and stained without shaking, the mucilage phenotypes of the protease mutants looked very similar to that of the wild type except for *ara12-1* (Figure 4.6), which has been shown to have a defect in mucilage extrusion (Rautengarten et al., 2008). However, when seeds were orbitally rotated for 2 h, *scpl35-1/aspg1-1* and
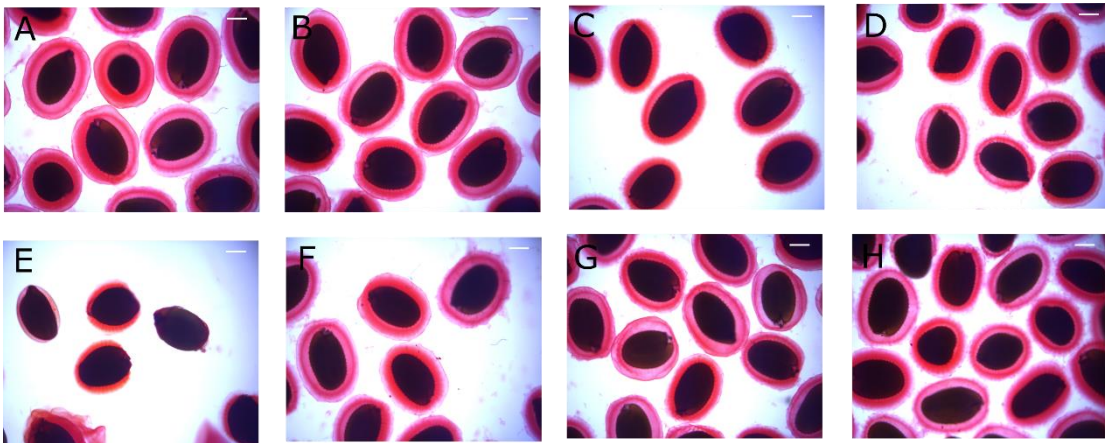
Figure 4.6: Seed mucilage phenotypes of protease mutants hydrated and stained without shaking

Mature dry seeds of wild type (A), *aspg1-1* (B), *rd21a-2* (C), *scpl35-1* (D), *ara12-1* (E), *rd21a-2/aspg1-1* (F), *scpl35-1/aspg1-1* (G), and *rd21a-2/scpl35-1/aspg1-1* (H)   immersed in water for 15 min before stained with ruthenium red. Scale bar = 200 μm.

rd21a-2/*scpl35-2/aspg1-1* and to a lesser extent *rd21a-2/aspg1-1* mutant seeds had smaller adherent mucilage halos (Figure 4.7). In contrast, *scpl35-1*, *rd21a-2* and *aspg1-1* single mutants showed normal seed mucilage halos. Mucilage of *ara12-1* still doesn't extrude well (Figure 4.7). To determine the sizes of mucilage halos, I measured the width of mucilage halos in seeds of

each different genotype. All the mucilage halos of seeds in all protease mutants were significantly smaller than that of wildtype seeds (Table 4.1). Consistent with what was shown in Figure 4.7, *scpl35-1/aspg1-1* and *rd21a-2/scpl35-2/aspg1-1* mutants had the smallest mucilage halos. These data suggest that the mucilage in these mutants is not as adherent as that of wild type. Because the sizes of mucilage halos were quite variable, I also calculated the percentage of seeds with halo widths smaller than 60 µm. All of protease mutants had a higher proportion of seeds with small mucilage halos than wild type, with *scpl35-1/aspg1-1* and *rd21a-2/scpl35-2/aspg1-1* mutants having the highest percentages (> 30 %) (Table 4.1). Because cellulose is required for the attachment of adherent mucilage to seeds (Griffiths et al., 2014, 2015), seeds were stained with a cellulose dye calcofluor white to examine cellulose structure of mucilage. However, no significant changes in cellulose were observed in any of the mutants (Figure 4.8).
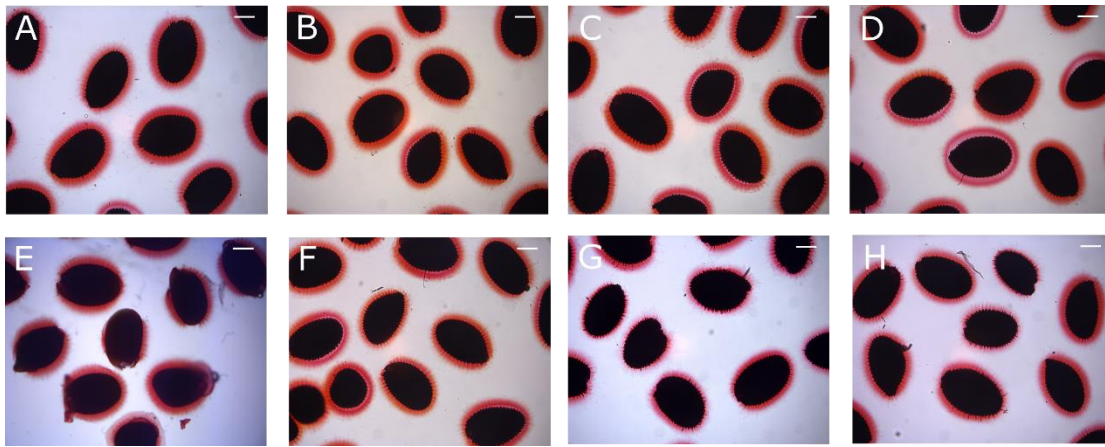
Figure 4.7: Seed mucilage phenotypes of protease mutants hydrated and stained with shaking

Mature dry seeds of wildtype (A), *aspg1-1* (B), *rd21a-2* (C), *scpl35-1* (D), *ara12-1* (E), *rd21a-2/aspg1-1* (F), *scpl35-1/aspg1-1* (G), and *rd21a-2/scpl35-1/aspg1-1* (H) mutants were immersed in water and rotated for 2 h before staining with ruthenium red. Scale bar = 200 µm.

Table 4.1: Average width of mucilage halo and percentage of seeds with small halos in wild type and protease mutants

Mucilage halos of 84 seeds in each mutant were measured with three experimental repeats. Standard deviation of three repeats was calculated. A one-way ANOVA was carried to test if the difference between mutants and wild type seeds is statistically significant. * means p-value $<$ 0.05, while ** means p-value < 0.01.

| Genotype	Average width of mucilage halo (µm)	Percentage of seeds with halo < 60 µm (%)
wild type	77.1±1.7	3.2±1.1
aspg1-1	67.5±2.4**	18.7±3.7**
rd21a-2	65.7±1.4**	24.2±9.0*
scpl35-1	69.6±2.1*	15.1±3.0**
rd21a-2/aspg1-1	64.1±1.7**	23.0±3.1**
scpl35-1/aspg1-1	60.1±2.3**	37.7±2.4**
rd21a-2/scpl35-1/aspg1-1	60.1±3.6**	40.1±6.2**
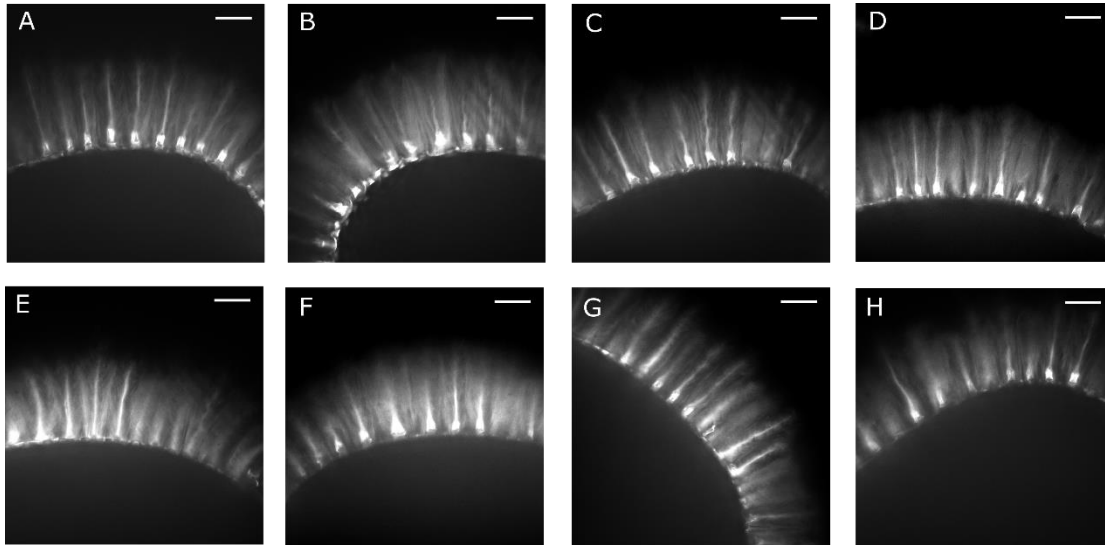
Figure 4.8: Seed mucilage phenotypes of protease mutants hydrated and stained with shaking

Mature dry seeds of wild type (A), *aspg1-1* (B), *rd21a-2* (C), *scpl35-1* (D), *ara12-1* (E), *rd21a-2/aspg1-1* (F), *scpl35-1/aspg1-1* (G), and *rd21a-2/scpl35-1/aspg1-1* (H) mutants were stained with calcofluor white. Scale bar = 20 µm.

4.3 Discussion

4.3.1 Mucilage proteins are degraded by proteases at the end of mucilage synthesis

In this chapter, I showed that the disappearance of MUM2 from the mucilage pocket is at least partially dependent on two proteases ASPG1 and RD21A. The loss of protease function reduces the degradation of MUM2. Further, both proteases accumulate in the cytoplasm during early stages of mucilage synthesis and appear in the mucilage pocket by 9 DPA. The timing of protease localization in the mucilage pocket is correlated with the timing of disappearance of MUM2 from the pocket. Taken together, these data suggest that the movement of the proteases into the mucilage pocket is the mechanism by which the cell degrades mucilage proteins abruptly at the end of mucilage synthesis.

In addition to MUM2-Citrine, the fluorescent signals of other tagged secreted proteins, including those not normally expressed in the seed coats, disappear at 9 DPA (this study; Tsai et al., 2017). This indicates that the degradation is general and not specific to one or a few mucilage proteins. However, not all proteins are targets because the proteases themselves are still present in the mucilage pocket at 9DPA. Considering that cell wall-modifying enzymes, including carbohydrate-active enzymes and probably oxidoreductases, account for large proportion of mucilage proteome (Tsai et al., 2017), the degradation of these cell wall proteins at the right time may be important for establishment of the desired mucilage properties.

4.3.2 Proteases regulate mucilage properties by degrading cell wall-modifying enzymes

Mucilage adherence defects are observed in all of the protease mutants to greater or lesser extents. These data indicate that the removal of mucilage proteins is required for normal mucilage adherence and raises the question as to how? Cellulosic rays are required for mucilage to be anchored to seed surfaces. Therefore, one possibility is that the detachment of the mucilage

may be due to alteration of ray structure. However, the results from calcofluor white staining shows that the structures of cellulosic rays remain unchanged in these mutants. Another possibility is that affinity of mucilage to the rays decreases. Xylans are important for binding of RGI to celluloses (Ralet et al., 2016), and removal of the arabinan and galactan side chains of RGI results in loosening of the mucilage (Dean et al., 2007; Macquet et al., 2007b; Arsovski et al., 2009), so the delayed degradation of RG-I modifying enzymes may result in over-trimming of the side chains. Mucilage proteins MUM2 and BXL1 have been shown to strongly influence the ability of mucilage to expand presumably through removal of mucilage RGI side chains (Dean et al., 2007; Macquet et al., 2007b; Arsovski et al., 2009). Thus in the absence of protease degradation their persistence in the mucilage could easily influence adherence.

The *rd21a-2/aspg1-1* mutants showed less severe mucilage defects than would have been expected from its effect of the degradation of MUM2-Citrine, while loss of SCPL35 showed more severe mucilage defects than were expected. One explanation for this apparent discrepancy is that RD21A/ASPG1 and SCPL35 degrade different suites of mucilage proteins all of which influence mucilage adherence.

4.3.3 The abrupt translocation of the proteases from the cytoplasm to the apoplast could involve vacuole fusion with plasma membrane or redirection of protein trafficking

It was observed in this study that RD21A-RFP localizes to a large compartment at the bottom of the seed coat epidermal cells that correlates with the position of the vacuole (Young et al., 2008). Thus it is likely that the protease is targeted to the vacuole during the early stages of mucilage synthesis (5-8 DPA). It appear abruptly throughout the mucilage pocket at 9 DPA, consistent with the fact that RD21A have been identified in the mucilage proteome (Tsai et al., 2017). Because both of the proteases have been identified in the extracellular space in proteomic

analysis of other cell types (Hooper et al., 2017), it is likely that they have a general role in degrading cell wall proteins.

The mechanism that directs deposition of RD21A-RFP to the vacuole and then later to the mucilage pocket is unclear but could have happened in one of two general ways. First, RD21A may be initially targeted to the vacuole, but at 9 DPA newly synthesize protein redirected to the mucilage pocket. VAMP727, a *v*-SNARE localized on vesicles targeted to vacuoles, was found to interact with a *t*-SNARE, SYP121, on the plasma membrane under stress conditions (Ebine et al., 2008, 2011). This suggests that the secretory pathway to vacuole is able to be redirected to the plasma membrane under certain conditions, so that the cargos destined for the vacuole end up in the apoplast. Phytaspase is a subtilisin-like protease involved in programmed cell death. It has been shown that the active phytaspase is continually produced and secreted to the apoplast in healthy leaf tissue and is relocated to the cytoplasm upon stress-induced programmed cell death. The mechanism for the translocation is still unknown (Chichkova et al., 2010). However, it is possible that redirection is a common strategy in plants to limit proteases from degrading their substrate until proper timing. Second, translocation of RD21A from the vacuole to the mucilage pocket could occur. Such direct transfer may happen through direct fusion of the vacuole to the mucilage pocket. Contact sites, between the vacuole and mucilage pocket, could be induced to form such that the proteases are released directly into the pocket at 9 DPA. It has been found that the vacuole membrane fuses with the plasma membrane to discharge anti-microbial proteins and compounds to the apoplast during pathogen-induced programmed cell death (Hatsugai et al., 2009), a situation comparable to mucilage cell which also undergo programmed cell death at the end of their differentiation process. Alternatively, it is also possible that the proteases are secreted directly from vacuoles to the plasma membrane. In animals, vacuolar type H^+-ATPase

(V-ATPase) is transported to the plasma membrane from lysosomes, an animal organelle with similar function as vacuoles, during osteoclast differentiation (Toyomura et al., 2003).

It has been found that RD21A is distributed in the vacuole in many studies (Yamada et al., 2001; Ondzighi et al., 2008), and it is also found to be released from the vacuole to the cytosol in stress conditions (Bogamuwa and Jang, 2016). In my study, I also confirmed that RD21A accumulates in the vacuoles. In addition, RD21A has been identified in the extracellular space in the other proteomic analyses including one on mature mucilage (Hooper et al., 2017; Tsai et al., 2017), which is also consistent with what I found in this study.

The spatiotemporal distribution of ASPG1 in seed coat epidermal cells has not been examined yet. In a previous study, it was shown that ASPG1 is localized to the ER (Yao et al., 2012). The close examination of how the construct was made in the paper reveals that the fluorescent protein was fused at the N-terminus, prior to the signal peptide. Since the signal peptide is normally cleaved after proteins go into the ER, the distribution of the fluorescent signal may not represent the location of ASPG1. In contrast, proteomic analyses show that ASPG1 is distributed in the apoplast including the mucilage pocket (Hooper et al., 2017; Tsai et al., 2017). Thus, it is likely that ASPG1also accumulates in the mucilage pocket at 9 DPA.

4.3.4   Failure in translocation of RD21A may be due to failure of protein processing

Many proteases are encoded as pro-proteins and then processed to mature functional polypeptides. Pro-domains have found to function as inhibitors of enzymatic activity in different protease families (Beers et al., 2004; Simões and Faro, 2004; Richau et al., 2012; Schaller et al., 2017). Therefore, pro-domains have to be removed to generate active mature enzymes. This removal can be done by autocatalysis or with help from other proteases. For example, RD21A contains a pro-domain at the N-terminus and proline-rich domain and granulin domain at the C-

terminus. Maturation of RD21A involves removal of the N-terminal domain and slow removal of the C-terminal domains (Yamada et al., 2001). Pro-domains are removed from the proproteins to generate intermediate RD21A (iRD21A), which also accumulates in the vacuole with mature RD21A (mRD21A). The iRD21A still has activity but tends to aggregate through the granulin domain at low pH (Yamada et al., 2001; Gu et al., 2012). It has been shown that the removal of the pro-domain is protease-mediated, although the existence of a proline-rich domain at the C-terminus is required for the removal. The removal of C-terminal domains is auto-catalytic (Gu et al., 2012).

I found that RD21A does not appear in the apoplast in every seed coat epidermal cell. This may result from the failure of protein processing. It has been shown that pro-domains of many proteases are required for targeting the proteins to the vacuoles and lysosomes in many organisms (Koelsch et al., 1994; Huete-Pérez et al., 1999). The pro-domains of proteases need to be removed prior to the protease entering the trans-Golgi network, in order for the proteases to be secreted by default. Therefore, if the proteases can not be processed efficiently, they may remain in the vacuole. However, it has not yet been tested whether the pro-domains of RD21A contain a vacuole-sorting signal. In addition, it is unknown if the processing of RD21A-RFP is defective. This can be tested by complementation of *rd21a-2/aspg1-1* mutant carrying *MUM2-Citrine* sequences; the amount MUM2-Citrine chimeric protein should be decrease in the double mutant if RD21A-RFP is functional. Another concern for RD21A is that the C-terminal domain is removed after RD21A reaches the vacuole such that the fluorescent signal does not represent the intracellular location of RD21A.

Chapter 5 : Investigating the unique intracellular distribution of PER36

5.1 Introduction

I have shown that, during mucilage synthesis, most secreted proteins are localized to the region of the mucilage pocket. Soluble proteins, such as MUM2, are typically found throughout the pocket while integral membrane proteins, such as CESA5, localize to the plasma membrane below the pocket. The only exception to this rule is the enzyme PER36, which a previous study has shown to localize to the primary wall surrounding the mucilage pocket (Kunieda et al., 2013). The unique features of PER36 that result in this specialized intracellular localization are unknown.

PER36 was found to be present in two forms with different molecular mass hypothesized to be due to N-glycosylation. (Kunieda et al., 2013). Different sizes of PER36 are localized to different subcellular regions, with a 65 kD form of PER36 in the soluble fraction and a 68 kD form in the microsomal fraction. N-glycosylation is a common post-translational modification for proteins in the endomembrane system or extracellular space. Glycans are first synthesized on the lipid carrier dilichol pyrophosphate in the ER. The glycans carrying 3 glucoses, 9 mannoses, and 2 N-acetylglucosamines, are then transferred *en bloc* to an asparagine of a protein with the consensus sequence Asn-X-Ser/Thr (X can be any amino acid except for Proline), although the consensus sites are not mandatorily glycosylated (An et al., 2009). The transferred glycans are trimmed in the ER to generate glycans composed of 8 mannoses and 2 N-acetylglucosamines, before glycoproteins leave the ER. Therefore, all glycoproteins carry high-mannose type glycans when leaving the ER. Mannose can be further removed from the glycans by mannosidases in the Golgi. Glycans can also be substituted with different sugars, such as fucoses and xyloses, in the Golgi to generate complex-type or hybrid-type glycans (reviewed by Lannoo and Van Damme,

2015). The degree of glycosylation, type of glycan, and sites of glycosylation in a protein may vary in different developmental stages, tissues, and species (Song et al., 2011; Ruiz-May et al., 2012; Arcalis et al., 2013).

N-glycosylation has been intensively studied in animals (Moremen et al., 2012). Glycosylation plays an important role in protein folding and protein quality control in the ER. Misfolded proteins are retained in the ER until they are folded properly or degraded through the ER associated degradation (ERAD) pathway. Also, N-glycosylation has been found to be involved in the regulation of enzyme activity/specificity, substrate binding of receptors, and protein stability (reviewed by Skropeta, 2009). In addition, attention has been drawn to the role of N-glycosylation in polarized trafficking of apical proteins to the apical domain of epithelial cells (reviewed by Vagin et al., 2009). It has been found that removal of glycan from apical proteins causes apical proteins to either shift from apical domains to basolateral domains or be retained in the Golgi (Gut et al., 1998; Vagin et al., 2009). Also, the addition of glycans to intracellular proteins or basolateral proteins allows them to be sorted to the apical domains (Vagin et al., 2009). The identity of receptors required for sorting apical proteins is still unclear.

In plants, N-glycosylation is involved in a variety of biological processes, including hormone signaling, pathogen immunity, self-incompatibility, and stress tolerance (Koiwa et al., 2003; Zhang et al., 2009; Häweker et al., 2010; Fanata et al., 2013; Wang et al., 2014; Yamamoto et al., 2014; Harmoko et al., 2016). N-glycosylation is found to be involved in protein folding and protein quality control in the ER (Vitale and Boston, 2008; Hüttner and Strasser, 2012). However, the molecular mechanism underlying how N-glycosylation influences these processes remains elusive. The effects of N-glycosylation were studied in only a few glycoproteins so far. It has been found in plants that N-glycosylation affects enzyme activity (Lige et al., 2001; Liebminger et al., 2013; Rips et al., 2014), substrate binding of receptors (Häweker et al., 2010;

Shen et al., 2014; Yamamoto et al., 2014), and protein stability (Lige et al., 2001; Liebminger et al., 2013; Rips et al., 2014). How glycosylation affects secretion is still unknown, although, in a few cases, intracellular retention of secreted glycoproteins has been observed upon the removal of glycans, suggesting that secretion is dependent on glycosylation (Häweker et al., 2010; Rips et al., 2014).

Cell wall proteins are commonly modified by N-glycosylation. When the protein compositions of apoplastic glycoproteins are compared to that of overall cell wall proteins in Arabidopsis, the ratios in each functional category are similar: carbohydrate-acting proteins (30.3% vs 27%), oxido-reductases (12.7% vs 11.6%), proteases (13.7% vs 15.6%), and proteins with interaction domains (11.8% vs 11%) (Minic et al., 2007; Duruflé et al., 2017), although the proportion may vary a little between species and tissues (Jamet et al., 2006; Minic et al., 2007; Albenne et al., 2013; Catalá et al., 2011; Zhang et al., 2011b; Ruiz-May et al., 2012; Bu et al., 2017). This indicates that N-glycosylation may play important roles in cell wall proteins of all functional categories. Given that a large proportion of the cell wall glycoproteins is cell-wall modifying in function (Minic et al., 2007), alteration of glycosylation would be expected to affect cell wall properties. Indeed, changes in cell wall properties have been observed in mutants with defects in N-glycosylation. For example, impaired cellulose biosynthesis has been commonly observed when glycosylation enzymes were mutated (Peng et al., 2000; Boisson et al., 2001; Zhang et al., 2009; Jadid et al., 2011; Fanata et al., 2013). In addition, the amount of highly methyl-esterified HG is greatly reduced in mutants defective in genes encoding mannosidases (Liebminger et al., 2009). Glycosylation may be important for cell wall-modifying enzymes to function properly. It has been found that the glycosylation is important for the enzymatic activity and subcellular targeting of KORRIGAN1 (KOR1), an endo-β-glucanase involved in cellulose biosynthesis (Liebminger et al., 2013; Rips et al., 2014). Other than what is

known about KOR1, little information concerning how glycosylation affects activity, distribution

and substrate affinity of cell wall-modifying enzymes is available. In a previous chapter, I

showed that cell wall properties were affected by the distribution of cell wall-modifying

enzymes. Since N-glycosylation has been shown to be involved in targeting proteins to different

cell domains and PER36 was located in a domain distinct from other proteins secreted at the

same time, I was interested in whether N-glycosylation might be involved in the polar

distribution of PER36.

In this chapter, I first investigated if a specific sequence of PER36 was required for its unique

distribution. Afterward, I tested if PER36 was glycosylated and how secretion and distribution of

PER36 was affected by de-glycosylation. Finally, I examined whether components of the

secretory pathway controlling other proteins associated with the mucilage pocket, such as

MUM2, also control that of PER36.

5.2 Results

5.2.1 PER36 has a different distribution pattern from the other proteins in the seed coat epidermis secreted during mucilage synthesis

A chimeric gene where *PER36* was translationally fused to *Citrine* was constructed to

examine the subcellular distribution of PER36 in the seed coat epidermal cells. Unlike *MUM4*,

which is expressed from 5 DPA to 10 DPA, *PER36* is expressed from 6 DPA to 8 DPA. Since I

used the MUM4 promoter to express the genes for all the other proteins, I constructed a *PER36-Citrine* chimeric gene under the control of the *MUM4p1.5* promoter so that the subcellular

localization results for *PER36* would be directly comparable. This construct was transformed

into a *per36-2* mutant background. The *per36-2* mucilage phenotype was rescued, by the

construct indicating that the *PER36-Citrine* is functional. The distribution of Citrine fluorescence

in seed coat epidermal cells was examined by confocal microscopy. Consistent with the previous study (Kunieda et al., 2013), PER36-Citrine was found in the primary cell wall at the junction of the outer and radial cell walls of seed coat epidermal cells from 5 DPA to 8 DPA (Figure 5.1 A to G, J). The distribution of PER36-Citrine after 8 DPA was not studied previously because the native *PER36* promoter was used, which only expresses from 6 DPA to 8 DPA (Kunieda et al., 2013). The distribution of PER36-Citrine remained the same at 9 DPA and 10 DPA, although small amounts of PER36-Citrine were observed in the developing columella cell wall (Figure 5.1 H, I, K, L). This pattern of distribution contrasts with all other mucilage proteins that I have tested, which localize to the mucilage pocket/columella or plasma membrane surrounding it (see Chapter 3). This suggests that the amino acid sequence of PER36 and not the timing of expression is what determines its uniques intracellular localization pattern.
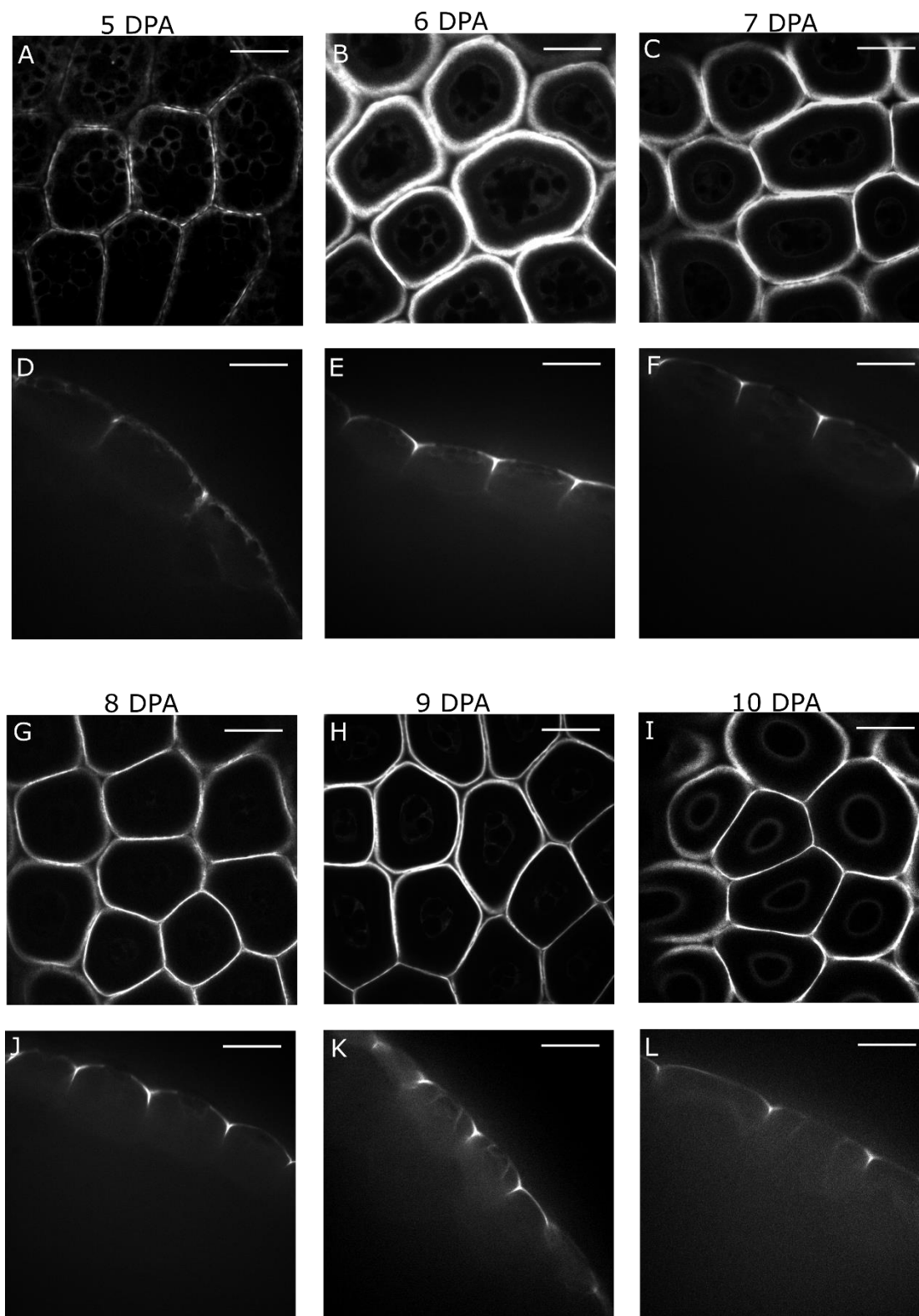
Figure 5.1: Distribution of PER36-Citrine in seed coat epidermis from 5 DPA to 10 DPA
(A) to (C) and (G) to (I) show transverse sections of seed coat epidermal cells. (D) to (F) and (J) to (L) show the longitudinal sections. Scale bar = 20 μm.

5.2.2 Certain domains of PER36 may be required for its unique distribution

To identify amino acid sequences of PER36 required for its unique distribution, three different truncated forms of PER36 including the predicted PER36 signal peptide, containing the first 28 amino acids in the N-terminus (PER36SP), amino acids 1 – 195 containing conserved region I and II of class III peroxidases (PER36$_{1-195}$) and amino acids 1 - 247 containing region I, II, and III of class III peroxidases (Mathé et al., 2010) (PER36$_{1-247}$) were translationally fused to Citrine (Figure 5.2 A). To make the distribution pattern comparable to that of full-length PER36-Citrine, the expression of the chimeric genes encoding different versions of tagged truncated *PER36* were driven by the *MUM4p1.5* promoter. Each construct was transformed into *per36-2* and the seed coats of transgenic plants were examined by confocal microscopy.

The fluorescence of PER36SP-Citrine accumulated in the mucilage pocket (Figure 5.2 B), similar to what was observed in MUM2-Citrine and secCitrine. These data suggest that the amino acid sequence of mature PER36 (without its signal peptide) is indeed required for its unique distribution in the primary cell wall. The fluorescence of PER36$_{1-195}$-Citrine and PER36$_{1-247}$-Citrine accumulated inside the cells (Figure 5.2 C, D) indicating that these truncated PER36 proteins are not secreted from the cell possibly because the truncation causes protein misfolding. Because of the retention, it not possible to know what aspect of the PER36 protein determines its polar distribution.
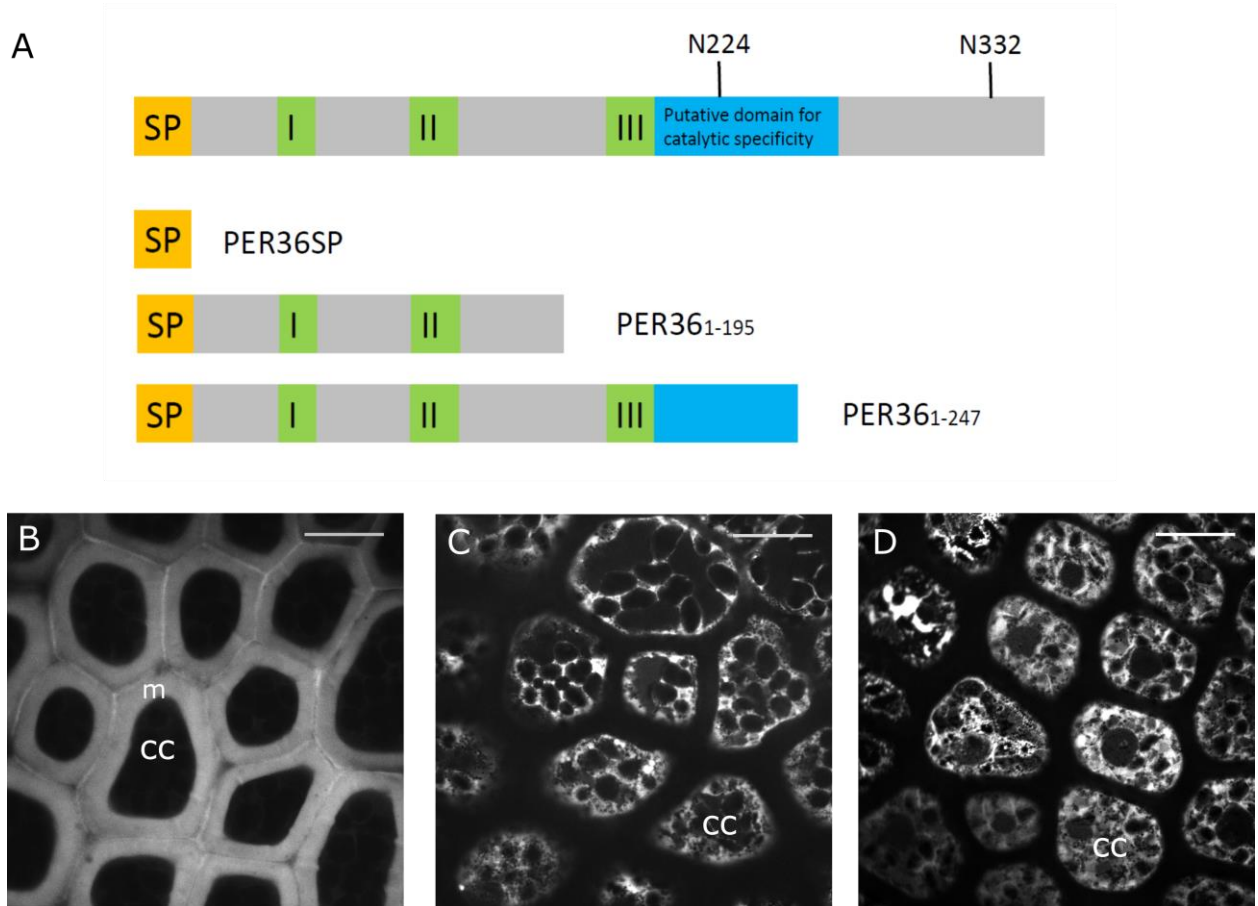
Figure 5.2: Distribution of truncated PER36-Citrine in seed coat epidermal cells at 7 DPA
(A) shows the protein structure of PER36. Conserved region I and III are heme-binding domains. Conserved region II is a conserved domain of unknown function. The blue box represents a putative domain for catalytic specificity, containing a loop in front of the substrate channel. PER36 also contains two predicted glycosylation sites. The domains of PER36 included in the three truncated versions that were constructed are shown. Confocal cross-sectional images of seed coat epidermal cells from lines carrying the following transgenic constructs are shown: *PER36SP-Citrine* (B), *PER36$_{1-195}$-Citrine* (C) and *PER36$_{1-247}$-Citrine* (D). Scale bar = 20 μm. cc: cytoplasmic columella; m: mucilage pocket.

To test if the sequence of PER36 was sufficient to bring another protein to the outer corner of primary cell walls, MUM2 was fused to PER36-Citrine to generate MUM2-PER36-Citrine chimeric protein. MUM2-PER36-Citrine fluorescence localized to the outer corner of the primary cell wall, similar to what was observed for PER36-Citrine (Figure 5.3A). Some of the

fluorescent signal was detected inside the cells, suggesting the chimeric proteins may not be

secreted as efficiently as PER36-Citrine. However, the size of the chimeric protein detected in

western blot analysis was the same as the size of PER36-Citrine (Figure 5.3 B). This suggested

that MUM2 was cleaved from MUM2-PER36-Citrine to produce PER36-Citrine. Hence, it is

still unclear whether the sequence of PER36 is sufficient to target an additional polypeptide to

the outer primary cell wall of seed coat epidermal cells.
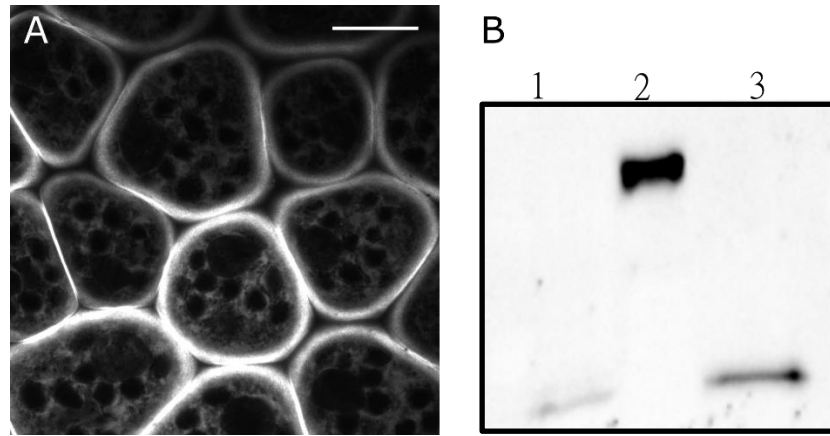
Figure 5.3: Distribution and molecular size of MUM2-PER36-Citrine
(A) shows the distribution of MUM2-PER36-Citrine in a cross section of seed coat epidermal
cells at 7 DPA. Scale bar = 20 μm. (B) shows a western blot where polypeptides containing
Citrine were detected among proteins extracted from siliques of *PER36-Citrine* (lane 1), *MUM2-Citrine* (lane 2), and *MUM2-PER36-Citrine* (lane 3) transgenic plants. Anti-GFP was used to
detect the Citrine domain of chimeric proteins.

5.2.3 PER36 is glycosylated in seed coats

To avoid possible protein misfolding caused by truncation, I focused on N-glycosylation sites of PER36. Because N-glycosylation has been shown to play a role in the targeting of proteins to the apical domains of animal epithelia cells (Vagin et al., 2009), I reasoned that N-glycosylation of PER36 might be involved in its cellular localization. In a previous study, it was found that PER36-GFPg4 had two different molecular masses of 68 and 65 kD. The 68 kD form of PER36 was first detected at 5 DPA. The 65 KD form appeared later at 6 DPA. The relative intensity of the two bands changed over time with the 68 kD form decreasing until only the 65 kD of PER36-GFPg4 was detected by 8 DPA. These data suggest that the 68 kD form of PER36 was processed to the 65 kD form of PER36-GFPg4 (Kunieda et al., 2013). The difference in molecular mass between the two forms of PER36-GFPg4 is roughly the same as the molecular weight of one N-linked glycan, suggesting that the difference may be due to N-glycosylation.

First, I repeated the experiments of Kunieda et al., confirming that two forms of PER36-Citrine exist at different development stages in the seed coats by conducting a western blot analysis. Proteins were extracted from siliques of ages 6 DPA to 10 DPA. Only the 68 kD form of PER36-Citrine was detected at 6 DPA, while only the 65 kD form was present at 10 DPA (Figure 5.4 A). Both forms were observed from 7 DPA to 9 DPA (Figure 5.4 A).

Next, I treated protein extracts from *PER36-Citrine* transgenic plants with de-glycosylation enzymes to test if PER36 is glycosylated. If so, the treatment would be expected to remove the glycan resulting in the loss of the 68 kD and an increase of 65 kD PER36-Citrine. Endo H and PNGase F are two de-glycosylation enzymes that remove different type N-linked glycans; Endo H removes glycans with high mannose content, while PNGase F removes all kinds of glycans except for the one with substitution of α-1,3-fucose residue on innermost N-acetylglucosamine (Maley et al., 1989; Tretter et al., 1991). When the protein extracts were treated with either of the

enzymes, the relative amount of 68 kD to 65 kD PER36-Citrine decreased dramatically (Figure 5.4 B). This experiment indicates that PER36 is glycosylated, and the difference of molecular mass between the two forms of PER36 results from N-glycosylation.

Finally, I investigated which site of PER36 might be glycosylated. Using the NetNGlyc program (Joshi and Gupta, 2015), PER36 had two predicted glycosylation sites at amino acid (a.a.) 224 and 322. Site-directed mutagenesis was conducted, replacing the asparagine (N) with a glutamine (Q) at each of the two sites. Three mutated versions of PER36 were generated, with either one site mutated (N244Q and N322Q) or both sites mutated (N12Q). The mutated versions of *PER36* were fused with *Citrine* and transformed into *per36-2* mutants. All of the mutated versions of *PER36* complemented *per36-2* mutants. Mutation of a glycosylation site is expected to result in a loss of glycosylation at that site, causing a band shift to lower molecular mass in a western blot. I found that only the 65 kD form of PER36 was present at 6 DPA in *PER36 (N224Q)-Citrine* transgenic plants, suggesting PER36 was glycosylated at a.a 224. However, although the majority of PER36 was present as the 65 kD form, a small amount of the 68 kD form of PER36 was observed from 7 DPA to 10 DPA, (Figure 5.4 B). In vitro de-glycosylation of PER36(N224Q)-Citrine with PNGase F confirmed that the small amount of 68 kD PER36(N224Q)-Citrine observed was the result of glycosylation (Figure 5.4 D). One explanation for the 68 kD form of PER36(N224Q)-Citrine observed is that glycosylation occurs less efficiently at a second site. If so, it is unlikely that the second site is at a.a. 332 since the western blot banding pattern of PER36(N332Q)-Citrine was similar to that of PER36-Citrine (Figure 5.4 C) and the banding pattern of PER36(N12Q)-Citrine was similar to PER36(N224Q)-Citrine (Figure 5.4 F). Instead, PER36 may be glycosylated at a non-conventional glycosylation site(s), such as Asn-X-Cys (Matsui et al., 2011) when the conventional site a.a 224 is not available. PER36 carries three putative Asn-X-Cys non-conventional glycosylation sites at a.a.

48, a.a. 86, and a.a. 128.
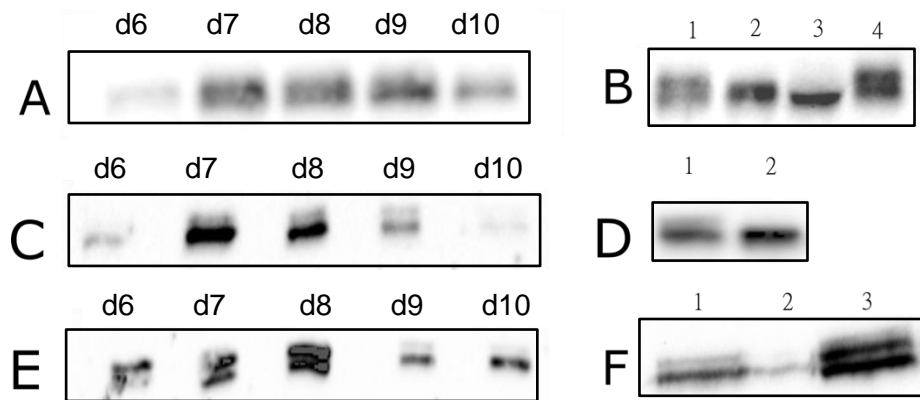
Figure 5.4: Western blots of PER36-Citrine and deglycosylated PER36-Citrine
(A), (C), (E) show that different sizes of bands are detected in siliques from 6 to 10 DPA (from left to right) in *PER36-Citrine* (A), *PER36(N224Q)-Citrine* (C), and *PER36(N332Q)-Citrine* (E) transgenic plants. (B) shows band shifts of PER36-Citrine with treatment of PNGase F (lane 2) and Endo H (lane 3) in comparison with no de-glycosylation (lane 1 and 4). (D) shows band shifts of PER36(N224Q)-Citrine with treatment of PNGase F (lane 2) in comparison to untreated one (lane 1). (F) shows the comparison of band sizes between PER36-Citrine from siliques of 7 DPA (lane 3) and PER36(N12Q)-Citrine from siliques of 7 DPA (lane 1) and from siliques of 9 DPA (lane 2).

5.2.4 Glycosylation is involved in the proper folding of PER36 and likely secretion in seed coats

To find out whether glycosylation is required for PER36 targeting, the distribution of the mutated PER36-Citrine in seed coats was examined by confocal microscopy. Consistent with the normal glycosylation pattern observed in the western blot analysis of PER36(N322Q)-Citrine (Figure 5.4 E), most fluorescent signal of PER36(N322Q)-Citrine was detected in the outer corners of cell walls (Figure 5.5 B, E). In contrast, the majority of PER36(N224Q)-Citrine and PER36(N12Q)-Citrine was distributed inside the cells (Figure 5.5 A, D; C, F). A small amount of PER36(N224Q)-Citrine was observed in the outer corner of the cell wall similar to what was seen for PER36-Citrine. Consistently, *per36-2* mutant was also complemented by all of the three mutated PER36s. However, the PER36(N224Q)-Citrine observed in the cell wall could represent the fraction that is glycosylated (Figure 5.4 B). For this reason, it is not possible to conclude from these experiments whether glycosylation is required for PER36 localization in the cell wall.
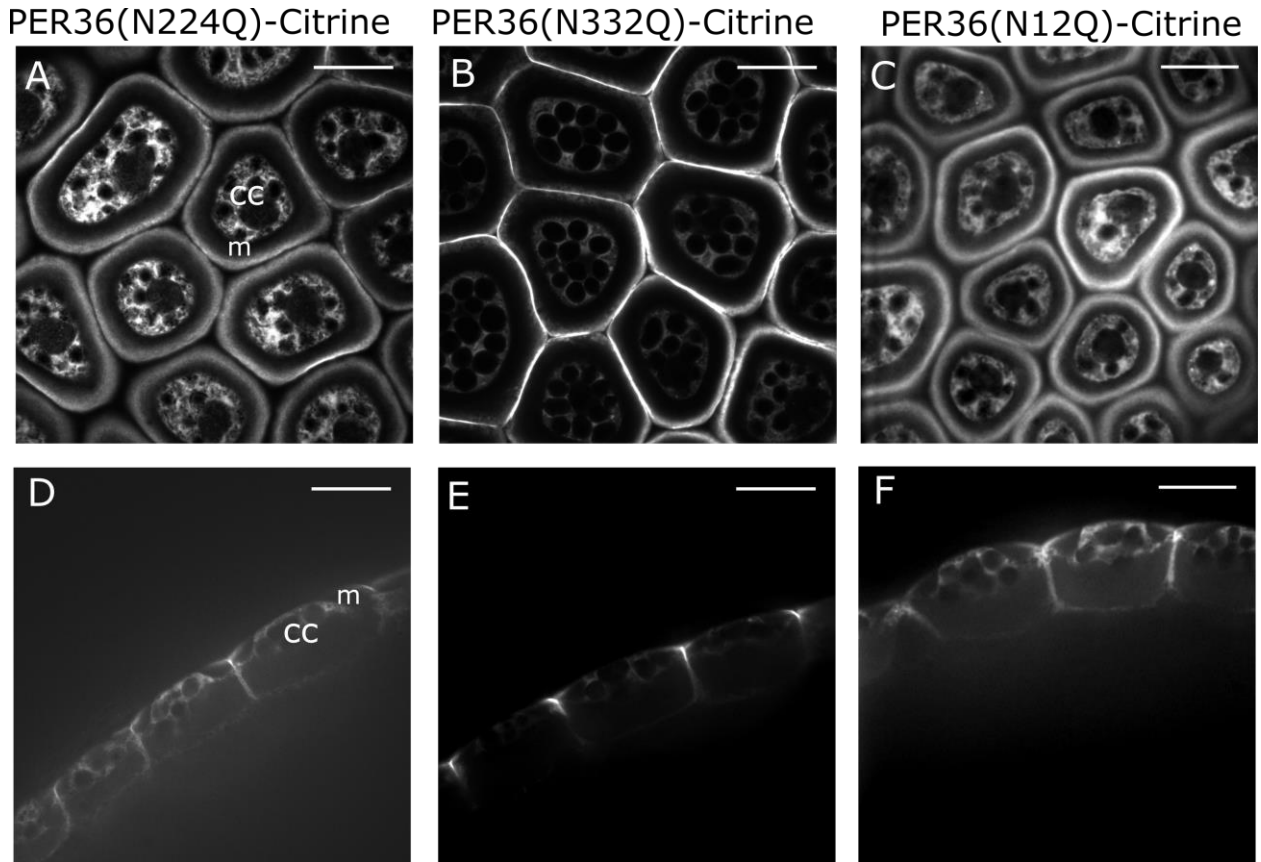
Figure 5.5: Distribution of PER36(N224Q)-Citrine, PER36(N322Q)-Citrine, and PER36(N12Q)-Citrine in seed coat epidermis at 7 DPA

(A) to (C) show transverse sections of seed coats. (D) to (F) show longitudinal sections. Scale bar = 20 μm. cc: cytoplasmic columella; m: mucilage pocket.

The retention of PER36(N224Q)-Citrine in the cytoplasm could be due to improper protein folding. The N224Q substitution could cause misfolding in one of two ways. The change in amino acid could cause protein instability directly. Alternatively, glycosylation has be shown to be important for protein folding and protein quality control in the ER (reviewed by Lannoo and Van Damme, 2015). Therefore, the intracellular localization of PER36(N224Q)-Citrine could be due to the lack of glycosylation. To distinguish between these two possibilities, I sought a different method, other than manipulation of amino acid sequence, to examine the localization of non-glycosylated PER36. Glycoproteins sometimes have different patterns of glycosylation in

different tissues. This may be true for PER36, because it was present only as the 65 kD form in tissues other than the seed coat when expressed ectopically (*Pro35S:PER36-GFPg4*; Kunieda et al., 2013). For this reason, I examined the size and localization of PER36-GFPg4 in leaves of *Pro35S:PER36-GFPg4 per36-1* plants to that of PER36-Citrine extracted from siliques of *MUM4p1.5: PER36-Citrine per36-2* (the molecular weight of GFP4g is the same as that of Citrine). I found that PER36-GFP4g in leaves was predominantly 65 kD in size (Figure 5.6 B), indicating that PER36 was not glycosylated in leaves. The non-glycosylated PER36-GFP4g was found to accumulate inside the cells (Figure 5.6 A). These data suggest that glycosylation may be important for PER36 to be secreted properly.
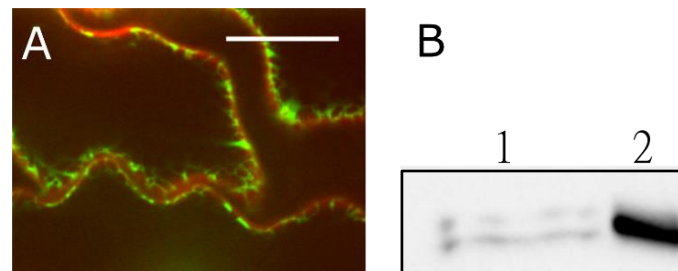
Figure 5.6: Distribution of PER36-GFP4g in leaf epidermis and a western blot of tagged PER36 from siliques and leaves

(A) shows the distribution of PER36-GFP4g (in green) with plasma membrane stained by FM4-64 (in red) in leaf epidermal cells. Scale bar = 20 μm. (B) shows PER36-GFPg4 from leaves (lane 2) and PER36-Citrine from siliques (lane 1).

Since non-glycosylated PER36 was not secreted from the cell, it is unclear whether glycosylation is involved in targeting PER36 to specific apoplastic domain. However, PER36 belongs to a large protein family of class III peroxidases, which contains 73 members in Arabidopsis. Each member has different putative glycosylation sites (Welinder et al., 2002), so some peroxidases closely related to PER36 lack the two predicted glycosylation sites at a.a. 224 and a.a. 322. Since these peroxidases don't have the glycosylation sites, the glycosylation at

these sites is not required for them to fold properly. According to the phylogenetic analysis (Tognolli et al., 2002) and results from the glycosylation prediction program NetNGlyc, the most closely-related peroxidases that lack these two predicted glycosylation sites were PEROXIDASE9 (PRX9) and PRX20, with 53% and 51% identity to PER36, respectively (Figure 5.7 A). PRX20 was chosen, because PRX9 has another predicted glycosylation site nearby (at a.a. 259). PRX72 (with 71% identity), which is the most closely related peroxidase to PER36 containing both predicted glycosylation sites, was also included as a positive control.

PRX20 and *PRX72* were fused to *Citrine* and the expression was driven by the *MUM4p1.5* promoter. The constructs were transformed into *per36-2* mutants and the distribution of fluorescent signal in seed coats of transgenic plants was characterized by confocal microscopy. *PRX72* partially complemented *per36-2* mutant, while *PRX20* did not. PRX20-Citrine was distributed in a punctate pattern inside the cells, suggesting that PRX20-Citrine accumulated in the endomembrane system (Figure 5.7 B, E), indicating that PRX20 was not secreted properly. In contrast, the majority of fluorescent signal of PRX72-Citrine was detected at the outer corner of the cell wall similar to PER36-Citrine, with weaker signal observed in the mucilage pocket (Figure 5.7 C, F). In addition, PRX72-Citrine disappeared from the mucilage pocket and accumulated along the columella at 9 DPA, although the fluorescent signal was still detectable in the outer corner of the primary cell walls (Figure 5.7 D, G). Although some signal of PER36-Citrine was also observed in the columella at 9 DPA (Figure 5.1 K), it was much weaker than that of PRX72-Citrine. These data suggest that PRX72 can be targeted in a manner similar to PER36 but perhaps less efficiently.
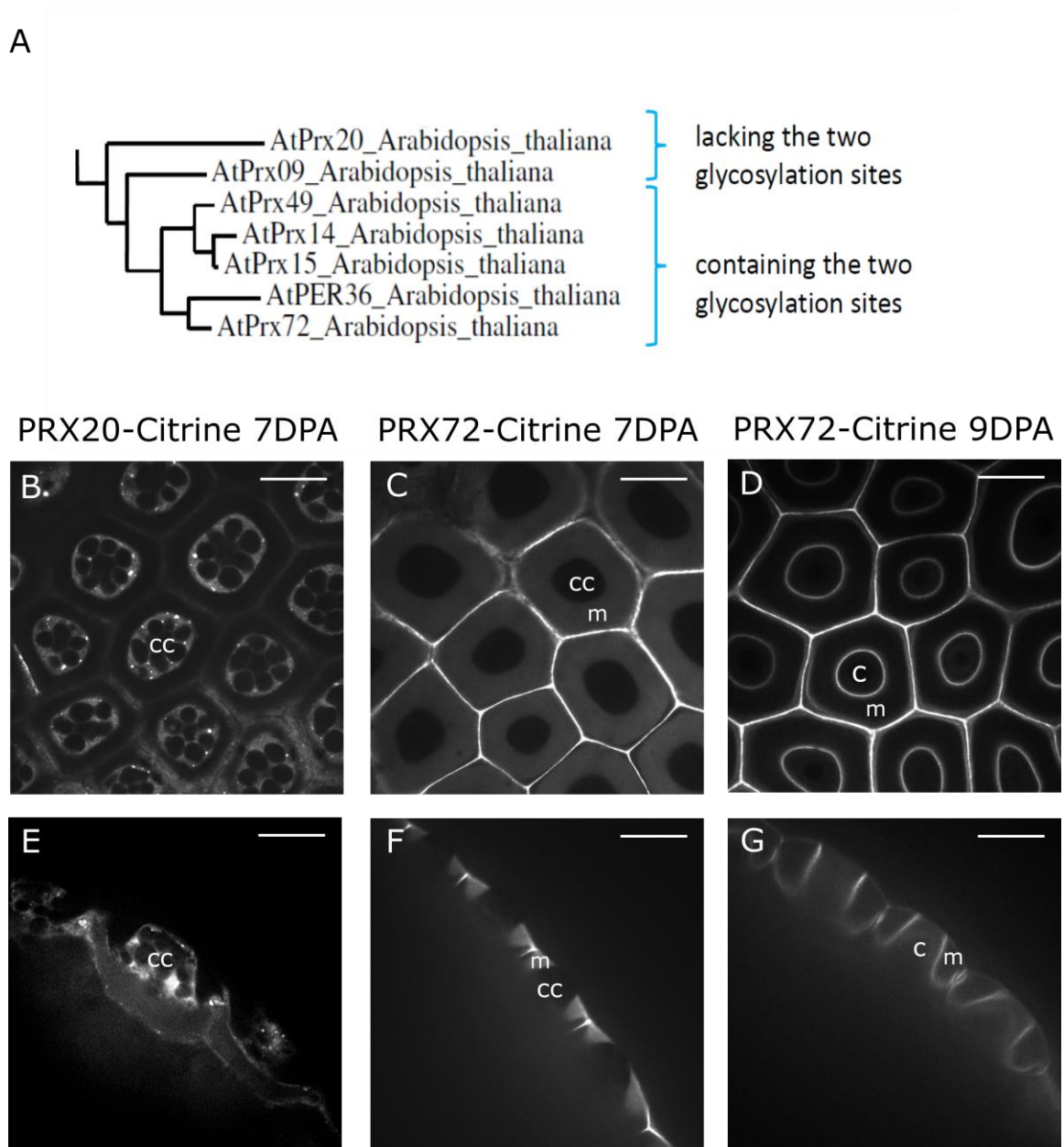
Figure 5.7: Phylogenetic relationship of PER36-related peroxidases and the distribution of two close-related peroxidases, PRX20-Citrine and PRX72-Citrine in seed coats

(A) shows a phylogenic trees of Arabdiopsis class III peroxidase regenerated according to Tognolli et al., 2001. Only the clade with PER36-related peroxidases is shown. (B) and (E) show the distribution of PRX20-Citrine in seed coat epidermal cells at 7 DPA. The distribution of PRX72-Citrine at 7 DPA (C, F) and 9 DPA (D, G) was also shown. (B) to (D) show transverse sections of seed coats. (E) to (G) show longitudinal sections. Scale bar = 20 μm. c: columella; cc: cytoplasmic columella; m: mucilage pocket.

5.2.5 Secretion of PER36 is mediated by ECH

Since that PER36 was distributed in a pattern different from other proteins secreted by the seed coat epidermal cells, I was curious to determine if PER36 was dependent on similar components of the secretory pathway. To test this hypothesis, *MUM4p1.5: PER36-Citrine* was crossed into an *ech* mutant background to determine if, like MUM2-Citrine (see section 3.2.5), the secretion of PER36-Citrine was dependent on ECH. PER36-Citrine was found to accumulate in the vacuole in *ech* mutants, although a strong fluorescent signal was detected in the outer corner of the cell walls (Figure 5.8 A, D). These data suggest that both MUM2 and PER36 secretion rely on ECH. Unexpectedly, PER36-Citrine accumulated in the mucilage pocket at 8 DPA and partially disappears from the pocket at 9 DPA (Figure 5.8 B, C, E, F), while fluorescence persists in the primary cell wall and accumulates in the developing columella.
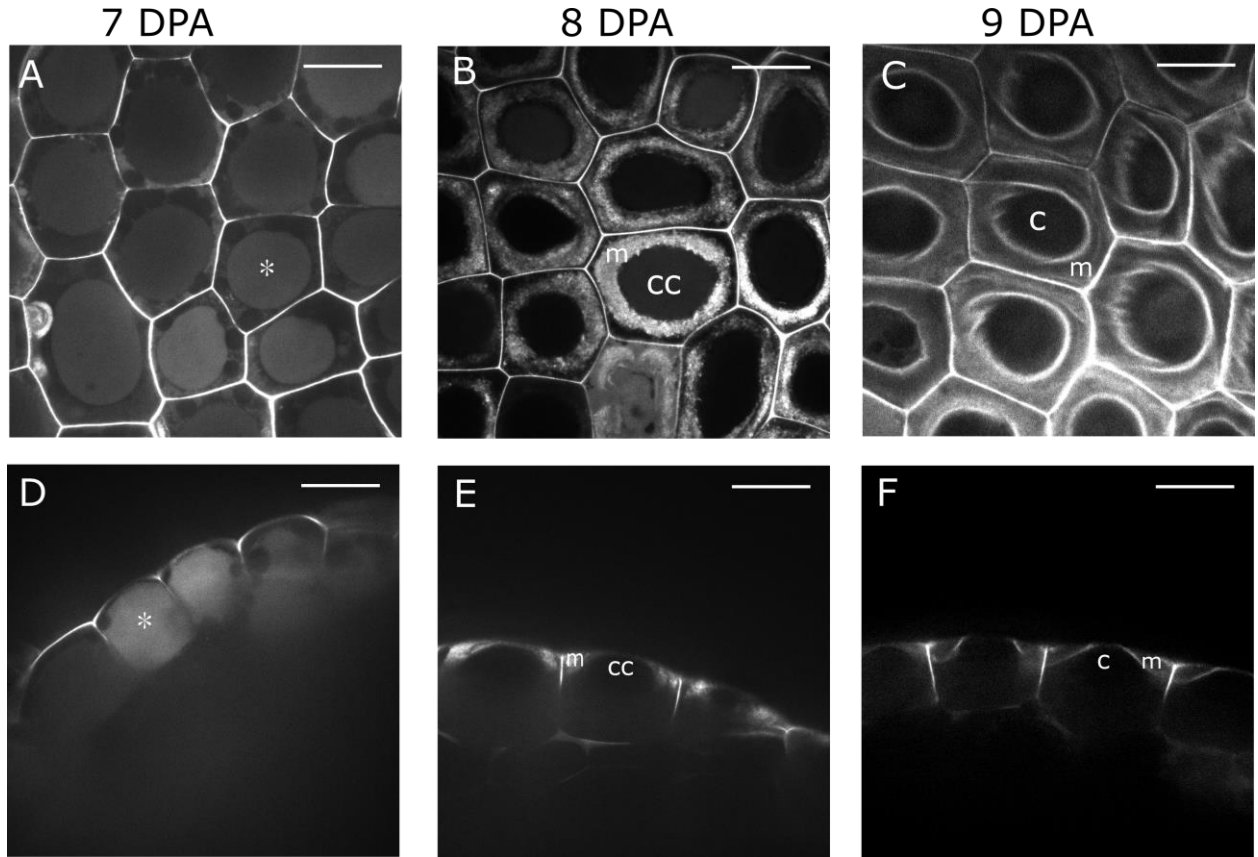
Figure 5.8: Distribution of PER36-Citrine in seed coats epidermal cells of an *ech* mutant from 7 DPA to 9 DPA

(A) to (C) show transverse sections of seed coats. (D) to (F) show longitudinal sections. Star marks (*) indicate where vacuoles are. Scale bar = 20 μm. c: columella; cc: cytoplasmic columella; m: mucilage pocket.

5.3 Discussion

5.3.1 PER36 is distributed in a unique pattern by an unknown mechanism

PER36 is distributed in a pattern distinct from other proteins in seed coat epidermal cells. To eliminate the possibility that temporal differences in the transcription of *PER36* result in the different localization from other mucilage proteins, *PER36* was placed under the control of the *MUM4p 1.5* promoter. Since the localization of PER36 was comparable regardless of whether the *MUM4p 1.5* or the native promoter was used (Kunieda et al., 2013; this work), the exact timing of transcription cannot account for the differences in localization.

PER36SP-Citrine, which includes only the signal peptide of PER36, was localized to the mucilage pocket and not the primary wall. Besides, PRX72, a peroxidase sharing 71% sequence identity with PER36, also accumulated in outer corner of primary cell wall. These data suggest that some aspect of the mature polypeptide sequence of these peroxidases is responsible for its localization to the primary cell wall. Some PRX72 was also found in the mucilage pocket. These data demonstrate that it is possible for a peroxidase to be located in the mucilage pocket. It is likely that whatever mechanism determines PER36 localization, the differences in amino acid sequence between PER36 and PRX72 make the process less efficient.

Features of PER36 that could influence its localization in the primary cell wall remain unknown because all changes I made to the mature amino acid sequence of PER36 resulted in poor or no secretion. However, aspects related to the PER36 amino acid sequence that could influence its localization include glycosylation (section 5.3.2 and 5.3.3), interaction with its substrate in the wall (section 5.3.3 and 5.3.4) or interaction with another polypeptide (section 5.3.4).

5.3.2 Glycosylation of PER36 is required for its secretion

Several pieces of evidence presented in this chapter demonstrate a correlation between the N-glycosylation of PER36 and its ability to be secreted to the apoplast. First, the loss of glycosylation through the mutation of a putative glycosylation site resulted in the retention of PER36 in the cytoplasm. Second, in leaf cells, ectopically expressed PER36 was not glycosylated and accumulated in the cytoplasm. Third, the PER36-related peroxidase PRX20, which lacks the two putative glycosylation sites, was also found to accumulate in the cytoplasm.

N-Glycosylation may be important for proteins to exit the Golgi. It has been found in animals that some apical proteins accumulate in the Golgi when glycans were removed (Gut et al., 1998). When basolateral targeting signals were removed from some non-glycosylated basolateral proteins, accumulation in the Golgi was also observed. In addition, when glycans were added to the non-glycosylated basolateral proteins without sorting signals, the glycosylated truncated basolateral proteins were sorted to the apical domains. These examples suggest that the exit of Golgi is signal-mediated (Gut et al., 1998), and N-linked glycan can act as one of the signals. However, it is believed that protein secretion in plants does not require any specific signal. It is unknown why the proteins can not be secreted when signals are removed.

Glycosylation may also be important for protein folding and quality control; the misfolded protein would be retained in the ER and be degraded by ERAD pathways eventually (Vitale and Boston, 2008; Hüttner and Strasser, 2012). The failure in secretion of non-glycosylated PER36 may be due to ER retention. In contrast, non-glycosylated proteins can reach the Golgi by escaping from the ERAD pathway. It has been found in yeast that some defective secretory proteins escape from the ERAD pathways and are sorted in the Golgi to the vacuole for degradation (Vitale and Boston, 2008). In plants, non-glycosylated KOR1 was found to be sorted to the vacuole possibly because non-glycosylated KOR1 is unstable (Rips et al., 2014). It is

possible that PRX20 is transported to the Golgi to be degraded in the vacuole, too.

In my studies, I showed that N-glycosylation is required for PER36 secretion, but whether glycosylation was responsible for targeting to different apoplastic domains remains unclear.

5.3.3 Glycosylation may be involved in enzyme activity, stability and substrate binding

Glycosylation may play other important roles in the function of PER36. First, it has been found that glycosylation is important for enzymatic activity and stability of a peanut peroxidase (Lige et al., 2001), although another study showed that glycosylation is not involved in enzyme activity of a horseradish peroxidase (Tams and Welinder, 1995). I found the PER36(N224Q) and PER36(N12Q) were more likely to be degraded than wild type PER36 when proteins were denatured by heat, suggesting that non-glycosylated PER36 may be less stable. In addition, glycosylation can provide steric protection from protease digestion (Rudd et al., 2001; Escrevente et al., 2008). The non-glycosylated PER36 may be more accessible for proteases to digest. Although the *per36-2* mutants were complemented by the mutated versions of PER36, I could not conclude if glycosylation affected enzymatic activity because a small amount of mutated PER36 was glycosylated and secreted and this glycosylated protein may have been sufficient for activity.

Second, glycosylation may affect substrate binding. PER36 is glycosylated at a.a. 224, which is located in the putative substrate-binding domains of peroxidases (Mathé et al., 2010). It has been shown that N-glycosylation can either increase ligand-binding ability or hinder access to substrate (Skropeta, 2009). PER36 is processed from a large form (glycosylated) to a small form (de-glycosylated). The glycosylated form was present in the microsomal fraction, while the de-glycosylated form was in the soluble fraction (Kunieda et al., 2013), indicating that glycan was removed from PER36 after secretion. Therefore, it is more likely that the glycan on the PER36

may block the access to substrates.

A difference in substrate binding and stability resulting from glycosylation may contribute to protein distribution. PRX72 was present in both the outer corners of primary cell walls and in the mucilage pocket, while PER36 was only present in the primary cell wall. PRX72 has the two glycosylation sites and may be glycosylated at a.a. 224. However, it is unknown if the glycan on PRX72 is removed after PRX72 is secreted. Failure to efficiently remove glycan from the substrate-binding domains of PRX72 may reduce its affinity to substrates in the primary cell wall. Therefore, unbound PRX72 may remain in the mucilage pocket. Also, it has been found that glycosylation changes substrate specificity (Skropeta, 2009). Glycosylated PRX72 may be able to bind primary cell wall, mucilage, and columella. Further, glycosylation may protect glycoprotein from protease digestion (Rudd et al., 2001; Escrevente et al., 2008). I showed that the disappearance of MUM2 from the mucilage pocket was due to degradation by proteases. It is possible that de-glycosylated PER36 in the pocket is digested by proteases such as SCPL35 from 6 DPA to 8 DPA, while glycosylated PRX72 is not.

5.3.4 Hypothetical mechanisms of polar distribution of PER36

PER36 was mis-sorted to the vacuole in the *ech* mutant similar to MUM2, suggesting that PER36 may share the same secretory pathway with MUM2. The question of how PER36 is deposited in the cell wall rather than the mucilage pocket remains unanswered. At least three models could explain the observed unique distribution of PER36 (Figure 5.9). First, (Figure 5.9 A; Protease digestion model) PER36 is secreted early 5-6 DPA and associated with the cell wall before the membrane is separated from the cell wall by mucilage secretion. Subsequently PER36 secreted to the pocket is degraded. Second, (Figure 5.9 B; Transportation model) PER36 is secreted to the mucilage pocket and the protein is transported to the primary cell wall by an

unknown mechanism. Only the PER36 transported to the wall persists. Third, (Figure 5.9C; Two secretory pathways model) PER36 is targeted to the junction between membrane and the outer radial primary cell wall where the membrane meets the cell wall by an unknown secretory mechanism.
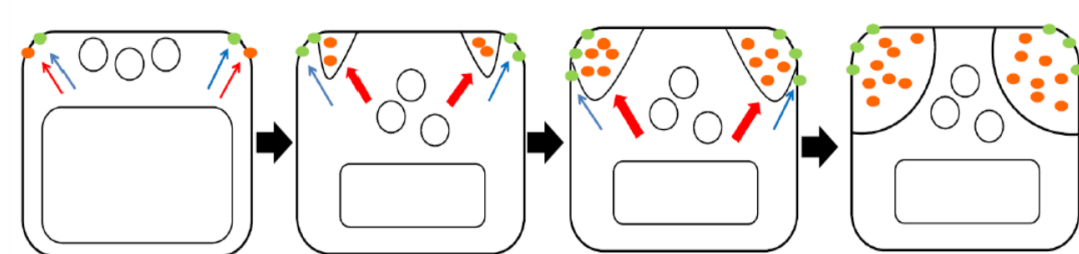
Figure 5.9: Three hypothetical models for mechanisms of PER36 distribution

The Protease Digestion model (Figure 5.9 A) is most likely because it is the simplest requiring no components for transport or secretion. Also, I showed that cell wall proteins in the mucilage pocket can be degraded, and a protease, SCPL35, was secreted to the mucilage pocket during the

period of MUM2 and mucilage secretion (Chapter 4). This model suggests that all proteins, including MUM2 and PER36 are targeted to the same domains of the cell. However, there is some difference between the distribution patterns of MUM2-Citrine and PER36-Citrine even prior to the formation of the mucilage pocket. Although like PER36-Citrine, strong MUM2-Citrine fluorescent signal was detected at the junction where radial and outer periclinal cell walls meet, weaker signal was detected around the entire outside of the cell. In contrast, PER36-Citrine fluorescent signal was only observed in the junction. The reason for this difference is unclear.

In the Transportation model (Figure 5.9 B), PER36 may be transferred to the outer corner of primary cell wall by some unknown transport proteins. It is also possible that PER36 has a strong affinity for the substrates residing the cell wall and therefore remain in the wall once there. However, to date, no such transport proteins have been identified and fluorescence that could account for PER36-Critine in transport has not been observed in the pocket. Also, how the transport proteins are able to target a specific domain of the cell wall is also unknown.

The Two Secretory Pathway model requires establishment of a novel secretory pathway, so it seems to be the least likely of three models.

None of the three pathways are mutually exclusive. It is possible the more than one mechanism is involved in the distribution of PER36. For example, some PER36 may be transported to the junction between radial and outer periclinal cell walls, while other may be digested by proteases in mucilage pocket. More evidence is required to determine which if any of the hypotheses is correct.

Chapter 6 : Conclusions

6.1   Major findings of this work

Plant cells deposit large amounts of cell wall polysaccharides to the apoplast. Cell wall proteins, which may play roles in modification of cell wall properties, are also secreted to the apoplast. Spatiotemporal deposition of different cell wall components is important for morphogenesis and cellular functions. However, a comprehensive answer to the question of how plants are able to deposit cell wall components in a polar manner remains elusive. In addition, how the cell wall polysaccharides are secreted and how the distribution is related to the modifying enzyme are largely unknown, too.

Arabidopsis seed coat epidermal cells are considered to be a good model for studying biosynthesis and secretion of cell wall components because they deposit a large amount of pectin-rich mucilage and cell wall proteins in a polar manner to a region of the apoplast called the mucilage pocket. In my thesis research, I found that in Arabidopsis seed coat epidermal cells the polar distribution of mucilage and cell wall proteins such as MUM2, is 1) most likely achieved through polar secretion and 2) determined by cell type and not by target protein sequence. Soluble secreted proteins ectopically expressed in seed coat epidermal cells such as MUM2 are found in the mucilage pocket. However, the distribution of MUM2 is nonpolar in tissues other than seed coats. That the secretory pathway appears to target cargo to the mucilage pocket during the period of mucilage secretion is also supported by the fact that VAMP721-containing vesicles were found to fuse only to the region of the plasma membrane surrounding the mucilage pocket. Also, the distribution of VAMP721 was disrupted in the same way as that of MUM2 and mucilage in *ech* mutants, suggesting both of MUM2 and mucilage are secreted in a polar manner, through a VAMP721-mediated pathway. This also suggests that cell wall

proteins and polysaccharides share in common at least some elements of their secretory pathway in seed coats. My results establish that polar secretion in seed coat epidermal cells involves redirection of the secretory pathway from nonpolar to polar during differentiation and provide a basis for future studies in secretion of cell wall components in Arabidopsis seed coats.

At the end of secretion, soluble proteins in the mucilage pocket abruptly disappear due to protein degradation. In the case of MUM2, this degradation is mediated by ASPG1 and RD21A, two proteases secreted to the mucilage pocket at the end of MUM2 secretion. Although some studies suggest that proteases may degrade cell wall proteins (Rautengurten et al., 2008), my work provides strong evidence showing the removal of cell wall proteins from a specific domain through degradation by proteases. Also, my research suggests that the timing of degradation of cell wall proteins is regulated by the timing of translocation of the protease RD21A, although the mechanism of the translocation is unknown.

In addition to polar secretion and protease degradation, there may be other mechanisms determining the distribution of cell wall proteins. PER36 is uniquely distributed in the primary cell walls adjacent to the mucilage. I found the sequence of PER36 is required for the unique distribution pattern; PER36SP-Citrine was distributed in a similar pattern as MUM2-Citrine. Also, PER36 was secreted by ECH-mediated pathway, suggesting that PER36 is likely secreted to the pocket but is localized only to the outer corner of the cell walls by unknown mechanisms. The fact that PRX72 accumulated in both mucilage pocket and the outer corner of the primary cell wall suggests that the mechanism determining accumulation in the primary cell wall may be different from the mechanism of removal from the mucilage pocket. Knowledge concerning the degradation of proteins in the mucilage pocket will be important when attempting to target valuable transgenic proteins to the mucilage pocket of crop species.

6.2 Perspectives and future directions

My thesis research shows that polar secretion contributes to polar distribution of cell wall components, and cell wall proteins and polysaccharide may share a secretory pathway, at least in part. However, the molecular mechanisms that establish polarity in seed coat epidermal cells remain unknown. To identify components of this mechanism, forward or reverse genetics could be employed. For example, a forward genetic screen identifying mutants that miss-target MUM2-Citrine could be conducted to identify genes encoding proteins needed for polar secretion. On the other hand mutants defective for genes already identified as being involved in polar secretion, such as members in ROP family, could be examined for their effect on MUM2 secretion.

Although polar secretion seems the most likely mechanism for polar distribution of mucilage and proteins in seed coat epidermal cells, we can't rule out the possibility that polarity is also generated through asymmetric endocytosis where secreted products in one region of the cell are removed from some regions and not others. To test this hypothesis, I could investigate whether the polar distribution patterns of MUM2 and mucilage are lost when endocytosis is blocked by chemical and genetic manipulation.

In my studies, I also show that the degradation of MUM2 after 8 DPA is regulated by the translocation of protease RD21A. However, the distribution of ASPG1 is still unknown. Transgenic plants carrying ASPG1-RFP can be used to examine how the distribution of ASPG1-RFP is related to disappearance of fluorescent signal of MUM2-Citrine. Besides, the mechanism controlling protease targeting is unknown. I have suggested that the pro-domain of the proteases might be involved in targeting proteases to the vacuole. I can test if the pro-domain carries a vacuole-sorting signal by examining the distribution of fluorescent protein-tagged pro-domains. One possibility for translocation is that the trafficking route to the vacuole is redirected to the

plasma membrane at 9 DPA. To test this hypothesis, I can examine if the distribution pattern of trafficking components on the vesicles destined for the vacuole, such as VAMP727, changes at 9 DPA. Another possible mechanism for the translocation is that the pro-domains carrying vacuole-sorting signals are processed at 9 DPA before the pro-proteins are sorted in the trans-Golgi network. The processing of the proteases at different developmental stages of seeds can be examined by western blot analysis. By combining western blot analysis and suborganellar fractionation, I can understand where ASPG1 and RD21A are processed in the endomembrane system at different developmental stages.

PER36 has a unique distribution in seed coats. To explain the unique pattern, I proposed three models, a protease digestion model, a transportation model and a two-secretory-pathway model. To determine which of these models might be correct, I could investigate if PER36 is secreted together with MUM2 by co-immunolabeling; if PER36 and MUM2 are found in the same vesicle, they must be secreted together. In addition, I could test if the absence of PER36 in the mucilage pocket is due to protein degradation by crossing PER36-Citrine into the protease mutants.

Although many cell wall proteins are glycosylated, how glycosylation affects cell wall proteins remains largely unexplored. In my studies, I found that PER36 is glycosylated, and that this glycosylation may be important for its secretion. It has been suggested that glycosylation is required for some secretory proteins to exit the Golgi (Gut et al., 1998). I can test this hypothesis by adding a glycosylation site equivalent to the N224 of PER36 to PRX20, which is retained in the cytoplasm of seed coat epidermal cells, to see if the modified PRX20 would be secreted. In addition to PER36, MUM2 also has several putative glycosylation sites. I confirmed that MUM2 is also glycosylated by treating it with de-glycosylation enzymes (data not shown). It would be interesting to test how MUM2 is affected by glycosylation.

References

Abramoff, M.D., Magalhães, P.J., and Ram, S.J. (2004). Image processing with ImageJ. Biophotonics Int.

Alassimone, J., Naseer, S., and Geldner, N. (2010). A developmental framework for endodermal differentiation and polarity. Proc. Natl. Acad. Sci. **107**: 5214–5219.

Albenne, C., Canut, H., and Jamet, E. (2013). Plant cell wall proteomics: the leadership of Arabidopsis thaliana. Front. Plant Sci. **4**.

Alberts, B., Johnson, A., Lewis, J., Raff, M., Roberts, K., and Walter, P. (2002). Molecular Biology of the Cell 4th ed. (Garland Science).

An, H.J., Froehlich, J.W., and Lebrilla, C.B. (2009). Determination of glycosylation sites and site-specific heterogeneity in glycoproteins. Curr. Opin. Chem. Biol. **13**: 421–426.

Anderson, C.T. (2016). We be jammin': an update on pectin biosynthesis, trafficking and dynamics. J. Exp. Bot. **67**: 495–502.

Anderson, C.T., Wallace, I.S., and Somerville, C.R. (2012). Metabolic click-labeling with a fucose analog reveals pectin delivery, architecture, and dynamics in Arabidopsis cell walls. Proc. Natl. Acad. Sci. **109**: 1329–1334.

Angers, C.G. and Merz, A.J. (2011). New links between vesicle coats and Rab-mediated vesicle targeting. Semin. Cell Dev. Biol. **22**: 18–26.

Arcalis, E., Stadlmann, J., Rademacher, T., Marcel, S., Sack, M., Altmann, F., and Stoger, E. (2013). Plant species and organ influence the structure and subcellular localization of recombinant glycoproteins. Plant Mol. Biol. **83**: 105–117.

Arsovski, A.A., Haughn, G.W., and Western, T.L. (2010). Seed coat mucilage cells of Arabidopsis thaliana as a model for plant cell wall research. Plant Signal. Behav. **5**: 796–801.

Arsovski, A.A., Popma, T.M., Haughn, G.W., Carpita, N.C., McCann, M.C., and Western, T.L. (2009). AtBXL1 Encodes a Bifunctional β-d-Xylosidase/α-l-Arabinofuranosidase Required for Pectic Arabinan Modification in Arabidopsis Mucilage Secretory Cells. Plant Physiol. **150**: 1219–1234.

Atmodjo, M.A., Hao, Z., and Mohnen, D. (2013). Evolving Views of Pectin Biosynthesis. Annu. Rev. Plant Biol. **64**: 747–779.

Atmodjo, M.A., Sakuragi, Y., Zhu, X., Burrell, A.J., Mohanty, S.S., Atwood, J.A., Orlando, R., Scheller, H.V., and Mohnen, D. (2011). Galacturonosyltransferase (GAUT)1 and GAUT7 are the core of a plant cell wall pectin biosynthetic homogalacturonan:galacturonosyltransferase complex. Proc. Natl. Acad. Sci. **108**: 20225–20230.

Bard, F. and Malhotra, V. (2006). The Formation of TGN-to-Plasma-Membrane Transport Carriers. Annu. Rev. Cell Dev. Biol. **22**: 439–455.

Batoko, H., Zheng, H.-Q., Hawes, C., and Moore, I. (2000). A Rab1 GTPase Is Required for Transport between the Endoplasmic Reticulum and Golgi Apparatus and for Normal Golgi Movement in Plants. Plant Cell **12**: 2201–2217.

Beers, E.P., Jones, A.M., and Dickerman, A.W. (2004). The S8 serine, C1A cysteine and A1 aspartic protease families in Arabidopsis. Phytochemistry **65**: 43–58.

Bogamuwa, S. and Jang, J.-C. (2016). Plant Tandem CCCH Zinc Finger Proteins Interact with ABA, Drought, and Stress Response Regulators in Processing-Bodies and Stress Granules. PLOS ONE **11**: e0151574.

Boisson, M., Gomord, V., Audran, C., Berger, N., Dubreucq, B., Granier, F., Lerouge, P., Faye, L., Caboche, M., and Lepiniec, L. (2001). Arabidopsis glucosidase I mutants reveal a critical role of N-glycan trimming in seed development. EMBO J. **20**: 1010–1019.

Bosch, M., Cheung, A.Y., and Hepler, P.K. (2005). Pectin Methylesterase, a Regulator of Pollen Tube Growth. Plant Physiol. **138**: 1334–1346.

Bosch, M. and Hepler, P.K. (2005). Pectin Methylesterases and Pectin Dynamics in Pollen Tubes. Plant Cell **17**: 3219–3226.

Boutté, Y., Jonsson, K., McFarlane, H.E., Johnson, E., Gendre, D., Swarup, R., Friml, J., Samuels, L., Robert, S., and Bhalerao, R.P. (2013). ECHIDNA-mediated post-Golgi trafficking of auxin carriers for differential cell elongation. Proc. Natl. Acad. Sci. **110**: 16259–16264.

Bove, J., Vaillancourt, B., Kroeger, J., Hepler, P.K., Wiseman, P.W., and Geitmann, A. (2008). Magnitude and Direction of Vesicle Dynamics in Growing Pollen Tubes Using Spatiotemporal Image Correlation Spectroscopy and Fluorescence Recovery after Photobleaching. Plant Physiol. **147**: 1646–1658.

Bradford, M.M. (1976). A rapid and sensitive method for the quantitation of microgram quantities of protein utilizing the principle of protein-dye binding. Anal. Biochem. **72**: 248–254.

Bu, T., Shen, J., Chao, Q., Shen, Z., Yan, Z., Zheng, H., and Wang, B. (2017). Dynamic N-glycoproteome analysis of maize seedling leaves during de-etiolation using Concanavalin A lectin affinity chromatography and a nano-LC–MS/MS-based iTRAQ approach. Plant Cell Rep. **36**: 1943–1958.

Burton, R.A., Gidley, M.J., and Fincher, G.B. (2010). Heterogeneity in the chemistry, structure and function of plant cell walls. Nat. Chem. Biol. **6**: 724.

Caffall, K.H. and Mohnen, D. (2009). The structure, function, and biosynthesis of plant cell wall pectic polysaccharides. Carbohydr. Res. **344**: 1879–1900.

Caffall, K.H., Pattathil, S., Phillips, S.E., Hahn, M.G., and Mohnen, D. (2009). Arabidopsis thaliana T-DNA Mutants Implicate GAUT Genes in the Biosynthesis of Pectin and Xylan in Cell Walls and Seed Testa. Mol. Plant **2**: 1000–1014.

Cai, H., Reinisch, K., and Ferro-Novick, S. (2007). Coats, Tethers, Rabs, and SNAREs Work Together to Mediate the Intracellular Destination of a Transport Vesicle. Dev. Cell **12**: 671–682.

Canut, H., Albenne, C., and Jamet, E. (2016). Post-translational modifications of plant cell wall proteins and peptides: A survey from a proteomics point of view. Biochim. Biophys. Acta BBA - Proteins Proteomics **1864**: 983–990.

Carol, R.J., Takeda, S., Linstead, P., Durrant, M.C., Kakesova, H., Derbyshire, P., Drea, S., Zarsky, V., and Dolan, L. (2005). A RhoGDP dissociation inhibitor spatially regulates growth in root hair cells. Nature **438**: 1013.

Castanheira, P., Samyn, B., Sergeant, K., Clemente, J.C., Dunn, B.M., Pires, E., Beeumen, J.V., and Faro, C. (2005). Activation, Proteolytic Processing, and Peptide Specificity of Recombinant Cardosin A. J. Biol. Chem. **280**: 13047–13054.

Catalá, C., Howe, K.J., Hucko, S., Rose, J.K.C., and Thannhauser, T.W. (2011). Towards characterization of the glycoproteome of tomato (Solanum lycopersicum) fruit using Concanavalin A lectin affinity chromatography and LC-MALDI-MS/MS analysis. PROTEOMICS **11**: 1530–1544.

Chan, J., Crowell, E., Eder, M., Calder, G., Bunnewell, S., Findlay, K., Vernhettes, S., Höfte, H., and Lloyd, C. (2010). The rotation of cellulose synthase trajectories is microtubule dependent and influences the texture of epidermal cell walls in Arabidopsis hypocotyls. J Cell Sci **123**: 3490–3495.

Chang, F., Gu, Y., Ma, H., and Yang, Z. (2013). AtPRK2 Promotes ROP1 Activation via RopGEFs in the Control of Polarized Pollen Tube Growth. Mol. Plant **6**: 1187–1201.

Chebli, Y. and Geitmann, A. (2017). Cellular growth in plants requires regulation of cell wall biochemistry. Curr. Opin. Cell Biol. **44**: 28–35.

Chen, Y.-G., Siddhanta, A., Austin, C.D., Hammond, S.M., Sung, T.-C., Frohman, M.A., Morris, A.J., and Shields, D. (1997). Phospholipase D Stimulates Release of Nascent Secretory Vesicles from the trans-Golgi Network. J. Cell Biol. **138**: 495–504.

Chichkova, N.V., Shaw, J., Galiullina, R.A., Drury, G.E., Tuzhikov, A.I., Kim, S.H., Kalkum, M., Hong, T.B., Gorshkova, E.N., Torrance, L., Vartapetian, A.B., and Taliansky, M. (2010). Phytaspase, a relocalisable cell death promoting plant protease with caspase specificity. EMBO J. **29**: 1149–1161.

Choi, Y., Lee, Y., and Hwang, J.-U. (2014). Arabidopsis ROP9 and ROP10 GTPases differentially regulate auxin and ABA responses. J. Plant Biol. **57**: 245–254.

Chow, C.-M., Neto, H., Foucart, C., and Moore, I. (2008). Rab-A2 and Rab-A3 GTPases Define a trans-Golgi Endosomal Membrane Domain in Arabidopsis That Contributes Substantially to the Cell Plate. Plant Cell **20**: 101–123.

Clough, S.J. and Bent, A.F. (1998). Floral dip: a simplified method for Agrobacterium-mediated transformation of Arabidopsis thaliana. Plant J. **16**: 735–743.

Cocuron, J.-C., Lerouxel, O., Drakakaki, G., Alonso, A.P., Liepman, A.H., Keegstra, K., Raikhel, N., and Wilkerson, C.G. (2007). A gene from the cellulose synthase-like C family encodes a β-1,4 glucan synthase. Proc. Natl. Acad. Sci. **104**: 8550–8555.

Cosgrove, D.J. (2005). Growth of the plant cell wall. Nat. Rev. Mol. Cell Biol. **6**: 850.

Cosgrove, D.J. (2014). Re-constructing our models of cellulose and primary cell wall assembly. Curr. Opin. Plant Biol. **22**: 122–131.

De Caroli, M., Lenucci, M.S., Di Sansebastiano, G.-P., Dalessandro, G., De Lorenzo, G., and Piro, G. (2011). Protein trafficking to the cell wall occurs through mechanisms distinguishable from default sorting in tobacco. Plant J. **65**: 295–308.

Dean, G., Cao, Y., Xiang, D., Provart, N.J., Ramsay, L., Ahad, A., White, R., Selvaraj, G., Datla, R., and Haughn, G. (2011). Analysis of Gene Expression Patterns during Seed Coat Development in Arabidopsis. Mol. Plant **4**: 1074–1091.

Dean, G.H., Jin, Z., Shi, L., Esfandiari, E., McGee, R., Nabata, K., Lee, T., Kunst, L., Western, T.L., and Haughn, G.W. (2017). Identification of a seed coat-specific promoter fragment from the Arabidopsis MUCILAGE-MODIFIED4 gene. Plant Mol. Biol. **95**: 33–50.

Dean, G.H., Zheng, H., Tewari, J., Huang, J., Young, D.S., Hwang, Y.T., Western, T.L., Carpita, N.C., McCann, M.C., Mansfield, S.D., and Haughn, G.W. (2007). The Arabidopsis MUM2 Gene Encodes a β-Galactosidase Required for the Production of Seed Coat Mucilage with Correct Hydration Properties. Plant Cell **19**: 4007–4021.

DeBono, A. (2011). The role and behavior of Arabidopsis thaliana lipid transfer proteins during cuticular wax deposition.

Delage, E., Puyaubert, J., Zachowski, A., and Ruelland, E. (2013). Signal transduction pathways involving phosphatidylinositol 4-phosphate and phosphatidylinositol 4,5-bisphosphate: Convergences and divergences among eukaryotic kingdoms. Prog. Lipid Res. **52**: 1–14.

Derksen, J., Rutten, T., Lichtscheidl, I.K., Win, A.H.N. de, Pierson, E.S., and Rongen, G. (1995). Quantitative analysis of the distribution of organelles in tobacco pollen tubes: implications for exocytosis and endocytosis. Protoplasma **188**: 267–276.

Dettmer, J. and Friml, J. (2011). Cell polarity in plants: when two do the same, it is not the same.... Curr. Opin. Cell Biol. **23**: 686–696.

Dettmer, J., Hong-Hermesdorf, A., Stierhof, Y.-D., and Schumacher, K. (2006). Vacuolar H+-ATPase Activity Is Required for Endocytic and Secretory Trafficking in Arabidopsis. Plant Cell **18**: 715–730.

Ding, Y., Wang, J., Wang, J., Stierhof, Y.-D., Robinson, D.G., and Jiang, L. (2012). Unconventional protein secretion. Trends Plant Sci. **17**: 606–615.

Doyle, S.M., Haeger, A., Vain, T., Rigal, A., Viotti, C., Łangowska, M., Ma, Q., Friml, J., Raikhel, N.V., Hicks, G.R., and Robert, S. (2015). An early secretory pathway mediated by GNOM-LIKE 1 and GNOM is essential for basal polarity establishment in Arabidopsis thaliana. Proc. Natl. Acad. Sci. **112**: E806–E815.

Drakakaki, G. (2015). Polysaccharide deposition during cytokinesis: Challenges and future perspectives. Plant Sci. **236**: 177–184.

Drakakaki, G. and Dandekar, A. (2013). Protein secretion: How many secretory routes does a plant cell have? Plant Sci. **203**–**204**: 74–78.

Driouich, A., Follet-Gueye, M.-L., Bernard, S., Kousar, S., Chevalier, L., Vicré-Gibouin, M., and Lerouxel, O. (2012). Golgi-Mediated Synthesis and Secretion of Matrix Polysaccharides of the Primary Cell Wall of Higher Plants. Front. Plant Sci. **3**.

Driouich, A., Staehelin, L.A., and Faye, L. (1994). Structural and functional organization of the Golgi apparatus in plant cells. Plant Physiol. Biochem. **32**: 732–749.

Driouich, A., Zhang, G.F., and Staehelin, L.A. (1993). Effect of Brefeldin A on the Structure of the Golgi Apparatus and on the Synthesis and Secretion of Proteins and Polysaccharides in Sycamore Maple (Acer pseudoplatanus) Suspension-Cultured Cells. Plant Physiol. **101**: 1363–1373.

Duruflé, H., Clemente, H.S., Balliau, T., Zivy, M., Dunand, C., and Jamet, E. (2017). Cell wall proteome analysis of Arabidopsis thaliana mature stems. PROTEOMICS **17**: 1600449.

Ebine, K. et al. (2011). A membrane trafficking pathway regulated by the plant-specific RAB GTPase ARA6. Nat. Cell Biol. **13**: 853.

Ebine, K., Okatani, Y., Uemura, T., Goh, T., Shoda, K., Niihama, M., Morita, M.T., Spitzer, C., Otegui, M.S., Nakano, A., and Ueda, T. (2008). A SNARE Complex Unique to Seed Plants Is Required for Protein Storage Vacuole Biogenesis and Seed Development of Arabidopsis thaliana. Plant Cell **20**: 3006–3021.

Escrevente, C., Morais, V.A., Keller, S., Soares, C.M., Altevogt, P., and Costa, J. (2008). Functional role of N-glycosylation from ADAM10 in processing, localization and activity of the enzyme. Biochim. Biophys. Acta BBA - Gen. Subj. **1780**: 905–913.

Fanata, W.I.D. et al. (2013). N-glycan maturation is crucial for cytokinin-mediated development and cellulose synthesis in Oryza sativa. Plant J. **73**: 966–979.

Fayant, P., Girlanda, O., Chebli, Y., Aubin, C.-É., Villemure, I., and Geitmann, A. (2010). Finite Element Model of Polar Growth in Pollen Tubes. Plant Cell **22**: 2579–2593.

Feraru, E., Feraru, M.I., Kleine-Vehn, J., Martinière, A., Mouille, G., Vanneste, S., Vernhettes, S., Runions, J., and Friml, J. (2011). PIN Polarity Maintenance by the Cell Wall in Arabidopsis. Curr. Biol. **21**: 338–343.

Figueiredo, D.D., Batista, R.A., Roszak, P.J., Hennig, L., and Köhler, C. (2016). Auxin production in the endosperm drives seed coat development in Arabidopsis. eLife **5**: e20542.

Fischer, U., Ikeda, Y., Ljung, K., Serralbo, O., Singh, M., Heidstra, R., Palme, K., Scheres, B., and Grebe, M. (2006). Vectorial Information for Arabidopsis Planar Polarity Is Mediated by Combined AUX1, EIN2, and GNOM Activity. Curr. Biol. **16**: 2143–2149.

Francoz, E., Ranocha, P., Nguyen-Kim, H., Jamet, E., Burlat, V., and Dunand, C. (2015). Roles of cell wall peroxidases in plant development. Phytochemistry **112**: 15–21.

Fraser, C.M., Rider, L.W., and Chapple, C. (2005). An Expression and Bioinformatics Analysis of the Arabidopsis Serine Carboxypeptidase-Like Gene Family. Plant Physiol. **138**: 1136–1148.

Fu, Y., Gu, Y., Zheng, Z., Wasteneys, G., and Yang, Z. (2005). Arabidopsis Interdigitating Cell Growth Requires Two Antagonistic Pathways with Opposing Action on Cell Morphogenesis. Cell **120**: 687–700.

Fujimoto, M. and Ueda, T. (2012). Conserved and Plant-Unique Mechanisms Regulating Plant Post-Golgi Traffic. Front. Plant Sci. **3**.

Galway, M.E., Heckman, J.W., and Schiefelbein, J.W. (1997). Growth and ultrastructure of Arabidopsis root hairs: the rhd3 mutation alters vacuole enlargement and tip growth. Planta **201**: 209–218.

Geitmann, A. and Parre, E. (2004). The local cytomechanical properties of growing pollen tubes correspond to the axial distribution of structural cellular elements. Sex. Plant Reprod. **17**: 9–16.

Geitmann, A. and Steer, M. (2006). The Architecture and Properties of the Pollen Tube Cell Wall. In The Pollen Tube, Plant Cell Monographs. (Springer, Berlin, Heidelberg), pp. 177–200.

Geldner, N., Anders, N., Wolters, H., Keicher, J., Kornberger, W., Muller, P., Delbarre, A., Ueda, T., Nakano, A., and Jürgens, G. (2003). The Arabidopsis GNOM ARF-GEF Mediates Endosomal Recycling, Auxin Transport, and Auxin-Dependent Plant Growth. Cell **112**: 219–230.

Gendre, D., Jonsson, K., Boutté, Y., and Bhalerao, R.P. (2015). Journey to the cell surface—the central role of the trans-Golgi network in plants. Protoplasma **252**: 385–398.

Gendre, D., McFarlane, H.E., Johnson, E., Mouille, G., Sjödin, A., Oh, J., Levesque-Tremblay, G., Watanabe, Y., Samuels, L., and Bhalerao, R.P. (2013). Trans-Golgi Network Localized ECHIDNA/Ypt Interacting Protein Complex Is Required for the Secretion of Cell Wall Polysaccharides in Arabidopsis. Plant Cell **25**: 2633–2646.

Gendre, D., Oh, J., Boutté, Y., Best, J.G., Samuels, L., Nilsson, R., Uemura, T., Marchant, A., Bennett, M.J., Grebe, M., and Bhalerao, R.P. (2011). Conserved Arabidopsis ECHIDNA protein mediates trans–Golgi-network trafficking and cell elongation. Proc. Natl. Acad. Sci. **108**: 8048–8053.

Griffiths, J.S. and North, H.M. (2017). Sticking to cellulose: exploiting Arabidopsis seed coat mucilage to understand cellulose biosynthesis and cell wall polysaccharide interactions. New Phytol. **214**: 959–966.

Griffiths, J.S., Šola, K., Kushwaha, R., Lam, P., Tateno, M., Young, R., Voiniciuc, C., Dean, G., Mansfield, S.D., DeBolt, S., and Haughn, G.W. (2015). Unidirectional Movement of Cellulose Synthase Complexes in Arabidopsis Seed Coat Epidermal Cells Deposit Cellulose Involved in Mucilage Extrusion, Adherence, and Ray Formation. Plant Physiol. **168**: 502–520.

Griffiths, J.S., Tsai, A.Y.-L., Xue, H., Voiniciuc, C., Šola, K., Seifert, G.J., Mansfield, S.D., and Haughn, G.W. (2014). SALT-OVERLY SENSITIVE5 Mediates Arabidopsis Seed

Coat Mucilage Adherence and Organization through Pectins. Plant Physiol. **165**: 991–1004.

Gu, C., Shabab, M., Strasser, R., Wolters, P.J., Shindo, T., Niemer, M., Kaschani, F., Mach, L., and Hoorn, R.A.L. van der (2012). Post-Translational Regulation and Trafficking of the Granulin-Containing Protease RD21 of Arabidopsis thaliana. PLOS ONE **7**: e32422.

Gu, F., Crump, C.M., and Thomas, G. (2001). Trans-Golgi network sorting. Cell. Mol. Life Sci. CMLS **58**: 1067–1084.

Gu, Y., Fu, Y., Dowd, P., Li, S., Vernoud, V., Gilroy, S., and Yang, Z. (2005). A Rho family GTPase controls actin dynamics and tip growth via two counteracting downstream pathways in pollen tubes. J Cell Biol **169**: 127–138.

Gu, Y., Li, S., Lord, E.M., and Yang, Z. (2006). Members of a Novel Class of Arabidopsis Rho Guanine Nucleotide Exchange Factors Control Rho GTPase-Dependent Polar Growth. Plant Cell **18**: 366–381.

Gut, A., Kappeler, F., Hyka, N., Balda, M.S., Hauri, H.-P., and Matter, K. (1998). Carbohydrate-mediated Golgi to cell surface transport and apical targeting of membrane proteins. EMBO J. **17**: 1919–1929.

Hachez, C., Laloux, T., Reinhardt, H., Cavez, D., Degand, H., Grefen, C., Rycke, R.D., Inzé, D., Blatt, M.R., Russinova, E., and Chaumont, F. (2014). Arabidopsis SNAREs SYP61 and SYP121 Coordinate the Trafficking of Plasma Membrane Aquaporin PIP2;7 to Modulate the Cell Membrane Water Permeability. Plant Cell **26**: 3132–3147.

Harmoko, R. et al. (2016). N-glycan containing a core α1,3-fucose residue is required for basipetal auxin transport and gravitropic response in rice (Oryza sativa). New Phytol. **212**: 108–122.

Harpaz-Saad, S., McFarlane, H.E., Xu, S., Divi, U.K., Forward, B., Western, T.L., and Kieber, J.J. (2011). Cellulose synthesis via the FEI2 RLK/SOS5 pathway and CELLULOSE SYNTHASE 5 is required for the structure of seed coat mucilage in Arabidopsis. Plant J. **68**: 941–953.

Harrison, M.J. and Ivanov, S. (2017). Exocytosis for endosymbiosis: membrane trafficking pathways for development of symbiotic membrane compartments. Curr. Opin. Plant Biol. **38**: 101–108.

Hatsugai, N., Iwasaki, S., Tamura, K., Kondo, M., Fuji, K., Ogasawara, K., Nishimura, M., and Hara-Nishimura, I. (2009). A novel membrane fusion-mediated plant immunity against bacterial pathogens. Genes Dev. **23**: 2496–2506.

Haughn, G. and Chaudhury, A. (2005). Genetic analysis of seed coat development in Arabidopsis. Trends Plant Sci. **10**: 472–477.

Haughn, G.W. and Somerville, C. (1986). Sulfonylurea-resistant mutants of Arabidopsis thaliana. Mol. Gen. Genet. MGG **204**: 430–434.

Haughn, G.W. and Western, T.L. (2012). Arabidopsis Seed Coat Mucilage is a Specialized Cell Wall that Can be Used as a Model for Genetic Analysis of Plant Cell Wall Structure and Function. Front. Plant Sci. **3**.

Häweker, H., Rips, S., Koiwa, H., Salomon, S., Saijo, Y., Chinchilla, D., Robatzek, S., and Schaewen, A. von (2010). Pattern Recognition Receptors Require N-Glycosylation to Mediate Plant Immunity. J. Biol. Chem. **285**: 4629–4636.

He, B. and Guo, W. (2009). The exocyst complex in polarized exocytosis. Curr. Opin. Cell Biol. **21**: 537–542.

Hellens, R.P., Edwards, E.A., Leyland, N.R., Bean, S., and Mullineaux, P.M. (2000). pGreen: a versatile and flexible binary Ti vector for Agrobacterium-mediated plant transformation. Plant Mol. Biol. **42**: 819–832.

Hepler, P.K., Rounds, C.M., and Winship, L.J. (2013). Control of cell wall extensibility during pollen tube growth. Mol. Plant **6**: 998–1017.

Hooper, C.M., Castleden, I.R., Tanz, S.K., Aryamanesh, N., and Millar, A.H. (2017). SUBA4: the interactive data analysis centre for Arabidopsis subcellular protein locations. Nucleic Acids Res. **45**: D1064–D1074.

Hoorn, R.A.L. van der (2008). Plant Proteases: From Phenotypes to Molecular Mechanisms. Annu. Rev. Plant Biol. **59**: 191–223.

Hu, R., Li, J., Wang, X., Zhao, X., Yang, X., Tang, Q., He, G., Zhou, G., and Kong, Y. (2016a). Xylan synthesized by Irregular Xylem 14 (IRX14) maintains the structure of seed coat mucilage in Arabidopsis. J. Exp. Bot. **67**: 1243–1257.

Hu, R., Li, J., Yang, X., Zhao, X., Wang, X., Tang, Q., He, G., Zhou, G., and Kong, Y. (2016b). Irregular xylem 7 (IRX7) is required for anchoring seed coat mucilage in Arabidopsis. Plant Mol. Biol. **92**: 25–38.

Huang, W.-J., Liu, H.-K., McCormick, S., and Tang, W.-H. (2014). Tomato Pistil Factor STIG1 Promotes in Vivo Pollen Tube Growth by Binding to Phosphatidylinositol 3-Phosphate and the Extracellular Domain of the Pollen Receptor Kinase LePRK2. Plant Cell **26**: 2505–2523.

Huete-Pérez, J.A., Engel, J.C., Brinen, L.S., Mottram, J.C., and McKerrow, J.H. (1999). Protease Trafficking in Two Primitive Eukaryotes Is Mediated by a Prodomain Protein Motif. J. Biol. Chem. **274**: 16249–16256.

Hüttner, S. and Strasser, R. (2012). Endoplasmic Reticulum-Associated Degradation of Glycoproteins in Plants. Front. Plant Sci. **3**.

Hwang, J.-U., Vernoud, V., Szumlanski, A., Nielsen, E., and Yang, Z. (2008). A Tip-Localized RhoGAP Controls Cell Polarity by Globally Inhibiting Rho GTPase at the Cell Apex. Curr. Biol. **18**: 1907–1916.

Ichikawa, M., Hirano, T., Enami, K., Fuselier, T., Kato, N., Kwon, C., Voigt, B., Schulze-Lefert, P., Baluška, F., and Sato, M.H. (2014). Syntaxin of Plant Proteins SYP123 and SYP132 Mediate Root Hair Tip Growth in Arabidopsis thaliana. Plant Cell Physiol. **55**: 790–800.

Jadid, N., Mialoundama, A.S., Heintz, D., Ayoub, D., Erhardt, M., Mutterer, J., Meyer, D., Alioua, A., Dorsselaer, A.V., Rahier, A., Camara, B., and Bouvier, F. (2011). DOLICHOL PHOSPHATE MANNOSE SYNTHASE1 Mediates the Biogenesis of Isoprenyl-Linked Glycans and Influences Development, Stress Response, and Ammonium Hypersensitivity in Arabidopsis. Plant Cell **23**: 1985–2005.

Jamet, E., Canut, H., Boudart, G., and Pont-Lezica, R.F. (2006). Cell wall proteins: a new insight through proteomics. Trends Plant Sci. **11**: 33–39.

Jeon, B.W., Hwang, J.-U., Hwang, Y., Song, W.-Y., Fu, Y., Gu, Y., Bao, F., Cho, D., Kwak, J.M., Yang, Z., and Lee, Y. (2008). The Arabidopsis Small G Protein ROP2 Is Activated by Light in Guard Cells and Inhibits Light-Induced Stomatal Opening. Plant Cell **20**: 75–87.

Jones, M.A., Raymond, M.J., Yang, Z., and Smirnoff, N. (2007). NADPH oxidase-dependent reactive oxygen species formation required for root hair growth depends on ROP GTPase. J. Exp. Bot. **58**: 1261–1270.

Jones, M.A., Shen, J.-J., Fu, Y., Li, H., Yang, Z., and Grierson, C.S. (2002). The Arabidopsis Rop2 GTPase Is a Positive Regulator of Both Root Hair Initiation and Tip Growth. Plant Cell **14**: 763–776.

Joshi, H.J. and Gupta, R. (2015). Eukaryotic Glycosylation: Online Methods for Site Prediction on Protein Sequences. In Glycoinformatics, Methods in Molecular Biology. (Humana Press, New York, NY), pp. 127–137.

Kang, B.-H., Nielsen, E., Preuss, M.L., Mastronarde, D., and Staehelin, L.A. (2011). Electron Tomography of RabA4b- and PI-4Kβ1-Labeled Trans Golgi Network Compartments in Arabidopsis. Traffic **12**: 313–329.

Kaothien, P., Ok, S.H., Shuai, B., Wengier, D., Cotter, R., Kelley, D., Kiriakopolos, S., Muschietti, J., and McCormick, S. (2005). Kinase partner protein interacts with the LePRK1 and LePRK2 receptor kinases and plays a role in polarized pollen tube growth. Plant J. **42**: 492–503.

Kasmi, F.E., Krause, C., Hiller, U., Stierhof, Y.-D., Mayer, U., Conner, L., Kong, L., Reichardt, I., Sanderfoot, A.A., and Jürgens, G. (2013). SNARE complexes of different composition jointly mediate membrane fusion in Arabidopsis cytokinesis. Mol. Biol. Cell **24**: 1593–1601.

Kim, H., O'Connell, R., Maekawa-Yoshikawa, M., Uemura, T., Neumann, U., and Schulze-Lefert, P. (2014). The powdery mildew resistance protein RPW8.2 is carried on VAMP721/722 vesicles to the extrahaustorial membrane of haustorial complexes. Plant J. **79**: 835–847.

Kitakura, S., Vanneste, S., Robert, S., Löfke, C., Teichmann, T., Tanaka, H., and Friml, J. (2011). Clathrin Mediates Endocytosis and Polar Distribution of PIN Auxin Transporters in Arabidopsis. Plant Cell **23**: 1920–1931.

Klahre, U., Becker, C., Schmitt, A.C., and Kost, B. (2006). Nt-RhoGDI2 regulates Rac/Rop signaling and polar cell growth in tobacco pollen tubes. Plant J. **46**: 1018–1031.

Kleine-Vehn, J. et al. (2011). Recycling, clustering, and endocytosis jointly maintain PIN auxin carrier polarity at the plasma membrane. Mol. Syst. Biol. **7**: 540.

Kleine-Vehn, J., Dhonukshe, P., Sauer, M., Brewer, P.B., Wiśniewska, J., Paciorek, T., Benková, E., and Friml, J. (2008). ARF GEF-Dependent Transcytosis and Polar Delivery of PIN Auxin Carriers in Arabidopsis. Curr. Biol. **18**: 526–531.

Koelsch, G., Mareš, M., Metcalf, P., and Fusek, M. (1994). Multiple functions of pro-parts of aspartic proteinase zymogens. FEBS Lett. **343**: 6–10.

Koh, E., Carmieli, R., Mor, A., and Fluhr, R. (2016). Singlet oxygen induced membrane disruption and serpin-protease balance in vacuolar driven cell death in Arabidopsis thaliana. Plant Physiol. **171**: 1616–1625.

Koiwa, H., Li, F., McCully, M.G., Mendoza, I., Koizumi, N., Manabe, Y., Nakagawa, Y., Zhu, J., Rus, A., Pardo, J.M., Bressan, R.A., and Hasegawa, P.M. (2003). The STT3a Subunit Isoform of the Arabidopsis Oligosaccharyltransferase Controls Adaptive Responses to Salt/Osmotic Stress. Plant Cell **15**: 2273–2284.

Kong, Y., Zhou, G., Abdeen, A.A., Schafhauser, J., Richardson, B., Atmodjo, M.A., Jung, J., Wicker, L., Mohnen, D., Western, T., and Hahn, M.G. (2013). GALACTURONOSYLTRANSFERASE-LIKE5 Is Involved in the Production of Arabidopsis Seed Coat Mucilage. Plant Physiol. **163**: 1203–1217.

Kost, B. (2008). Spatial control of Rho (Rac-Rop) signaling in tip-growing plant cells. Trends Cell Biol. **18**: 119–127.

Kulich, I., Cole, R., Drdová, E., Cvrčková, F., Soukup, A., Fowler, J., and Žárský, V. (2010). Arabidopsis exocyst subunits SEC8 and EXO70A1 and exocyst interactor ROH1 are involved in the localized deposition of seed coat pectin. New Phytol. **188**: 615–625.

Kunieda, T., Shimada, T., Kondo, M., Nishimura, M., Nishitani, K., and Hara-Nishimura, I. (2013). Spatiotemporal Secretion of PEROXIDASE36 Is Required for Seed Coat Mucilage Extrusion in Arabidopsis. Plant Cell **25**: 1355–1367.

Kutschera, U. (2008). The Growing Outer Epidermal Wall: Design and Physiological Role of a Composite Structure. Ann. Bot. **101**: 615–621.

Kwon, C. et al. (2008). Co-option of a default secretory pathway for plant immune responses. Nature **451**: 835.

Lampl, N., Alkan, N., Davydov, O., and Fluhr, R. (2013). Set-point control of RD21 protease activity by AtSerpin1 controls cell death in Arabidopsis. Plant J. **74**: 498–510.

Lancelle, S.A. and Hepler, P.K. (1992). Ultrastructure of freeze-substituted pollen tubes of Lilium longiflorum. Protoplasma **167**: 215–230.

Łangowski, Ł., Růžička, K., Naramoto, S., Kleine-Vehn, J., and Friml, J. (2010). Trafficking to the Outer Polar Domain Defines the Root-Soil Interface. Curr. Biol. **20**: 904–908.

Łangowski, Ł., Wabnik, K., Li, H., Vanneste, S., Naramoto, S., Tanaka, H., and Friml, J. (2016). Cellular mechanisms for cargo delivery and polarity maintenance at different polar domains in plant cells. Cell Discov. **2**: 16018.

Lannoo, N. and Van Damme, E.J.M. (2015). Review/N-glycans: The making of a varied toolbox. Plant Sci. **239**: 67–83.

Lee, Y., Rubio, M.C., Alassimone, J., and Geldner, N. (2013). A Mechanism for Localized Lignin Deposition in the Endodermis. Cell **153**: 402–412.

Lee, Y.J., Szumlanski, A., Nielsen, E., and Yang, Z. (2008). Rho-GTPase–dependent filamentous actin dynamics coordinate vesicle targeting and exocytosis during tip growth. J. Cell Biol. **181**: 1155–1168.

Leucci, M.R., Sansebastiano, G.-P.D., Gigante, M., Dalessandro, G., and Piro, G. (2007). Secretion marker proteins and cell-wall polysaccharides move through different secretory pathways. Planta **225**: 1001–1017.

Levesque-Tremblay, G. (2014). Pectin methyl esterification functions in seed development and germination.

Li, R., Rodriguez-Furlan, C., Wang, J., Ven, W. van de, Gao, T., Raikhel, N.V., and Hicks, G.R. (2017). Different Endomembrane Trafficking Pathways Establish Apical and Basal Polarities. Plant Cell **29**: 90–108.

Li, S., Chen, M., Yu, D., Ren, S., Sun, S., Liu, L., Ketelaar, T., Emons, A.-M.C., and Liu, C.-M. (2013). EXO70A1-Mediated Vesicle Trafficking Is Critical for Tracheary Element Development in Arabidopsis. Plant Cell **25**: 1774–1786.

Li, Y.-Q., Mareck, A., Faleri, C., Moscatelli, A., Liu, Q., and Cresti, M. (2002). Detection and localization of pectin methylesterase isoforms in pollen tubes of Nicotiana tabacum L. Planta **214**: 734–740.

Li Zixing, Kang Jun, Sui Ning, and Liu Dong (2012). ROP11 GTPase is a Negative Regulator of Multiple ABA Responses in Arabidopsis. J. Integr. Plant Biol. **54**: 169–179.

Liebminger, E., Grass, J., Altmann, F., Mach, L., and Strasser, R. (2013). Characterizing the Link between Glycosylation State and Enzymatic Activity of the Endo-β1,4-glucanase KORRIGAN1 from Arabidopsis thaliana. J. Biol. Chem. **288**: 22270–22280.

Liebminger, E., Hüttner, S., Vavra, U., Fischl, R., Schoberer, J., Grass, J., Blaukopf, C., Seifert, G.J., Altmann, F., Mach, L., and Strasser, R. (2009). Class I α-Mannosidases Are Required for N-Glycan Processing and Root Development in Arabidopsis thaliana. Plant Cell **21**: 3850–3867.

Lige, B., Ma, S., and van Huystee, R.B. (2001). The Effects of the Site-Directed Removal of N-Glycosylation from Cationic Peanut Peroxidase on Its Function. Arch. Biochem. Biophys. **386**: 17–24.

Lin, D. et al. (2012). A ROP GTPase-Dependent Auxin Signaling Pathway Regulates the Subcellular Distribution of PIN2 in Arabidopsis Roots. Curr. Biol. **22**: 1319–1325.

Lipka, V., Kwon, C., and Panstruga, R. (2007). SNARE-Ware: The Role of SNARE-Domain Proteins in Plant Biology. Annu. Rev. Cell Dev. Biol. **23**: 147–174.

Lu, Q.S., Dela Paz, J., Pathmanathan, A., Chiu, R.S., Tsai, A.Y.-L., and Gazzarrini, S. (2010). The C-terminal domain of FUSCA3 negatively regulates mRNA and protein levels, and mediates sensitivity to the hormones abscisic acid and gibberellic acid in Arabidopsis. Plant J. **64**: 100–113.

Macquet, A., Ralet, M.-C., Kronenberger, J., Marion-Poll, A., and North, H.M. (2007a). In situ, Chemical and Macromolecular Study of the Composition of Arabidopsis thaliana Seed Coat Mucilage. Plant Cell Physiol. **48**: 984–999.

Macquet, A., Ralet, M.-C., Loudet, O., Kronenberger, J., Mouille, G., Marion-Poll, A., and North, H.M. (2007b). A Naturally Occurring Mutation in an Arabidopsis Accession Affects a β-d-Galactosidase That Increases the Hydrophilic Potential of Rhamnogalacturonan I in Seed Mucilage. Plant Cell **19**: 3990–4006.

Mao, H., Nakamura, M., Viotti, C., and Grebe, M. (2016). A Framework for Lateral Membrane Trafficking and Polar Tethering of the PEN3 ATP-Binding Cassette Transporter. Plant Physiol. **172**: 2245–2260.

Martinière, A. et al. (2012). Cell wall constrains lateral diffusion of plant plasma-membrane proteins. Proc. Natl. Acad. Sci. **109**: 12805–12810.

Mathé, C., Barre, A., Jourda, C., and Dunand, C. (2010). Evolution and expression of class III peroxidases. Arch. Biochem. Biophys. **500**: 58–65.

Maley, F., Trimble, R.B., Tarentino, A.L., and Plummer, T.H. (1989). Characterization of glycoproteins and their associated oligosaccharides through the use of endoglycosidases. Anal. Biochem. **180**: 195–204.

McFarlane, H.E., Döring, A., and Persson, S. (2014). The Cell Biology of Cellulose Synthesis. Annu. Rev. Plant Biol. **65**: 69–94.

McFarlane, H.E., Watanabe, Y., Gendre, D., Carruthers, K., Levesque-Tremblay, G., Haughn, G.W., Bhalerao, R.P., and Samuels, L. (2013). Cell Wall Polysaccharides are Mislocalized to the Vacuole in echidna Mutants. Plant Cell Physiol. **54**: 1867–1880.

Mendu, V., Griffiths, J.S., Persson, S., Stork, J., Downie, A.B., Voiniciuc, C., Haughn, G.W., and DeBolt, S. (2011). Subfunctionalization of Cellulose Synthases in Seed Coat Epidermal Cells Mediates Secondary Radial Wall Synthesis and Mucilage Attachment. Plant Physiol. **157**: 441–453.

Minic, Z., Jamet, E., Négroni, L., Arsene der Garabedian, P., Zivy, M., and Jouanin, L. (2007). A sub-proteome of Arabidopsis thaliana mature stems trapped on Concanavalin A is enriched in cell wall glycoside hydrolases. J. Exp. Bot. **58**: 2503–2512.

Moore, P.J., Swords, K.M., Lynch, M.A., and Staehelin, L.A. (1991). Spatial organization of the assembly pathways of glycoproteins and complex polysaccharides in the Golgi apparatus of plants. J. Cell Biol. **112**: 589–602.

Moremen, K.W., Tiemeyer, M., and Nairn, A.V. (2012). Vertebrate protein glycosylation: diversity, synthesis and function. Nat. Rev. Mol. Cell Biol. **13**: 448.

Mugford, S.T. and Osbourn, A. (2010). Evolution of serine carboxypeptidase-like acyltransferases in the monocots. Plant Signal. Behav. **5**: 193–195.

Muschietti, J., Eyal, Y., and McCormick, S. (1998). Pollen Tube Localization Implies a Role in Pollen–Pistil Interactions for the Tomato Receptor-like Protein Kinases LePRK1 and LePRK2. Plant Cell **10**: 319–330.

Nagawa, S., Xu, T., Lin, D., Dhonukshe, P., Zhang, X., Friml, J., Scheres, B., Fu, Y., and Yang, Z. (2012). ROP GTPase-Dependent Actin Microfilaments Promote PIN1 Polarization by Localized Inhibition of Clathrin-Dependent Endocytosis. PLOS Biol. **10**: e1001299.

Nagawa, S., Xu, T., and Yang, Z. (2010). RHO GTPase in plants. Small GTPases **1**: 78–88.

Nakagawa, T., Nakamura, S., Tanaka, K., Kawamukai, M., Suzuki, T., Nakamura, K., Kimura, T., and Ishiguro, S. (2008). Development of R4 Gateway Binary Vectors (R4pGWB) Enabling High-Throughput Promoter Swapping for Plant Research. Biosci. Biotechnol. Biochem. **72**: 624–629.

Nakayama, T., Shinohara, H., Tanaka, M., Baba, K., Ogawa-Ohnishi, M., and Matsubayashi, Y. (2017). A peptide hormone required for Casparian strip diffusion barrier formation in Arabidopsis roots. Science **355**: 284–286.

Naramoto, S., Kleine-Vehn, J., Robert, S., Fujimoto, M., Dainobu, T., Paciorek, T., Ueda, T., Nakano, A., Montagu, M.C.E.V., Fukuda, H., and Friml, J. (2010). ADP-ribosylation factor machinery mediates endocytosis in plant cells. Proc. Natl. Acad. Sci. **107**: 21890–21895.

Nelson, W.J. (2003). Adaptation of core mechanisms to generate cell polarity. Nature **422**: 766-774.

Oda, Y. (2015). Cortical microtubule rearrangements and cell wall patterning. Front. Plant Sci. **6**.

Oda, Y. and Fukuda, H. (2012). Initiation of Cell Wall Pattern by a Rho- and Microtubule-Driven Symmetry Breaking. Science **337**: 1333–1336.

Oda, Y. and Fukuda, H. (2013). The dynamic interplay of plasma membrane domains and cortical microtubules in secondary cell wall patterning. Front. Plant Sci. **4**.

Oda, Y., Iida, Y., Kondo, Y., and Fukuda, H. (2010). Wood Cell-Wall Structure Requires Local 2D-Microtubule Disassembly by a Novel Plasma Membrane-Anchored Protein. Curr. Biol. **20**: 1197–1202.

Oikawa, A., Lund, C.H., Sakuragi, Y., and Scheller, H.V. (2013). Golgi-localized enzyme complexes for plant cell wall biosynthesis. Trends Plant Sci. **18**: 49–58.

Oka, T. and Jigami, Y. (2006). Reconstruction of de novo pathway for synthesis of UDP-glucuronic acid and UDP-xylose from intrinsic UDP-glucose in Saccharomyces cerevisiae. FEBS J. **273**: 2645–2657.

Ondzighi, C.A., Christopher, D.A., Cho, E.J., Chang, S.-C., and Staehelin, L.A. (2008). Arabidopsis Protein Disulfide Isomerase-5 Inhibits Cysteine Proteases during Trafficking to Vacuoles before Programmed Cell Death of the Endothelium in Developing Seeds. Plant Cell **20**: 2205–2220.

Paredez, A.R., Somerville, C.R., and Ehrhardt, D.W. (2006). Visualization of Cellulose Synthase Demonstrates Functional Association with Microtubules. Science **312**: 1491–1495.

Park, M. and Jürgens, G. (2012). Membrane Traffic and Fusion at Post-Golgi Compartments. Front. Plant Sci. **2**.

Parre, E. and Geitmann, A. (2005). Pectin and the role of the physical properties of the cell wall in pollen tube growth of Solanum chacoense. Planta **220**: 582–592.

Passardi, F., Penel, C., and Dunand, C. (2004). Performing the paradoxical: how plant peroxidases modify the cell wall. Trends Plant Sci. **9**: 534–540.

Paul, M.J. and Frigerio, L. (2007). Coated vesicles in plant cells. Semin. Cell Dev. Biol. **18**: 471–478.

Pei, W., Du, F., Zhang, Y., He, T., and Ren, H. (2012). Control of the actin cytoskeleton in root hair development. Plant Sci. **187**: 10–18.

Peng, L., Hocart, C.H., Redmond, J.W., and Williamson, R.E. (2000). Fractionation of carbohydrates in Arabidopsis root cell walls shows that three radial swelling loci are specifically involved in cellulose production. Planta **211**: 406–414.

Potocký, M., Jones, M.A., Bezvoda, R., Smirnoff, N., and Žárský, V. (2007). Reactive oxygen species produced by NADPH oxidase are involved in pollen tube growth. New Phytol. **174**: 742–751.

Preuss, M.L., Schmitz, A.J., Thole, J.M., Bonner, H.K.S., Otegui, M.S., and Nielsen, E. (2006). A role for the RabA4b effector protein PI-4Kβ1 in polarized expansion of root hair cells in Arabidopsis thaliana. J Cell Biol **172**: 991–998.

Preuss, M.L., Serna, J., Falbel, T.G., Bednarek, S.Y., and Nielsen, E. (2004). The Arabidopsis Rab GTPase RabA4b Localizes to the Tips of Growing Root Hair Cells. Plant Cell **16**: 1589–1603.

Pumplin, N., Zhang, X., Noar, R.D., and Harrison, M.J. (2012). Polar localization of a symbiosis-specific phosphate transporter is mediated by a transient reorientation of secretion. Proc. Natl. Acad. Sci. **109**: E665–E672.

Qiu, J.-L., Jilk, R., Marks, M.D., and Szymanski, D.B. (2002). The Arabidopsis SPIKE1 Gene Is Required for Normal Cell Shape Control and Tissue Development. Plant Cell **14**: 101–118.

Ralet, M.-C., Crépeau, M.-J., Vigouroux, J., Tran, J., Berger, A., Sallé, C., Granier, F., Botran, L., and North, H.M. (2016). Xylans Provide the Structural Driving Force for Mucilage Adhesion to the Arabidopsis Seed Coat. Plant Physiol. **171**: 165–178.

Rautengarten, C., Usadel, B., Neumetzler, L., Hartmann, J., Büssis, D., and Altmann, T. (2008). A subtilisin-like serine protease essential for mucilage release from Arabidopsis seed coats. Plant J. **54**: 466–480.

Rehman, R.U. and Sansebastiano, G.-P.D. (2014). Plant Rab GTPases in Membrane Trafficking and Signalling. In Plant signaling: Understanding the molecular crosstalk (Springer, New Delhi), pp. 51–73.

Richau, K.H., Kaschani, F., Verdoes, M., Pansuriya, T.C., Niessen, S., Stüber, K., Colby, T., Overkleeft, H.S., Bogyo, M., and Hoorn, R.A.L.V. der (2012). Subclassification and Biochemical Analysis of Plant Papain-Like Cysteine Proteases Displays Subfamily-Specific Characteristics. Plant Physiol. **158**: 1583–1599.

Ringli, C., Baumberger, N., Diet, A., Frey, B., and Keller, B. (2002). ACTIN2 Is Essential for Bulge Site Selection and Tip Growth during Root Hair Development of Arabidopsis. Plant Physiol. **129**: 1464–1472.

Rips, S., Bentley, N., Jeong, I.S., Welch, J.L., Schaewen, A. von, and Koiwa, H. (2014). Multiple N-Glycans Cooperate in the Subcellular Targeting and Functioning of Arabidopsis KORRIGAN1. Plant Cell **26**: 3792–3808.

Robert, S., Chary, S.N., Drakakaki, G., Li, S., Yang, Z., Raikhel, N.V., and Hicks, G.R. (2008). Endosidin1 defines a compartment involved in endocytosis of the brassinosteroid

receptor BRI1 and the auxin transporters PIN2 and AUX1. Proc. Natl. Acad. Sci. **105**: 8464–8469.

Robinson, D.G. and Pimpl, P. (2014). Clathrin and post-Golgi trafficking: a very complicated issue. Trends Plant Sci. **19**: 134–139.

Röckel, N., Wolf, S., Kost, B., Rausch, T., and Greiner, S. (2008). Elaborate spatial patterning of cell-wall PME and PMEI at the pollen tube tip involves PMEI endocytosis, and reflects the distribution of esterified and de-esterified pectins. Plant J. **53**: 133–143.

Rodriguez-Boulan, E. and Müsch, A. (2005). Protein sorting in the Golgi complex: Shifting paradigms. Biochim. Biophys. Acta BBA - Mol. Cell Res. **1744**: 455–464.

Rudd, P.M., Elliott, T., Cresswell, P., Wilson, I.A., and Dwek, R.A. (2001). Glycosylation and the Immune System. Science **291**: 2370–2376.

Ruiz-May, E., Kim, S.-J., Brandizzi, F., and Rose, J.K.C. (2012). The Secreted Plant N-Glycoproteome and Associated Secretory Pathways. Front. Plant Sci. **3**.

Saez-Aguayo, S. et al. (2017). UUAT1 Is a Golgi-Localized UDP-Uronic Acid Transporter That Modulates the Polysaccharide Composition of Arabidopsis Seed Mucilage. Plant Cell **29**: 129–143.

Saez-Aguayo, S., Ralet, M.-C., Berger, A., Botran, L., Ropartz, D., Marion-Poll, A., and North, H.M. (2013). PECTIN METHYLESTERASE INHIBITOR6 Promotes Arabidopsis Mucilage Release by Limiting Methylesterification of Homogalacturonan in Seed Coat Epidermal Cells. Plant Cell **25**: 308–323.

Saito, C. and Ueda, T. (2009). Chapter 4 Functions of RAB and SNARE Proteins in Plant Life. In International Review of Cell and Molecular Biology, International Review of Cell and Molecular Biology. (Academic Press), pp. 183–233.

Satiat-Jeunemaitre, B. and Hawes, C. (1993). The distribution of secretory products in plant cells is affected by brefeldin A. Cell Biol. Int. **17**: 183–193.

Schaller, A., Stintzi, A., Rivas, S., Serrano, I., Chichkova, N.V., Vartapetian, A.B., Martínez, D., Guiamét, J.J., Sueldo, D.J., van der Hoorn, R.A.L., Ramírez, V., and Vera, P. (2017). From structure to function – a family portrait of plant subtilases. New Phytol.

Scheller, H.V. and Ulvskov, P. (2010). Hemicelluloses. Annu. Rev. Plant Biol. **61**: 263–289.

Seguí-Simarro, J.M., Austin, J.R., White, E.A., and Staehelin, L.A. (2004). Electron Tomographic Analysis of Somatic Cell Plate Formation in Meristematic Cells of Arabidopsis Preserved by High-Pressure Freezing. Plant Cell **16**: 836–856.

Sénéchal, F. et al. (2014). Arabidopsis PECTIN METHYLESTERASE17 is co-expressed with and processed by SBT3.5, a subtilisin-like serine protease. Ann. Bot. **114**: 1161–1175.

Shen, J., Ding, Y., Gao, C., Rojo, E., and Jiang, L. (2014). N-linked glycosylation of AtVSR1 is important for vacuolar protein sorting in Arabidopsis. Plant J. **80**: 977–992.

Sherrier, D.J. and VandenBosch, K.A. (1994). Secretion of cell wall polysaccharides in Vicia root hairs. Plant J. **5**: 185–195.

Shi, H., Kim, Y., Guo, Y., Stevenson, B., and Zhu, J.-K. (2003). The Arabidopsis SOS5 Locus Encodes a Putative Cell Surface Adhesion Protein and Is Required for Normal Cell Expansion. Plant Cell **15**: 19–32.

Shindo, T., Misas-Villamil, J.C., Hörger, A.C., Song, J., and Hoorn, R.A.L. van der (2012). A Role in Immunity for Arabidopsis Cysteine Protease RD21, the Ortholog of the Tomato Immune Protease C14. PLOS ONE **7**: e29317.

Simões, I. and Faro, C. (2004). Structure and function of plant aspartic proteinases. Eur. J. Biochem. **271**: 2067–2075.

Skropeta, D. (2009). The effect of individual N-glycans on enzyme activity. Bioorg. Med. Chem. **17**: 2645–2653.

Somssich, M., Khan, G.A., and Persson, S. (2016). Cell Wall Heterogeneity in Root Development of Arabidopsis. Front. Plant Sci. **7**: 1242.

Song, W., Henquet, M.G.L., Mentink, R.A., van Dijk, A.J., Cordewener, J.H.G., Bosch, D., America, A.H.P., and van der Krol, A.R. (2011). N-glycoproteomics in plants: Perspectives and challenges. J. Proteomics **74**: 1463–1474.

St Johnston, D. and Ahringer, J. (2010). Cell Polarity in Eggs and Epithelia: Parallels and Diversity. Cell **141**: 757–774.

Staehelin, A. and Moore, I. (1995). The Plant Golgi Apparatus: Structure, Functional Organization and Trafficking Mechanisms. Annu. Rev. Plant Physiol. Plant Mol. Biol. **46**: 261–288.

Steinwand, B.J., Xu, S., Polko, J.K., Doctor, S.M., Westafer, M., and Kieber, J.J. (2014). Alterations in Auxin Homeostasis Suppress Defects in Cell Wall Function. PLOS ONE **9**: e98193.

Stenmark, H. (2009). Rab GTPases as coordinators of vesicle traffic. Nat. Rev. Mol. Cell Biol. **10**: 513.

Stenzel, I., Ischebeck, T., König, S., Hołubowska, A., Sporysz, M., Hause, B., and Heilmann, I. (2008). The Type B Phosphatidylinositol-4-Phosphate 5-Kinase 3 Is Essential for Root Hair Formation in Arabidopsis thaliana. Plant Cell **20**: 124–141.

Stoops, E.H. and Caplan, M.J. (2014). Trafficking to the Apical and Basolateral Membranes in Polarized Epithelial Cells. J. Am. Soc. Nephrol. **25**: 1375–1386.

Sullivan, S., Ralet, M.-C., Berger, A., Diatloff, E., Bischoff, V., Gonneau, M., Marion-Poll, A., and North, H.M. (2011). CESA5 Is Required for the Synthesis of Cellulose with a Role in Structuring the Adherent Mucilage of Arabidopsis Seeds. Plant Physiol. **156**: 1725–1739.

Takano, J., Noguchi, K., Yasumori, M., Kobayashi, M., Gajdos, Z., Miwa, K., Hayashi, H., Yoneyama, T., and Fujiwara, T. (2002). Arabidopsis boron transporter for xylem loading. Nature **420**: 337.

Takano, J., Tanaka, M., Toyoda, A., Miwa, K., Kasai, K., Fuji, K., Onouchi, H., Naito, S., and Fujiwara, T. (2010). Polar localization and degradation of Arabidopsis boron transporters through distinct trafficking pathways. Proc. Natl. Acad. Sci. **107**: 5220–5225.

Takeda, S., Gapper, C., Kaya, H., Bell, E., Kuchitsu, K., and Dolan, L. (2008). Local Positive Feedback Regulation Determines Cell Shape in Root Hair Cells. Science **319**: 1241–1244.

Tams, J.W. and Welinder, K.G. (1995). Mild Chemical Deglycosylation of Horseradish Peroxidase Yields a Fully Active, Homogeneous Enzyme. Anal. Biochem. **228**: 48–55.

Tan, L. et al. (2013). An Arabidopsis Cell Wall Proteoglycan Consists of Pectin and Arabinoxylan Covalently Linked to an Arabinogalactan Protein. Plant Cell **25**: 270–287.

Tao, L., Cheung, A.Y., and Wu, H. (2002). Plant Rac-Like GTPases Are Activated by Auxin and Mediate Auxin-Responsive Gene Expression. Plant Cell **14**: 2745–2760.

Tognolli, M., Penel, C., Greppin, H., and Simon, P. (2002). Analysis and expression of the class III peroxidase large gene family in Arabidopsis thaliana. Gene **288**: 129–138.

Toyomura, T., Murata, Y., Yamamoto, A., Oka, T., Sun-Wada, G.-H., Wada, Y., and Futai, M. (2003). From Lysosomes to the Plasma Membrane LOCALIZATION OF VACUOLAR TYPE H+-ATPase WITH THE a3 ISOFORM DURING OSTEOCLAST DIFFERENTIATION. J. Biol. Chem. **278**: 22023–22030.

Toyooka, K., Goto, Y., Asatsuma, S., Koizumi, M., Mitsui, T., and Matsuoka, K. (2009). A Mobile Secretory Vesicle Cluster Involved in Mass Transport from the Golgi to the Plant Cell Exterior. Plant Cell **21**: 1212–1229.

Tretter, V., Altmann, F., and März, L. (1991). Peptide-N4-(N-acetyl-β-glucosaminyl)asparagine amidase F cannot release glycans with fucose attached $\alpha 1 \rightarrow 3$ to the asparagine-linked N-acetylglucosamine residue. Eur. J. Biochem. **199**: 647–652.

Tsai, A.Y.-L., Kunieda, T., Rogalski, J., Foster, L.J., Ellis, B.E., and Haughn, G.W. (2017). Identification and characterization of seed coat mucilage proteins. Plant Physiol. **173**: 1059–1074.

Tsiatsiani, L., Gevaert, K., and Van Breusegem, F. (2012). Natural substrates of plant proteases: how can protease degradomics extend our knowledge? Physiol. Plant. **145**: 28–40.

Tsugama, D., Liu, S., and Takano, T. (2011). A rapid chemical method for lysing Arabidopsis cells for protein analysis. Plant Methods **7**: 22.

Turbant, A., Fournet, F., Lequart, M., Zabijak, L., Pageau, K., Bouton, S., and Van Wuytswinkel, O. (2016). PME58 plays a role in pectin distribution during seed coat mucilage extrusion through homogalacturonan modification. J. Exp. Bot. **67**: 2177–2190.

Ueda, T., Sato, M.H., and Uemura, T. (2012). The Role of RAB GTPases and SNARE Proteins in Plant Endocytosis and Post-Golgi Trafficking. In Endocytosis in Plants (Springer, Berlin, Heidelberg), pp. 201–216.

Usadel, B., Kuschinsky, A.M., Rosso, M.G., Eckermann, N., and Pauly, M. (2004). RHM2 Is Involved in Mucilage Pectin Synthesis and Is Required for the Development of the Seed Coat in Arabidopsis. Plant Physiol. **134**: 286–295.

Vagin, O., Kraut, J.A., and Sachs, G. (2009). Role of N-glycosylation in trafficking of apical membrane proteins in epithelia. Am. J. Physiol.-Ren. Physiol. **296**: F459–F469.

Vitale, A. and Boston, R.S. (2008). Endoplasmic Reticulum Quality Control and the Unfolded Protein Response: Insights from Plants. Traffic **9**: 1581–1588.

Vitale, A. and Denecke, J. (1999). The Endoplasmic Reticulum—Gateway of the Secretory Pathway. Plant Cell **11**: 615–628.

Voiniciuc, C., Dean, G.H., Griffiths, J.S., Kirchsteiger, K., Hwang, Y.T., Gillett, A., Dow, G., Western, T.L., Estelle, M., and Haughn, G.W. (2013). FLYING SAUCER1 Is a Transmembrane RING E3 Ubiquitin Ligase That Regulates the Degree of Pectin Methylesterification in Arabidopsis Seed Mucilage. Plant Cell **25**: 944–959.

Voiniciuc, C., Günl, M., Schmidt, M.H.-W., and Usadel, B. (2015a). Highly Branched Xylan Made by IRREGULAR XYLEM14 and MUCILAGE-RELATED21 Links Mucilage to Arabidopsis Seeds. Plant Physiol. **169**: 2481–2495.

Voiniciuc, C., Schmidt, M.H.-W., Berger, A., Yang, B., Ebert, B., Scheller, H.V., North, H.M., Usadel, B., and Guenl, M. (2015b). MUCI10 Produces Galactoglucomannan That Maintains Pectin and Cellulose Architecture in Arabidopsis Seed Mucilage. Plant Physiol. **169**: 403–420.

Wang, H., Zhuang, X., Wang, X., Law, A.H.Y., Zhao, T., Du, S., Loy, M.M.T., and Jiang, L. (2016). A Distinct Pathway for Polar Exocytosis in Plant Cell Wall Formation. Plant Physiol. **172**: 1003–1018.

Wang, J., Ding, Y., Wang, J., Hillmer, S., Miao, Y., Lo, S.W., Wang, X., Robinson, D.G., and Jiang, L. (2010). EXPO, an Exocyst-Positive Organelle Distinct from Multivesicular Endosomes and Autophagosomes, Mediates Cytosol to Cell Wall Exocytosis in Arabidopsis and Tobacco Cells. Plant Cell **22**: 4009–4030.

Wang, S., Xu, Y., Li, Z., Zhang, S., Lim, J.-M., Lee, K.O., Li, C., Qian, Q., Jiang, D.A., and Qi, Y. (2014). OsMOGS is required for N-glycan formation and auxin-mediated root development in rice (Oryza sativa L.). Plant J. **78**: 632–645.

Wang, S., Yoshinari, A., Shimada, T., Hara-Nishimura, I., Mitani-Ueno, N., Ma, J.F., Naito, S., and Takano, J. (2017). Polar Localization of the NIP5;1 Boric Acid Channel Is Maintained by Endocytosis and Facilitates Boron Transport in Arabidopsis Roots. Plant Cell **29**: 824–842.

Wang, T., Park, Y.B., Daniel, J.C., and Hong, M. (2015). Cellulose-Pectin Spatial Contacts Are Inherent to Never-Dried Arabidopsis thaliana Primary Cell Walls: Evidence from Solid-State NMR. Plant Physiol.: pp.00665.2015.

van Weering, J.R.T., Verkade, P., and Cullen, P.J. (2010). SNX–BAR proteins in phosphoinositide-mediated, tubular-based endosomal sorting. Semin. Cell Dev. Biol. **21**: 371–380.

Welinder, K.G., Justesen, A.F., Kjærsgård, I.V.H., Jensen, R.B., Rasmussen, S.K., Jespersen, H.M., and Duroux, L. (2002). Structural diversity and transcription of class III peroxidases from Arabidopsis thaliana. Eur. J. Biochem. **269**: 6063–6081.

Wengier, D., Valsecchi, I., Cabanas, M.L., Tang, W., McCormick, S., and Muschietti, J. (2003). The receptor kinases LePRK1 and LePRK2 associate in pollen and when expressed in yeast, but dissociate in the presence of style extract. Proc. Natl. Acad. Sci. **100**: 6860–6865.

Western, T.L., Burn, J., Tan, W.L., Skinner, D.J., Martin-McCaffrey, L., Moffatt, B.A., and Haughn, G.W. (2001). Isolation and Characterization of Mutants Defective in Seed Coat Mucilage Secretory Cell Development in Arabidopsis. Plant Physiol. **127**: 998–1011.

Western, T.L., Skinner, D.J., and Haughn, G.W. (2000). Differentiation of Mucilage Secretory Cells of the Arabidopsis Seed Coat. Plant Physiol. **122**: 345–356.

Western, T.L., Young, D.S., Dean, G.H., Tan, W.L., Samuels, A.L., and Haughn, G.W. (2004). MUCILAGE-MODIFIED4 Encodes a Putative Pectin Biosynthetic Enzyme Developmentally Regulated by APETALA2, TRANSPARENT TESTA GLABRA1, and GLABRA2 in the Arabidopsis Seed Coat. Plant Physiol. **134**: 296–306.

Willats, W.G.T., McCartney, L., and Knox, J.P. (2001). In-situ analysis of pectic polysaccharides in seed mucilage and at the root surface of Arabidopsis thaliana. Planta **213**: 37–44.

Windsor, J.B., Symonds, V.V., Mendenhall, J., and Lloyd, A.M. (2000). Arabidopsis seed coat development: morphological differentiation of the outer integument. Plant J. **22**: 483–493.

Wolf, S. and Greiner, S. (2012). Growth control by cell wall pectins. Protoplasma **249**: 169–175.

Wolf, S., Rausch, T., and Greiner, S. (2009). The N-terminal pro region mediates retention of unprocessed type-I PME in the Golgi apparatus. Plant J. **58**: 361–375.

Worden, N., Park, E., and Drakakaki, G. (2012). Trans-Golgi Network—An Intersection of Trafficking Cell Wall ComponentsF. J. Integr. Plant Biol. **54**: 875–886.

Xu, T. et al. (2014). Cell Surface ABP1-TMK Auxin-Sensing Complex Activates ROP GTPase Signaling. Science **343**: 1025–1028.

Xu, T., Wen, M., Nagawa, S., Fu, Y., Chen, J.-G., Wu, M.-J., Perrot-Rechenmann, C., Friml, J., Jones, A.M., and Yang, Z. (2010). Cell Surface- and Rho GTPase-Based Auxin Signaling Controls Cellular Interdigitation in Arabidopsis. Cell **143**: 99–110.

Yamada, K., Matsushima, R., Nishimura, M., and Hara-Nishimura, I. (2001). A Slow Maturation of a Cysteine Protease with a Granulin Domain in the Vacuoles of Senescing Arabidopsis Leaves. Plant Physiol. **127**: 1626–1634.

Yamamoto, M., Tantikanjana, T., Nishio, T., Nasrallah, M.E., and Nasrallah, J.B. (2014). Site-Specific N-Glycosylation of the S-Locus Receptor Kinase and Its Role in the Self-Incompatibility Response of the Brassicaceae. Plant Cell **26**: 4749–4762.

Yao, X., Xiong, W., Ye, T., and Wu, Y. (2012). Overexpression of the aspartic protease ASPG1 gene confers drought avoidance in Arabidopsis. J. Exp. Bot. **63**: 2579–2593.

Yeaman, C., Grindstaff, K.K., and Nelson, W.J. (1999). New Perspectives on Mechanisms Involved in Generating Epithelial Cell Polarity. Physiol. Rev. **79**: 73–98.

Young, R.E., McFarlane, H.E., Hahn, M.G., Western, T.L., Haughn, G.W., and Samuels, A.L. (2008). Analysis of the Golgi Apparatus in Arabidopsis Seed Coat Cells during Polarized Secretion of Pectin-Rich Mucilage. Plant Cell **20**: 1623–1638.

Yu, L., Shi, D., Li, J., Kong, Y., Yu, Y., Chai, G., Hu, R., Wang, J., Hahn, M.G., and Zhou, G. (2014). CELLULOSE SYNTHASE-LIKE A2, a Glucomannan Synthase, Is Involved

in Maintaining Adherent Mucilage Structure in Arabidopsis Seed. Plant Physiol. **164**: 1842–1856.

Žárský, V., Cvrčková, F., Potocký, M., and Hála, M. (2009). Exocytosis and cell polarity in plants – exocyst and recycling domains. New Phytol. **183**: 255–272.

Zhang, D., Wengier, D., Shuai, B., Gui, C.-P., Muschietti, J., McCormick, S., and Tang, W.-H. (2008). The Pollen Receptor Kinase LePRK2 Mediates Growth-Promoting Signals and Positively Regulates Pollen Germination and Tube Growth. Plant Physiol. **148**: 1368–1379.

Zhang, G.F. and Staehelin, L.A. (1992). Functional Compartmentation of the Golgi Apparatus of Plant Cells: Immunocytochemical Analysis of High-Pressure Frozen- and Freeze-Substituted Sycamore Maple Suspension Culture Cells. Plant Physiol. **99**: 1070–1083.

Zhang, L., Zhang, H., Liu, P., Hao, H., Jin, J.B., and Lin, J. (2011a). Arabidopsis R-SNARE Proteins VAMP721 and VAMP722 Are Required for Cell Plate Formation. PLOS ONE **6**: e26129.

Zhang, M., Henquet, M., Chen, Z., Zhang, H., Zhang, Y., Ren, X., Van Der Krol, S., Gonneau, M., Bosch, D., and Gong, Z. (2009). LEW3, encoding a putative α-1,2-mannosyltransferase (ALG11) in N-linked glycoprotein, plays vital roles in cell-wall biosynthesis and the abiotic stress response in Arabidopsis thaliana. Plant J. **60**: 983–999.

Zhang, Y., Giboulot, A., Zivy, M., Valot, B., Jamet, E., and Albenne, C. (2011b). Combining various strategies to increase the coverage of the plant cell wall glycoproteome. Phytochemistry **72**: 1109–1123.

Zhang, Y. and McCormick, S. (2007). A distinct mechanism regulating a pollen-specific guanine nucleotide exchange factor for the small GTPase Rop in Arabidopsis thaliana. Proc. Natl. Acad. Sci. **104**: 18830–18835.

Zheng, L., Baumann, U., and Reymond, J.-L. (2004). An efficient one-step site-directed and site-saturation mutagenesis protocol. Nucleic Acids Res. **32**: e115–e115.